

1
2
3
4
5
6
7
8
9
10
11
12
13
14
15
16
17
18
19
20
21
22
23
24
25
26
27
28
29
30

Global Sea Level Budget 1993-Present

WCRP Global Sea Level Budget Group*

*A full list of authors and their affiliations appears at the end of the paper

**Revised version
8 July 2018**

Corresponding author: Anny Cazenave, LEGOS, 18 Avenue Edouard Belin, 31401 Toulouse, Cedex 9, France; anny.cazenave@legos.obs-mip.fr

31 **Abstract**

32 Global mean sea level is an integral of changes occurring in the climate system in response to
33 unforced climate variability as well as natural and anthropogenic forcing factors. Its temporal
34 evolution allows detecting changes (e.g., acceleration) in one or more components. Study of the
35 sea level budget provides constraints on missing or poorly known contributions, such as the
36 unsurveyed deep ocean or the still uncertain land water component. In the context of the World
37 Climate Research Programme Grand Challenge entitled “Regional Sea Level and Coastal
38 Impacts”, an international effort involving the sea level community worldwide has been
39 recently initiated with the objective of assessing the various data sets used to estimate
40 components of the sea level budget during the altimetry era (1993 to present). These data sets
41 are based on the combination of a broad range of space-based and in situ observations, model
42 estimates and algorithms. Evaluating their quality, quantifying uncertainties and identifying
43 sources of discrepancies between component estimates is extremely useful for various
44 applications in climate research. This effort involves several tens of scientists from about fifty
45 research teams/institutions worldwide (www.wcrp-climate.org/grand-challenges/gc-sea-level).
46 The results presented in this paper are a synthesis of the first assessment performed during
47 2017-2018. We present estimates of the altimetry-based global mean sea level (average rate of
48 3.1 ± 0.3 mm/yr and acceleration of 0.1 mm/yr² over 1993-present), as well as of the different
49 components of the sea level budget (2.9 Ocean mass change from GRACE Line 1383:
50 constraint Line 1386-1393: This is a very long sentence. Consider splitting it in several
51 sentences or us i), ii) and so on to list the major error sources. Line 1395: Remove on. Table
52 10, first row: please be more accurate with the column titles (also check all the other Tables) –
53 the first column should be “source” or “publication” and the last one “ocean mass trend SLE
54 (mm/yr)” or so. Table 10, Line 1398: ocean mass trend Line 1402-1404: I think this sentence
55 should be moved to the end of the next paragraph (Line 1413). It seems a bit lost here. Line
56 1409: Remove to. Line 1431: What is ΔC_{20} ? Table 11: same comment as for Table 10 – be
57 more accurate with the titles of the columns. E.g. first column should be “GRACE data product”
58 or so, and second “linear trend (mm/yr)” or so. Line 1481-1482: As far as I understood, it was
59 launched in March 2018, wasn’t it? (Instead of “is scheduled to be launched”) 3. Sea Level
60 Budget results Line 1532: Don’t you mean Table 13 instead of 12? Section 3.2.2: A very short
61 section. I think, even though you discuss it in the Discussion, in this section you should at least
62 comment on the large discrepancy between Row 7 and 8 in Table 13, and how it relates to the
63 large uncertainty in TWS. Line 1549-1551: Be more accurate: the table provides annual mean
64 values for the ensemble mean GMSL and the sum of components (GRACE-based ocean mass

65 and Argo-based thermosteric component). Line 1567: Is the residual trend statistically
66 significant? 5. Concluding Remarks Line 1728: for example Line 1730: Remove the long term
67 for NASA to a list of abbreviations at the end of the text.). We further examine closure of the
68 sea level budget, comparing the observed global mean sea level with the sum of components.
69 Ocean thermal expansion, glaciers, Greenland and Antarctica contribute by 42%, 21%, 15%
70 and 8% to the global mean sea level over the 1993-present. We also study the sea level budget
71 over 2005-present, using GRACE-based ocean mass estimates instead of sum of individual
72 mass components. Results show closure of the sea level budget within 0.3 mm/yr. Substantial
73 uncertainty remains for the land water storage component, as shown in examining individual
74 mass contributions to sea level.
75

76 **1. Introduction**

77
78 Global warming has already several visible consequences, in particular increase of the Earth's
79 mean surface temperature and ocean heat content (Rhein et al., 2013, Stocker et al., 2013),
80 melting of sea ice, loss of mass of glaciers (Gardner et al., 2013), and ice mass loss from the
81 Greenland and Antarctica ice sheets (Rignot et al., 2011, Shepherd et al., 2012). On average
82 over the last 50 years, about 93% of heat excess accumulated in the climate system because of
83 greenhouse gas emissions has been stored in the ocean, and the remaining 7% has been warming
84 the atmosphere and continents, and melting sea and land ice (von Schuckmann et al., 2016).
85 Because of ocean warming and land ice mass loss, sea level rises. Since the end of the last
86 deglaciation about 3000 years ago, sea level remained nearly constant (e.g., Lambeck et al.,
87 2010, Kemp et al., 2011, Kopp et al. 2014). However, direct observations from in situ tide
88 gauges available since the mid-to-late 19th century show that the 20th century global mean sea
89 level has started to rise again at a rate of 1.2 mm/yr to 1.9 mm/yr (Church and White, 2011,
90 Jevrejeva et al., 2014a, Hay et al., 2015, Dangendorf et al., 2017). Since the early 1990s, thi
91 rate, now measured by high-precision altimeter satellites, has increased to ~3 mm/yr on average
92 (Legeais et al., 2018, Nerem et al., 2018).

93 Accurate assessment of present-day global mean sea level variations and its components (ocean
94 thermal expansion, ice sheet mass loss, glaciers mass change, changes in land water storage,
95 etc.) is important for many reasons. The global mean sea level is an integral of changes
96 occurring in the Earth's climate system in response to unforced climate variability as well as
97 natural and anthropogenic forcing factors e.g., net contribution of ocean warming, land ice mass
98 loss, and changes in water storage in continental river basins. Temporal changes of the
99 components are directly reflected in the global mean sea level curve. If accurate enough, study
100 of the sea level budget provides constraints on missing or poorly known contributions, e.g., the
101 deep ocean or polar regions undersampled by current observing systems, or still uncertain
102 changes in water storage on land due to human activities (e.g. ground water depletion in
103 aquifers). Global mean sea level corrected for ocean mass change in principle allows one to
104 independently estimate temporal changes in total ocean heat content, from which the Earth's
105 energy imbalance can be deduced (von Schuckmann et al., 2016). The sea level and/or ocean
106 mass budget approach can also be used to constrain models of Glacial Isostatic Adjustment
107 (GIA). The GIA phenomenon has significant impact on the interpretation of GRACE-based
108 space gravimetry data over the oceans (for ocean mass change) and over Antarctica (for ice
109 sheet mass balance). However, there is still incomplete consensus on best estimates, a result of

110 uncertainties in deglaciation models and mantle viscosity structure. Finally, observed changes
111 of the global mean sea level and its components are fundamental for validating climate models
112 used for projections.

113 In the context of the Grand Challenge entitled “Regional Sea Level and Coastal Impacts” of the
114 World Climate Research Programme (WCRP), an international effort involving the sea level
115 community worldwide has been recently initiated with the objective of assessing the sea level
116 budget during the altimetry era (1993 to present). To estimate the different components of the
117 sea level budget, different data sets are used. These are based on the combination of a broad
118 range of space-based and in situ observations. Evaluating their quality, quantifying their
119 uncertainties, and identifying the sources of discrepancies between component estimates,
120 including the altimetry-based sea level time series, are extremely useful for various applications
121 in climate research.

122 Several previous studies have addressed the sea level budget over different time spans and
123 using different data sets (e.g., Cazenave et al., 2009, Leuliette and Willis, 2010, Church and
124 White, 2011, Chambers et al., 2017, Dieng et al., 2017, Chen et al., 2017, Nerem et al., 2018).
125 Assessments of the published literature have also been performed in past IPCC
126 (Intergovernmental Panel on Climate Change) reports (e.g., Church et al., 2013). Building on
127 these previous works, here we intend to provide a collective update of the global mean sea
128 level budget, involving the many groups worldwide interested in present-day sea level rise and
129 its components. We focus on observations rather than model-based estimates and consider the
130 high-precision altimetry era starting in 1993 that includes the period since the mid-2000s where
131 new observing systems, like the Argo float project (Roemmich et al., 2012) and the GRACE
132 space gravimetry mission (Tapley et al., 2004) that provide improved data sets of high value
133 for such a study. Only the global mean budget is considered here. Regional budget will be the
134 focus of a future assessment.

135 Section 2 describes for each component of the sea level budget equation the different data sets
136 used to estimate the corresponding contribution to sea level, discusses associated errors and
137 provides trend estimates for the two periods. Section 3 addresses the mass and sea level budgets
138 over the study periods. A discussion is provided in Section 4, followed by a conclusion.

139

140 **2. Methods and Data**

141 In this section, we briefly present the global mean sea level budget (sub section 2.1), then
142 provide, for each term of the budget equation, an assessment of the most up-to-date published

143 results. Multiple organisations and research groups routinely generate the basic measurements
 144 as well as the derived data sets and products used to study the sea level budget. Sub sections
 145 2.2 to 2.7 summarize the measurements and methodologies used to derive observed sea level,
 146 as well as steric and mass components. In most cases, we focus on observations but in some
 147 instances (e.g., for GIA corrections applied to the data), model-based estimates are the only
 148 available information.

149

150 **2.1 Sea level budget equation**

151 Global mean sea level (GMSL) change as a function of time t is usually expressed by the sea
 152 level budget equation:

$$153 \quad \text{GMSL}(t) = \text{GMSL}(t)_{\text{steric}} + \text{GMSL}(t)_{\text{ocean mass}} \quad (1)$$

154 where $\text{GMSL}(t)_{\text{steric}}$ refers to the contributions of ocean thermal expansion and salinity to sea
 155 level change, and $\text{GMSL}(t)_{\text{ocean mass}}$ refers to the change in mass of the oceans. Due to water
 156 conservation in the climate system, the ocean mass term (also noted as $M(t)_{\text{ocean}}$) can further be
 157 expressed as:

158

$$159 \quad \begin{aligned} &M(t)_{\text{ocean}} + M(t)_{\text{glaciers}} + M(t)_{\text{Greenland}} + M(t)_{\text{Antarctica}} + M(t)_{\text{TWS}} + M(t)_{\text{WV}} + M(t)_{\text{Snow}} \\ 160 &+ \text{uncertainty} = 0 \end{aligned} \quad (2)$$

161

162 where $M(t)_{\text{glaciers}}$, $M(t)_{\text{Greenland}}$, $M(t)_{\text{Antarctica}}$, $M(t)_{\text{TWS}}$, $M(t)_{\text{WV}}$, $M(t)_{\text{Snow}}$ represent temporal
 163 changes in mass of glaciers, Greenland and Antarctica ice sheets, terrestrial water storage
 164 (TWS), atmospheric water vapor (WV), and snow mass changes. The uncertainty is a result of
 165 uncertainties in all of the estimates and potentially missing mass terms, for example, permafrost
 166 melting.

167

168 From equation (2), we deduce:

169

$$170 \quad \begin{aligned} \text{GMSL}(t)_{\text{ocean mass}} = & - [M(t)_{\text{glaciers}} + M(t)_{\text{Greenland}} + M(t)_{\text{Antarctica}} + M(t)_{\text{TWS}} + M(t)_{\text{WV}} + M(t)_{\text{Snow}} \\ 171 & + \text{missing mass terms}] \end{aligned} \quad (3)$$

172

173 In the next subsections, we successively discuss the different terms of the budget (equations 1
 174 and 2) and how they are estimated from observations. We do not consider the atmospheric water
 175 vapor and snow components, assumed to be small. Two periods are considered: (1) 1993-

176 present (i.e. the entire altimetry era), and (2) 2005-present (i.e. the period covered by both Argo
177 and GRACE).

178

179 **2.2 Altimetry-based global mean sea level over 1993-present**

180 The launch of the TOPEX/Poseidon (T/P) altimeter satellite in 1992 led to a new paradigm for
181 measuring sea level from space, providing for the first time precise and globally distributed sea
182 level measurements at 10-day intervals. At the time of the launch of T/P, the measurements
183 were not expected to have sufficient accuracy for measuring GMSL changes. However, as the
184 radial orbit error decreased from ~10 cm at launch to ~1 cm presently, and other instrumental
185 and geophysical corrections applied to altimetry system improved (e.g., Stammer and
186 Cazenave, 2017), several groups regularly provided an altimetry-based GMSL time series (e.g.,
187 Nerem et al. 2010, Church et al. 2011, Ablain et al., 2015, Legeais et al., 2018). The initial T/P
188 GMSL time series was extended with the launch of Jason-1 (2001), Jason-2 (2008) and Jason-
189 3 (2016). By design, each of these missions has an overlap period with the previous one in order
190 to inter-compare the sea level measurements and estimate instrument biases (e.g., Nerem et al.,
191 2010; Ablain et al., 2015). This has allowed the construction of an uninterrupted GMSL time
192 series that is currently 25-year long.

193

194 **2.2.1 Global mean sea level datasets**

195 Six groups (AVISO/CNES, SL_cci/ESA, University of Colorado, CSIRO, NASA/GSFC,
196 NOAA) provide altimetry-based GMSL time series. All of them use 1-Hz altimetry
197 measurements derived from T/P, Jason-1, Jason-2 and Jason-3 as reference missions. These
198 missions provide the most accurate long-term stability at global and regional scales (Ablain et
199 al. 2009, 2017a), and are all on the same historical T/P ground track. This allows computation
200 of a long-term record of the GMSL from 1993 to present. In addition, complementary missions
201 (ERS-1, ERS-2, Envisat, Geosat Follow-on, CryoSat-2, SARAL/AltiKa and Sentinel-3A)
202 provide increased spatial resolution and coverage of high latitude ocean areas, poleward of
203 66°N/S latitude (e.g. the European Space Agency/ESA Climate Change Initiative/CCI sea level
204 data set; Legeais et al. 2018).

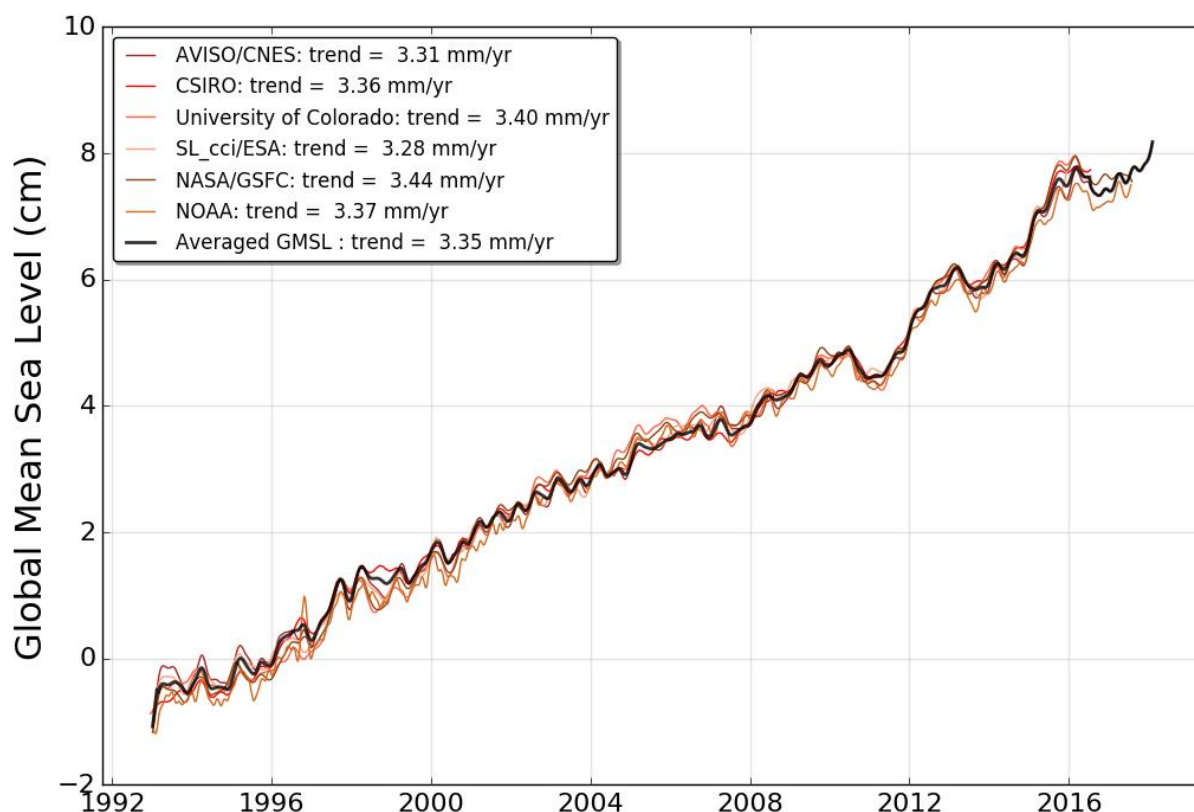
205 The above groups adopt different approaches when processing satellite altimetry data. The most
206 important differences concern the geophysical corrections needed to account for various
207 physical phenomena such as atmospheric propagation delays, sea state bias, ocean tides, and
208 the ocean response to atmospheric wind and pressure forcing. Other differences come from data

209 editing, methods to spatially average individual measurements during orbital cycles and link
 210 between successive missions (Masters et al. 2012; Henry et al. 2014).

211 Overall, the quality of the different GMSL time series is similar. Long-term trends agree well
 212 to within 6% of the signal, approximately 0.2 mm/yr (see Figure 1) within the GMSL trend
 213 uncertainty range (~ 0.3 mm/yr; see next section). The largest differences are observed at
 214 interannual time scales and during the first years (before 1999; see below). Here we use an
 215 ensemble mean GMSL based on averaging all individual GMSL time series.

216

217



218

219

220 *Figure 1: Evolution of GMSL time series from 6 different groups (AVISO/CNES, SL_cci/ESA,*
 221 *University of Colorado, CSIRO, NASA/GSFC, NOAA) products. Annual signals are removed*
 222 *and 6-month smoothing applied. All GMSL time series are centered in 1993 with zero mean. A*
 223 *GIA correction of -0.3 mm/yr has been subtracted to each data set.*

224 **2.2.2 Global mean sea level uncertainties and TOPEX-A drift**

225 Based on an assessment of all sources or uncertainties affecting the altimetric system (Ablain
 226 et al. 2017), the GMSL trend uncertainty (90% confidence interval) is estimated as ~ 0.4 mm/yr
 227 over the whole altimetry era (1993-2017). The main contribution to the uncertainty is the wet

228 tropospheric correction with a drift uncertainty in the range of 0.2-0.3 mm/yr (Legeais et al.
 229 2018) over a 10-year period. To a lesser extent, the orbit error (Couhert et al. 2015; Escudier et
 230 al., 2017) and the altimeter parameters' (range, sigma-0 and significant wave height/SWH)
 231 instability (Ablain et al., 2012) also contribute to the GMSL trend uncertainty, at the level of
 232 0.1 mm/yr. Furthermore, imperfect links between successive altimetry missions lead to another
 233 trend uncertainty of about 0.15 mm/yr over the 1993-2017 period (Zawadzki and Ablain, 2016).
 234 Uncertainties are higher during the first decade (1993-2002) where T/P measurements display
 235 larger errors at climatic scales. For instance, the orbit solutions are much more uncertain due to
 236 gravity field solutions calculated without GRACE data. Furthermore, the switch from TOPEX-
 237 A to TOPEX-B in February 1999 (with no overlap between the two instrumental observations)
 238 leads to an error of ~ 3 mm in the GMSL time series (Escudier et al., 2017).
 239 However, the most significant error that affects the first 6 years (January-1993 to February
 240 1999) of the T/P GMSL measurements is due to an instrumental drift of the TOPEX-A
 241 altimeter, not included in the formal uncertainty estimates discussed above. This effect on the
 242 GMSL time series was recently highlighted via comparisons with tide gauges (Valladeau et al.
 243 2012; Watson et al. 2015; Chen et al. 2017; Ablain et al. 2017), via a sea level budget approach
 244 (i.e., comparison with the sum of mass and steric components; Dieng et al., 2017) and by
 245 comparing with Poseidon-1 measurements (Zawadzki, personal communication). In a recent
 246 study, Beckley et al. (2017) asserted that the corresponding error on the 1993-1998 GMSL
 247 resulted from incorrect onboard calibration parameters.
 248 All three approaches conclude that during the period January 1993 to February 1999, the
 249 altimetry-based GMSL was overestimated. TOPEX-A drift correction was estimated close to
 250 1.5 mm/yr (in terms of sea level trend) with an uncertainty of ± 0.5 to ± 1.0 mm/yr (Watson et
 251 al. 2015; Chen et al. 2017; Dieng et al. 2017). Beckley et al. (2017) proposed to not apply the
 252 suspect onboard calibration correction on TOPEX-A measurements. The impact of this
 253 approach is similar to the TOPEX-A drift correction estimated by Dieng et al. (2017) and Ablain
 254 et al. (2017b). In the latter study, accurate comparison between TOPEX A-based GMSL and
 255 tide gauge measurements leads to a drift correction to about -1.0 mm/yr between January 1993
 256 and July 1995, and +3.0 mm/yr between August 1995 and February 1999, with an uncertainty
 257 of 1.0 mm/yr (with a 68% confidence level, see Table 1).
 258

TOPEX-A drift correction	to be subtracted from the first 6-years (Jan. 1993 to Feb. 1999)
---------------------------------	---

	of the uncorrected GMSL record
Watson et al. (2015)	1.5 +/- 0.5 mm/yr over Jan.1993/ Feb.1999
Chen et al. (2017); Dieng et al. (2017)	1.5 +/- 0.5 mm/yr over Jan.1993/ Feb.1999
Beckley et al. (2017)	No onboard calibration applied
Ablain et al. (2017b)	-1.0 +/- 1.0 mm/yr over Jan.1993/ Jul.1995 +3.0 +/-1.0 mm/yr over Aug.1995- Feb.1999

259 *Table 1. TOPEX-A GMSL drift corrections proposed by different studies*

260

261 **2.2.3 Global Mean Sea Level variations**

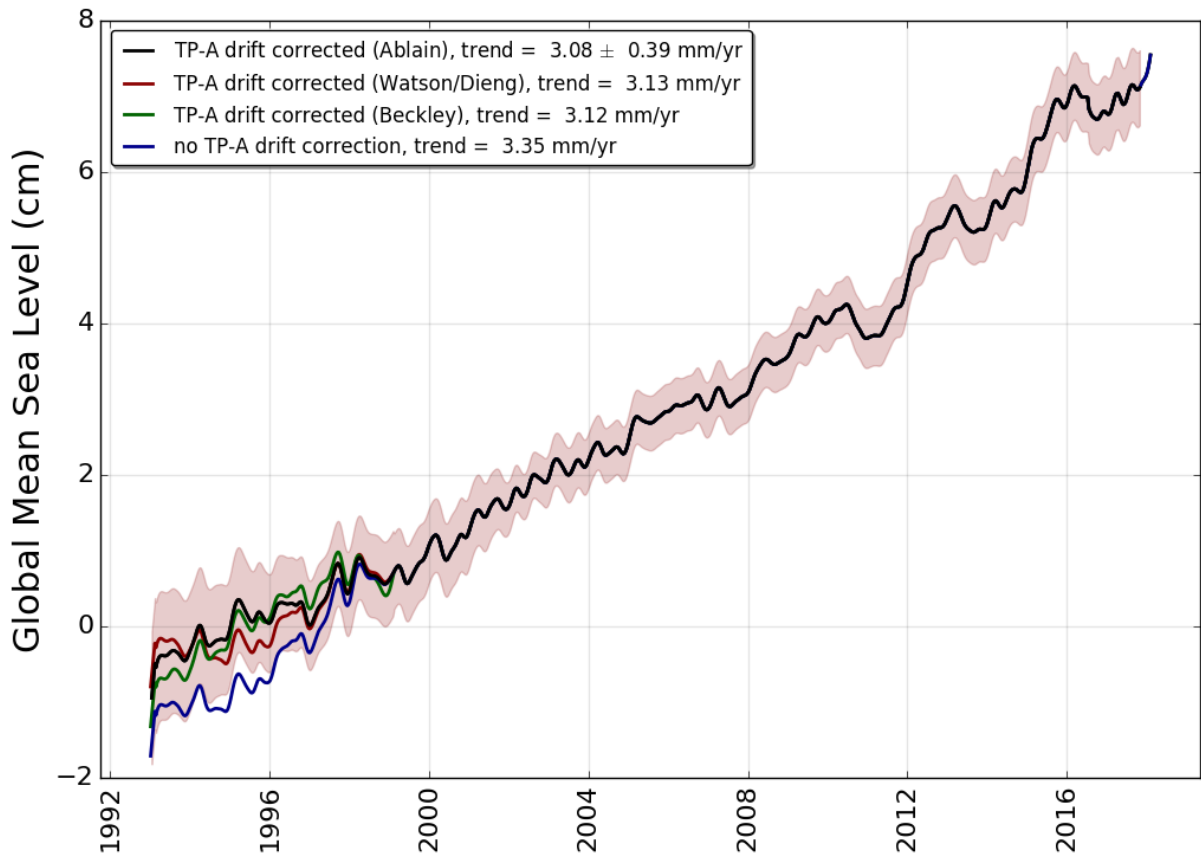
262

263 The ensemble mean GMSL rate after correcting for the TOPEX-A drift (for all of the proposed
 264 corrections) amounts to 3.1 mm/yr over 1993-2017 (Figure 2). This corresponds to a mean sea
 265 level rise of about 7.5 cm over the whole altimetry period. More importantly, the GMSL curve
 266 shows a net acceleration, estimated at 0.08 mm/yr² (Chen et al. 2017; Dieng et al. 2017) and
 267 0.084 +/- 0.025 mm/yr² (Nerem et al., 2018) (Note Watson et al. found a smaller acceleration
 268 after correcting for the instrumental bias over a shorter period up to the end of 2014.). GMSL
 269 trends calculated over 10-year moving windows illustrate this acceleration (Figure 3). GMSL
 270 trends are close to 2.5 mm/yr over 1993-2002 and 3.0 mm/yr over 1996-2005. After a slightly
 271 smaller trend over 2002-2011, the 2008-2017 trend reaches 4.2 mm/yr. Uncertainties (90%
 272 confidence interval) associated to these 10-year trends regularly decrease through time from
 273 1.3 mm/yr over 1993-2002 (corresponding to T/P data) to 0.65 mm/yr for 2008-2017
 274 (corresponding to Jason-2 and Jason-3 data).

275 Removing the trend from the GMSL time series highlights inter-annual variations (not shown).
 276 Their magnitudes depend on the period (+3 mm in 1998-1999, -5 mm in 2011-2012, and +10
 277 mm in 2015-2016) and are well correlated in time with El Niño and La Niña events (Nerem et
 278 al. 2010; Cazenave et al. 2014, Nerem et al., 2018). However, substantial differences (of 1-3
 279 mm) exist between the six detrended GMSL time series. This issue needs further investigation.

280

281



282

283

284 *Figure 2: Evolution of ensemble mean GMSL time series (average of the 6 GMSL products*
 285 *from AVISO/CNES, SL_cci/ESA, University of Colorado, CSIRO, NASA/GSFC, and NOAA).*
 286 *On the black, red and green curves, the TOPEX-A drift correction is applied respectively based*
 287 *on (Ablain et al, 2017b), (Watson et al. 2015; Dieng et al. 2017) and Beckley et al., 2017).*
 288 *Annual signal removed and 6-month smoothing applied; GIA correction also applied.*
 289 *Uncertainties (90% confidence interval) of correlated errors over a 1-year period are*
 290 *superimposed for each individual measurement (shaded area).*

291

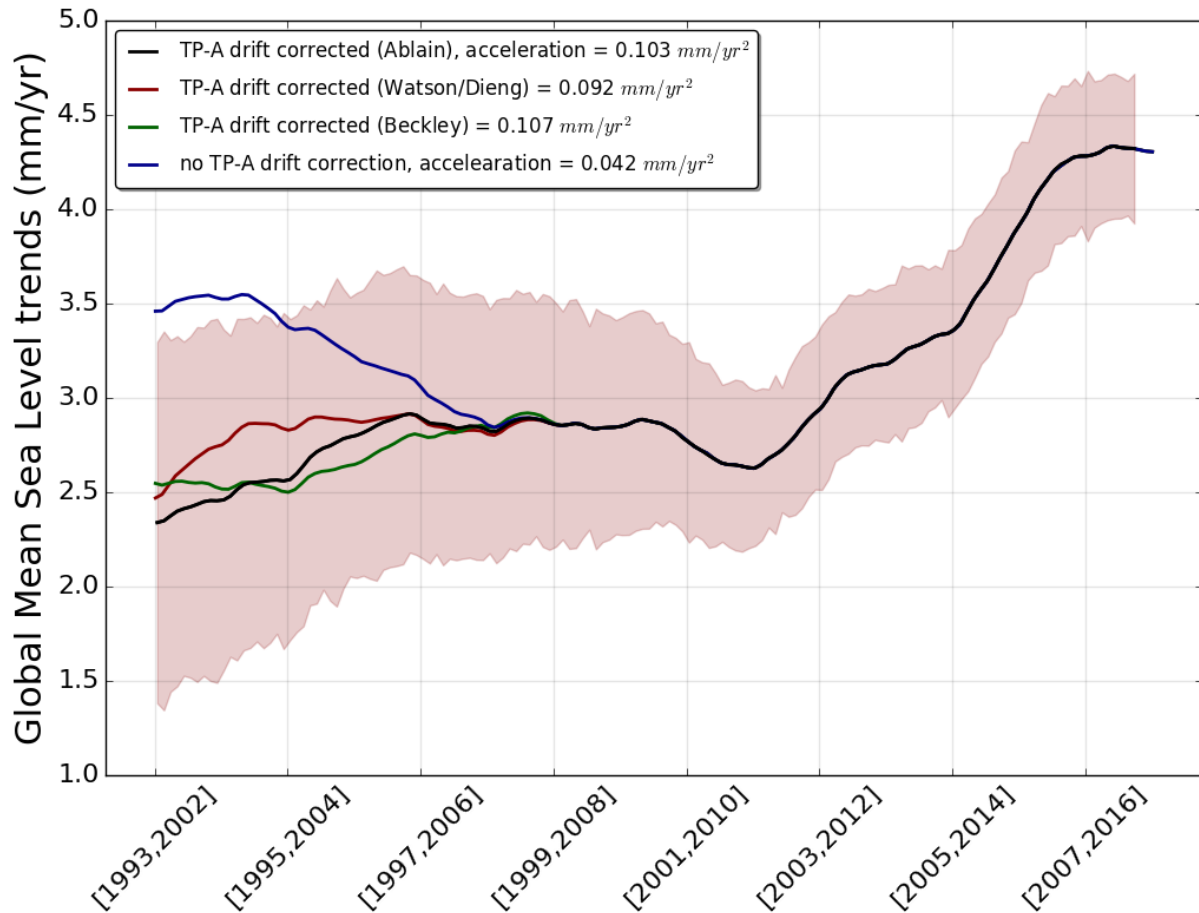
292

293

294

295

296



297

298

299 *Figure 3: Ensemble mean GMSL trends calculated over 10-year moving windows. On the black,*
 300 *red and green curves, the TOPEX-A drift correction is applied respectively based on (Ablain et*
 301 *al, 2017b), and Beckley et al., 2017). Uncorrected GMSL trends are shown by the blue curve.*
 302 *The shaded area represents trend uncertainty over 10-year periods (90% confidence interval).*

303

304 For the sea level budget assessment (section 3), we will use the ensemble mean GMSL time
 305 series corrected for the TOPEX A drift using the Ablain et al. (2017b) correction.

306

307 **2.2.4. Comparison with tide gauges**

308

309 Prior to 1992 global sea level rise estimates rely on the tide gauge measurements, and it is worth
 310 mentioning past attempts to produce global sea level reconstructions utilizing these
 311 measurements (e.g. Gornitz et al. 1982; Barnett 1984; Douglas 1991, 1997, 2001). Here we
 312 focus on global sea level reconstructions that overlap with satellite altimetry data over a
 313 substantial common time span. Some of these reconstructions rely on tide gauge data only
 314 (Jevrejeva et al. 2006, 2014; Merrifield et al. 2009; Wenzel and Schroter 2010; Ray and Douglas

315 2011; Hamlington et al. 2011, Spada and Galassi 2012; Thompson and Merrifield 2014;
316 Dangendorf et al. 2017; Frederikse et al. 2017). In addition, there are reconstructions that jointly
317 use satellite altimetry and tide gauge records (Church and White 2006, 2011) and
318 reconstructions which combines tide gauge records with ocean models (Meysignac et al. 2011)
319 or physics-based and model-derived geometries of the contributing processes (Hay et al. 2015).
320 For the period since 1993, with most of the world coastlines densely sampled, the rates of sea
321 level rise from all tide gauge based reconstructions and estimates from satellite altimetry agree
322 within their specific uncertainties, e.g., rates of $3.0 \pm 0.7 \text{ mm} \cdot \text{yr}^{-1}$ (Hay et al. 2015); 2.8 ± 0.5
323 $\text{mm} \cdot \text{yr}^{-1}$ (Church and White 2011; Rhein et al. 2013); $3.1 \pm 0.6 \text{ mm} \cdot \text{yr}^{-1}$ (Jevrejeva et al, 2014);
324 $3.1 \pm 1.4 \text{ mm} \cdot \text{yr}^{-1}$ (Dangendorf et al. 2017) and the estimate from satellite altimetry 3.2 ± 0.4
325 $\text{mm} \cdot \text{yr}^{-1}$ (Nerem et al. 2010; Rhein et al. 2013). However, classical tide gauge-based
326 reconstructions still tend to overestimate the inter-annual to decadal variability of global mean
327 sea level (e.g. Calafat et al., 2012; Dangendorf et al. 2015; Natarov et al. 2017) compared to
328 global mean sea level from satellite altimetry, due to limited and uneven spatial sampling of the
329 global ocean afforded by the tide gauge network. Sea level rise being non uniform, spatial
330 variability of sea-level measured at tide gauges is evidenced by 2D reconstruction methods. The
331 most widely used approach is the use of empirical orthogonal functions (EOF) calibrated with
332 the satellite altimetry data (e.g. Church and White, 2004). Alternatively, Choblet et al.
333 (2014) implemented a Bayesian inference method based on a Voronoi tessellation of the Earth's
334 surface to reconstruct sea level during the twentieth century. Considerable uncertainties remain
335 however in long term assessments due to poorly sampled ocean basins such as the South
336 Atlantic, or regions which are significantly influenced by open-ocean circulation (e.g.
337 Subtropical North Atlantic) (Frederikse et al. 2017). Uncertainties involved in specifying
338 vertical land motion corrections at tide gauges also impact tide gauge reconstructions (Jevrejeva
339 et al. 2014; Woppelmann and Marcos 2016; Hamlington et al. 2016). Frederikse et al. (2017)
340 recently also demonstrated that both global mean sea level reconstructed from tide gauges and
341 the sum of steric and mass contributors show a good agreement with altimetry estimates for the
342 overlapping period 1993-2014.

343

344 **2.3 Steric sea level**

345 Steric sea level variations result from temperature (T) and salinity (S) related density changes
346 of sea water associated to volume expansion and contraction. These are referred to as
347 thermosteric and halosteric components. Despite clear detection of regional salinity changes

348 and the dominance of the salinity effect on density changes at high latitudes (Rhein et al., 2013),
349 the halosteric contribution to present-day global mean steric sea level rise is negligible, as the
350 ocean's total salt content is essentially constant over multidecadal timescales (Gregory and
351 Lowe, 2000). Hence in this study, we essentially consider the thermosteric sea level component.
352 Averaged over the 20th century, ocean thermal expansion associated with ocean warming has
353 been the largest contribution to global mean sea level rise (Church et al., 2013). This remains
354 true for the altimetry period starting in the year 1993 (e.g., Chen et al. 2017; Dieng et al., 2017,
355 Nerem et al., 2018). But total land ice mass loss (from glaciers, Greenland and Antarctica)
356 during this period, now dominates the sea level budget (see section 3).

357 Until the mid-2000s, the majority of ocean temperature data have been retrieved from shipboard
358 measurements. These include vertical temperature profiles along research cruise tracks from
359 the surface sometimes all the way down to the bottom layer (e.g. Purkey and Johnson, 2010)
360 and upper-ocean broadscale measurements from ships of opportunity (Abraham et al., 2013).
361 These upper-ocean in situ temperature measurements however are limited to the upper 700 m
362 depth due to common use of expandable bathy thermographs (XBTs). Although the coverage
363 has been improved through time, large regions characterized by difficult meteorological
364 conditions remained undersampled, in particular the southern hemisphere oceans and the Arctic
365 area.

366

367 ***2.3.1 Thermosteric data sets***

368 Over the altimetry era, several research groups have produced gridded time series of
369 temperature data for different depth levels, based on XBTs (with additional data from
370 mechanical bathythermographs -MBTs- and conductivity-temperature-depth (CTD) devices
371 and moorings) and Argo float measurements. The temperature data have further been used to
372 provide thermosteric sea level products. These differ because of different strategies adopted for
373 data editing, temporal and spatial data gaps filling, mapping methods, baseline climatology and
374 instrument bias corrections (in particular the time-to-depth correction for XBT data, Boyer et
375 al., 2016).

376 The global ocean in situ observing system has been dramatically improved through the
377 implementation of the international Argo program of autonomous floats, delivering a unique
378 insight of the interior ocean from the surface down to 2000 m depth of the ice-free global ocean
379 (Roemmich et al., 2012, Riser et al., 2016). More than 80% of intially planned full deployment
380 of Argo float program was achieved during the year 2005, with quasi- global coverage of the
381 ice-free ocean by the start of 2006. At present, more than 3800 floats provide systematic T/S

382 data, with quasi (60°S-60°N latitude) global coverage down to 2000 m depth. A full overview
 383 on in situ ocean temperature measurements is given for example in Abraham et al. (2013).
 384 In this section, we consider a set of 11 direct (in situ) estimates, publically available over the
 385 entire altimetry era, to review global mean thermosteric sea level rise and, ultimately, to
 386 construct an ensemble mean timeseries. These data sets are:

- 387 1. CORA = Coriolis Ocean database for ReAnalysis, Copernicus Service, France
 388 marine.copernicus.eu/, product name :
 389 INSITU_GLO_TS_OA_REP_OBSERVATIONS_013_002_b
- 390 2. CSIRO (RSOI) = Commonwealth Scientific and Industrial Research
 391 Organisation/Reduced-Space Optimal Interpolation, Australia
- 392 3. ACECRC/IMAS-UTAS = Antarctic Climate and Ecosystem Cooperative Research
 393 Centre/Institute for Marine and Antarctic Studies-University of Tasmania, Australia
 394 http://www.cmar.csiro.au/sealevel/thermal_expansion_ocean_heat_timeseries.html
- 395 4. ICCES = International Center for Climate and Environment Sciences, Institute of
 396 Atmospheric Physics, China
 397 <http://ddl.escience.cn/f/PKFR>
- 398 5. ICDC = Integrated Climate Data Center, Universit of Hamburg, Germany
- 399 6. IPRC = International Pacific Research Center, University of Hawaii, USA
 400 [http://apdrc.soest.hawaii.edu/projects/Argo/data/gridded/On_standard_levels/index-](http://apdrc.soest.hawaii.edu/projects/Argo/data/gridded/On_standard_levels/index-1.html)
 401 [1.html](http://apdrc.soest.hawaii.edu/projects/Argo/data/gridded/On_standard_levels/index-1.html)
- 402 7. JAMSTEC = Japan Agency for Marine-Earth Science and Technology, Japan
 403 ftp://ftp2.jamstec.go.jp/pub/argo/MOAA_GPV/Glb_PRS/OI/
- 404 8. MRI/JMA = Meteorological Resarch Institute/Japan Meteorological Agency, Japan
 405 <https://climate.mri-jma.go.jp/~ishii/.wcrp/>
- 406 9. NCEI/NOAA = National Centers for Environmental Information/National Oceanic and
 407 Atmospheric Adinistration, USA
- 408 10. SIO = Scripps Institution of Oceanography, USA
 409 Deep/abyssal: <https://cchdo.ucsd.edu/>
- 410 11. SIO = Scripps Institution of Oceanography, USA
 411 Deep/abyssal: <https://cchdo.ucsd.edu/> (for the abyssal ocean)

412

413 Their characteristics are presented in Table 2.

414

415

416

417

418

419

420

Product/Institution		Period	Depth-integration (m)				Temporal resolution / Latitudinal range	Reference
			0-700	700 - 2000	0-2000	≥2000		
1	CORA	1993-2016	Y	Y	Y	---	Monthly 60°S-60°N	http://marine.copernicus.eu/services-portfolio/access-to-products/
2	CSIRO (RSOI)	2004-2017	Y/E (0-300)	Y/E	Y/E	---	Monthly 65°S-65°N	Roemmich et al. (2015); Wijffels et al. (2016)
3	CSIRO/ACE CRC/IMAS-UTAS	1970-2017	Y/E (0-300)	---	---	---	Yearly (3-yr run. mean) 65°S-65°N	Domingues et al. (2008); Church et al. (2011)
4	ICES	1970-2016	Y/E (0-300)	Y/E	Y/E	---	Yearly 89°S-89°N	Cheng and Zhu (2016); Cheng et al. (2017)
5	ICDC	1993-2016	Y (1993)	---	Y (2005)	---	Monthly	Gouretzki and Koltermann (2007)
6	IPRC	2005-2016	---	---	Y	---	Monthly	http://apdrc.soest.hawaii.edu/projects/argo
7	JAMSTEC	2005-2016	---	---	Y	---	Monthly	Hosoda et al. (2008)
8	MRI/JMA	1970-2016 (rel. to 1961-1990 averages)	Y/E (0-300)	Y/E	Y/E	---	Yearly 89°S-89°N	Ishii et al. (2017)
9	NCEI/NOAA	1970-2016	Y/E	Y/E	Y/E	---	Yearly 89°S-89°N	Antonov et al. (2005)
10	SIO	2005-2016	---	---	Y	---	Monthly	Roemmich and Gilson (2009)
11	SIO (Deep/abyssal)	1990-2010 (as of 01/2018)	---	---	---	Y/E	Linear trend 89°S-89°N, as an aggregation of 32	Purkey and Johnson (2010)

							deep ocean basins	
--	--	--	--	--	--	--	-------------------------	--

421 *Table 2: Compilation of available in situ datasets from different originators and/or*
 422 *contributors. The table indicates the time span covered by the data, the depth of intergration,*
 423 *as well as the temporal resolution and latitude coverage.*

424

425

426 **2.3.2 Individual estimates**

427

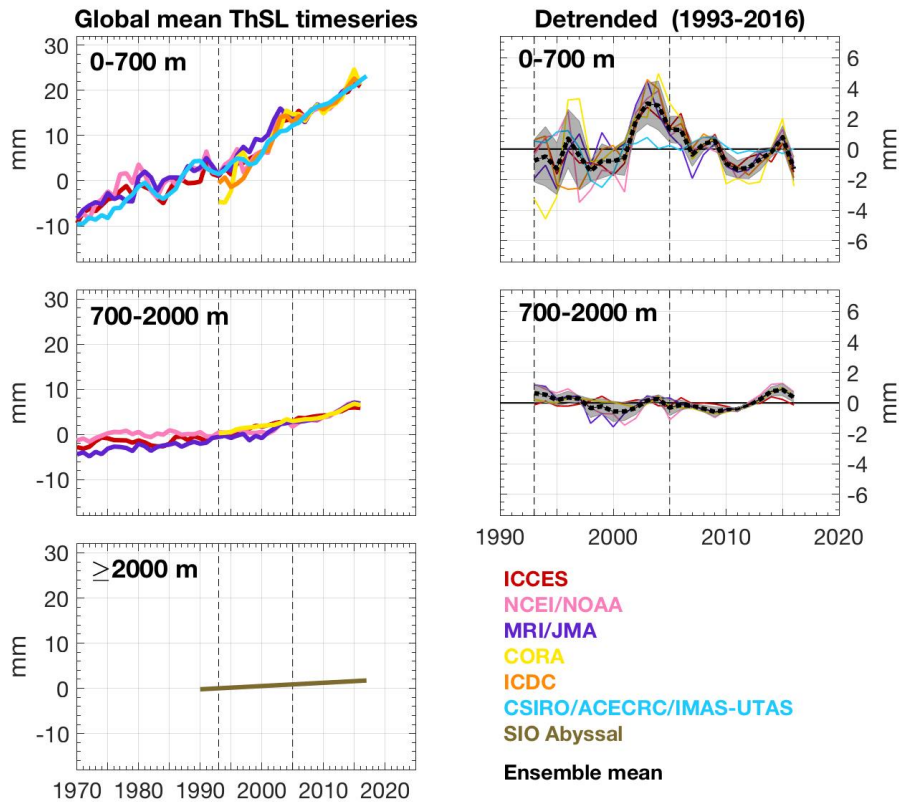
428 All in situ estimates compiled in this study show a steady rise in global mean thermosteric sea
 429 level, independent of depth-integration and decadal/multidecadal periods (Figure 4 and 5, left
 430 panels). As the deep/abyssal ocean estimate only illustrates the updated version of the linear
 431 trend from Purkey and Johnson (2010) for 1990-2010 extrapolated to 2016, it does not have
 432 any variability superimposed.

433 Interannual to decadal variability during the Altimeter era (since 1993) is similar for both 0-
 434 700 m and 700-2000 m, with larger amplitude in the upper ocean (Figure 4 and 5, right panels).
 435 For the 0-700 m, there is an apparent change in amplitude before/after the Argo era (since 2005),
 436 mostly due to a maximum (2-4 mm) around 2001-2004, except for one estimate. Higher
 437 amplitude and larger spread in variability between estimates before the Argo era is a symptom
 438 of the much sparser in situ coverage of the global ocean. Interannual variability over the Argo
 439 era (Figures 4 and 5, right panels) is mainly modulated by El Niño Southern Oscillation (ENSO)
 440 phases in the upper 500 m ocean, particularly for the Pacific, the largest ocean basin (Roemmich
 441 et al., 2011; Johnson and Birnbaum, 2017).

442 In terms of depth contribution, on average, the upper 300 m explains the same percentage
 443 (almost 70%) of the 0-700 m linear rate over both altimetry and Argo eras, but the contribution
 444 from the 0-700 m to 0-2000 m varies: about 75% for 1993-2016 and 65% for 2005-2016. Thus,
 445 the 700-2000 m contribution increases by 10% during the Argo decade, when the number of
 446 observations within 700-2000 m has significantly increased.

447

448

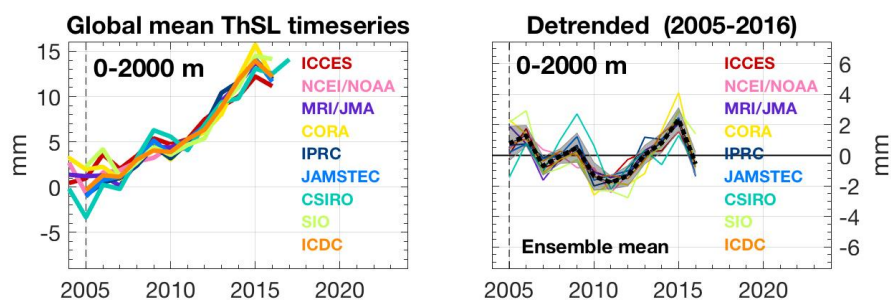


449

450 Figure 4. Left- panels. Annual mean global mean thermosteric anomaly timseries since 1970,
 451 from various research groups (colour) and for three depth-integrations: 0-700 m (top), 700-
 452 2000 m (middle), and below 2000 m (bottom). Vertical dashed lines are plotted along 1993 and
 453 2005. For comparison, all timeseries were offset arbitrarily. Right panels. Respective linearly
 454 detrended timeseries for 1993-2016. Black bold dashed line is the ensemble mean and gray
 455 shadow bar the ensemble spread (1-standard deviation). Units are mm.

456

457



458

459 Figure 5. Left- panel. Annual mean global mean thermosteric anomaly timseries since 2004,
 460 from various research groups (colour) in the upper 2000 m. A vertical dashed line is plotted
 461 along 2005. For comparison, all timeseries were offset arbitrarily. Right panel. Respective
 462 linearly detrended timeseries for 2005-2016. Black bold dashed line is the ensemble mean and
 463 gray shadow bar the ensemble spread (1-standard deviation). Units are mm.

464

465

466 *2.3.3. Ensemble mean thermosteric sea level*

467 Given that the global mean thermosteric sea level anomaly estimates compiled for this study
468 are not necessarily referenced to the same baseline climatology, they cannot be directly
469 averaged together to create an ensemble mean. To circumvent this limitation, we created an
470 ensemble mean in three steps, as explained below.

471 Firstly, we detrended the individual timeseries by removing a linear trend for 1993-2016 and
472 averaged together to obtain an “ensemble mean variability timeseries”. Secondly, we averaged
473 together the corresponding linear trends of the individual estimates to obtain an “ensemble
474 mean linear rate”. Thirdly, we combined this “ensemble mean linear rate” with the “ensemble
475 mean variability timeseries” to obtain the final ensemble mean timeseries. We applied the same
476 steps for the Argo era (2005-2016).

477 To maximise the number of individual estimates used in the final full-depth ensemble mean
478 timeseries, the three steps above were actually divided into depth-integrations and then
479 summed. For the Argo era, we summed 0-2000 m (9 estimates) and ≥ 2000 m (1 estimate). For
480 the altimetry era, we summed 0-700 m (6 estimates), 700-2000 (4 estimates) and ≥ 2000 m (1
481 estimate), although there is no statistical difference if the calculation was only based on the sum
482 of 0-2000 m (4 estimates) and ≥ 2000 m (1 estimate). There is also no statistical difference
483 between the full-depth ensemble mean timeseries created for the Altimeter and Argo eras during
484 their overlapping years (since 2005).

485 Figure 6 shows the full-depth ensemble mean timeseries over 1993-2016 and 2005-2016. It
486 reveals a global mean thermosteric sea level rise of about 30 mm over 1993-2016 (24 years) or
487 about 18 mm over 2005-2016 (12 years) , with a record high in 2015. These thermosteric
488 changes are equivalent to a linear rate of 1.32 ± 0.4 mm/yr and 1.31 ± 0.4 mm/yr
489 respectively.

490

491

492

493

494

495

496

497

498

499

500

501

502

**Global mean ThSL timeseries
Ensemble mean**

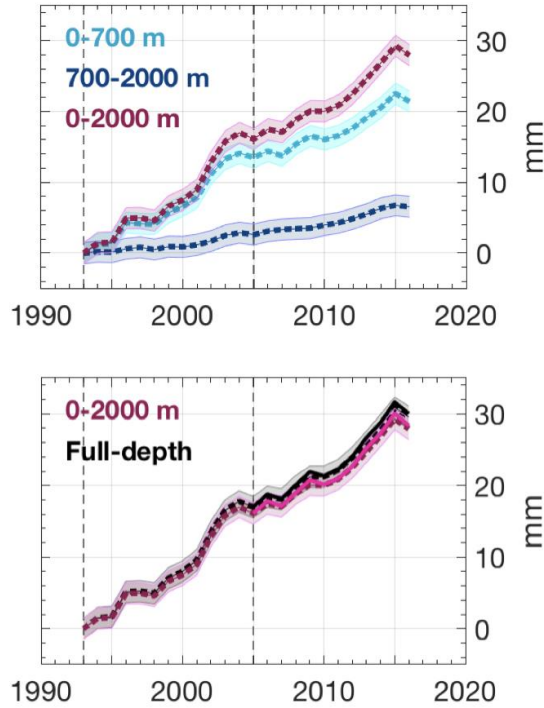
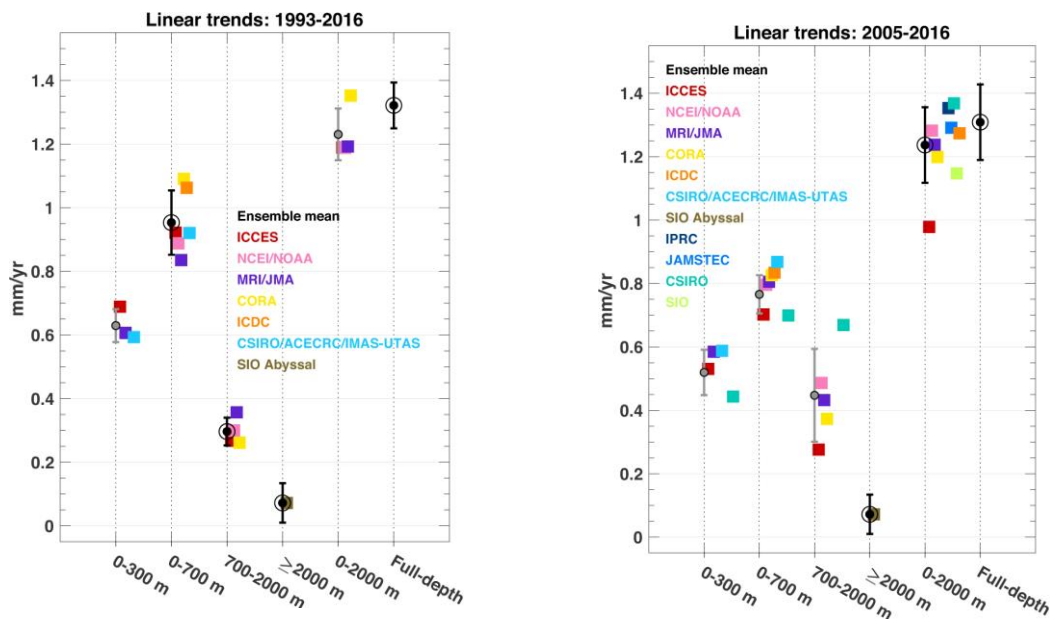


Figure 6: Ensemble mean timeseries for global mean thermosteric anomaly, for three-depth integrations (top) and for 0-2000 m and Full-depth (bottom). In the bottom panel, dashed lines are for the 1993-2016 period whereas solid lines are for 2005-2016. Error bars represent the ensemble spread (standard deviation). Units are mm.

Figure 7 shows thermosteric sea level trends for each of the data sets used over the 1993-2016 (left panel) and 2005-2016 (right panel) time spans and different depth ranges (including full depth), as well as associated ensemble mean trends. The full depth ensemble mean trend amounts to 1.3 +/- 0.4 mm/yr over 2005-2016. It is similar to the 1993-2016 ensemble mean trend, suggesting negligible acceleration of the thermosteric component over the altimetry era.



548 *Figure 7: Linear rates of global mean thermosteric sea level for depth-integrations (x-axis), for*
 549 *individual estimates and ensemble means, over 1993-2016 (left) and 2005-2016 (right). Ensemble*
 550 *mean rates with a black circle were used in the estimation of the timeseries described in Section 2.3.4.*
 551 *Errorbars are standard deviation due to spread of the estimates except for ≥ 2000 m. Units are mm/yr.*

552
553

554 **2.4 Glaciers**

555 Glaciers have strongly contributed to sea-level rise during the 20th century – around 40% - and
 556 will continue to be an important part of the projected sea-level change during the 21st century –
 557 around 30% (Kaser et al., 2006, Church et al., 2013, Gardner et al., 2013, Marzeion et al., 2014,
 558 Zemp et al., 2015; Huss and Hock, 2015). Because glaciers are time-integrated dynamic
 559 systems, a response lag of at least 10 years to a few hundred years is observed between changes
 560 in climate forcing and glacier shape, mainly depending on glacier length and slope
 561 (Johannesson et al., 1989, Bahr et al., 1998). Today, glaciers are globally (a notable exception
 562 is the Karakoram/Kunlun Shan region, e.g. Brun et al., 2017) in a strong disequilibrium with
 563 the current climate and are losing mass, due essentially to the global warming in the second
 564 half of the 20th century (Marzeion et al., 2018).

565 Global glacier mass changes are derived from in situ measurements of glacier mass changes or
 566 glacier length changes. Remote sensing methods measure elevation changes over entire glaciers
 567 based on differencing digital elevation models (DEMs) from satellite imagery between two
 568 epochs (or at points from repeat altimetry), surface flow velocities for determination of mass
 569 fluxes, and glacier mass changes from space-based gravimetry. Mass balance modeling driven
 570 by climate observations is also used (Marzeion et al., 2017 provide a review of these different
 571 methods).

572 Glacier contribution to sea level is primarily the result of their surface mass balance and
 573 dynamic adjustment, plus iceberg discharge and frontal ablation (below sea level) in the case
 574 of marine-terminating glaciers. The sum of worldwide glacier mass balances (MBs) does not
 575 correspond to the total glacier contribution to sea-level change for the following reasons:

576 - Glacier ice below sea level does not contribute to sea-level change, apart from a small
 577 lowering when replacing ice with seawater of a higher density. Total volume of glacier ice
 578 below sea level is estimated to be 10 – 60 mm sea-level equivalent (SLE, Huss and Farinotti,
 579 2012, Haeberli and Linsbauer, 2013, Huss and Hock, 2015).

580 - Incomplete transfer of melting ice from glaciers to the ocean: meltwater stored in lakes
 581 or wetlands, meltwater intercepted by natural processes and human activities (e.g. drainage to

582 lakes and aquifers in endorheic basins, impoundment in reservoirs, agriculture use of
583 freshwater, Loriaux and Casassa, 2013, Käab et al., 2015).

584 Despite considerable progress in observing methods and spatial coverage (Marzeion et al.,
585 2017), estimating glacier contribution to sea-level change remains challenging due to the
586 following reasons:

587 - Number of regularly observed glaciers (in the field) remains very low (0.25% of the
588 200 000 glaciers of the world have at least one observation and only 37 glaciers have multi
589 decade-long observations, Zemp et al. 2015).

590 - Uncertainty of the total glacier ice mass remains high (Figure 8, Grinsted et al., 2013,
591 Pfeffer et al., 2014, Farinotti et al., 2017, Frey et al. 2014).

592 - Uncertainties in glacier inventories and DEMs are not negligible. Sources of
593 uncertainties include debris-covered glaciers, disappearance of small glaciers, positional
594 uncertainties, wrongly mapped seasonal snow, rock glaciers, voids and artifacts in DEMs (Paul
595 et al., 2004, Bahr and Radić, 2012).

596 - Uncertainties of satellite retrieval algorithms from space-based gravimetry and
597 regional DEM differencing are still high, especially for global estimates (Gardner et al. 2013,
598 Marzeion et al., 2017, Chambers et al., 2017).

599 - Uncertainties of global glacier modeling (e.g. initial conditions, model assumptions
600 and simplifications, local climate conditions, Marzeion et al., 2012).

601 - Knowledge about some processes governing mass balance (e.g. wind redistribution
602 and metamorphism, sublimation, refreezing, basal melting) and dynamic processes (e.g. basal
603 hydrology, fracking, surging) remains limited (Farinotti et al., 2017).

604 An annual assessment of glacier contribution to sea-level change is difficult to perform from
605 ground-based or space-based observations except space-based gravimetry, due to the sparse and
606 irregular observation of glaciers, and the difficulty of assessing accurately the annual mass
607 balance variability. Global annual averages are highly uncertain because of the sparse coverage,
608 but successive annual balances are uncorrelated and therefore averages over several years are
609 known with greater confidence.

610

611 ***2.4.1 Glacier datasets***

612 The following datasets are considered, with a focus on the trends of annual mass changes:

613 1. Update of Gardner et al., 2013 (Reager et al., 2016), from satellite gravimetry and
614 altimetry, and glaciological records, called G16.

615 2. Update of Marzeion et al, 2012 (Marzeion et al., 2017), from global glacier modeling
616 and mass balance observations, called M17.

617 3. Update of Cogley (2009) (Marzeion et al., 2017), from geodetic and direct mass-
618 balance measurements, called C17.

619 4. Update of Leclercq et al., 2011 (Marzeion et al., 2017), from glacier length changes,
620 called L17.

621 5. Average of GRACE-based estimates of Marzeion et al. (2017), from spatial
622 gravimetry measurements, called M17-G.

623 In general it is not possible to align measurements of glacier mass balance with the calendar.
624 Most in-situ measurements are for glaciological years that extend between successive annual
625 minima of the glacier mass at the end of the summer melt season. Geodetic measurements have
626 start and end dates several years apart and are distributed irregularly through the calendar year;
627 some are corrected to align with annual mass minima but most are not. Consequently,
628 measurements discussed here for 1993-2016 (the altimetry era) and 2005-2016 (the GRACE
629 and Argo era) are offset by up to a few months from the nominal calendar years.

630 Peripheral glaciers around the Greenland and Antarctic ice sheets are not treated in detail in this
631 section (see sections 2.5 and 2.6 for mass-change estimates that combine the peripheral glaciers
632 with the Greenland Ice Sheet and Antarctic Ice Sheet respectively). This is primarily because
633 of the lack of observations (especially ground-based measurements) and also because of the
634 high spatial variability of mass balance in those regions, and the slightly different climate (e.g.
635 precipitation regime) and processes (e.g. refreezing). In the past, these regions have often been
636 neglected. However, Radić and Hock (2010) estimated the total ice mass of peripheral glaciers
637 around Greenland and Antarctica as 191 ± 70 mm SLE, with an actual contribution to sea-
638 level rise of around 0.23 ± 0.04 mm/yr (Radić and Hock, 2011). Gardner et al. (2013) found
639 a contribution from Greenland and Antarctic peripheral glaciers equal to 0.12 ± 0.05 mm/yr.
640 Note that some new or updated datasets for peripheral glaciers surrounding polar ice sheets are
641 under development and would hopefully be available in coming years in order to incorporate
642 Greenland and Antarctic peripheral glaciers in the estimates of global glacier mass changes.

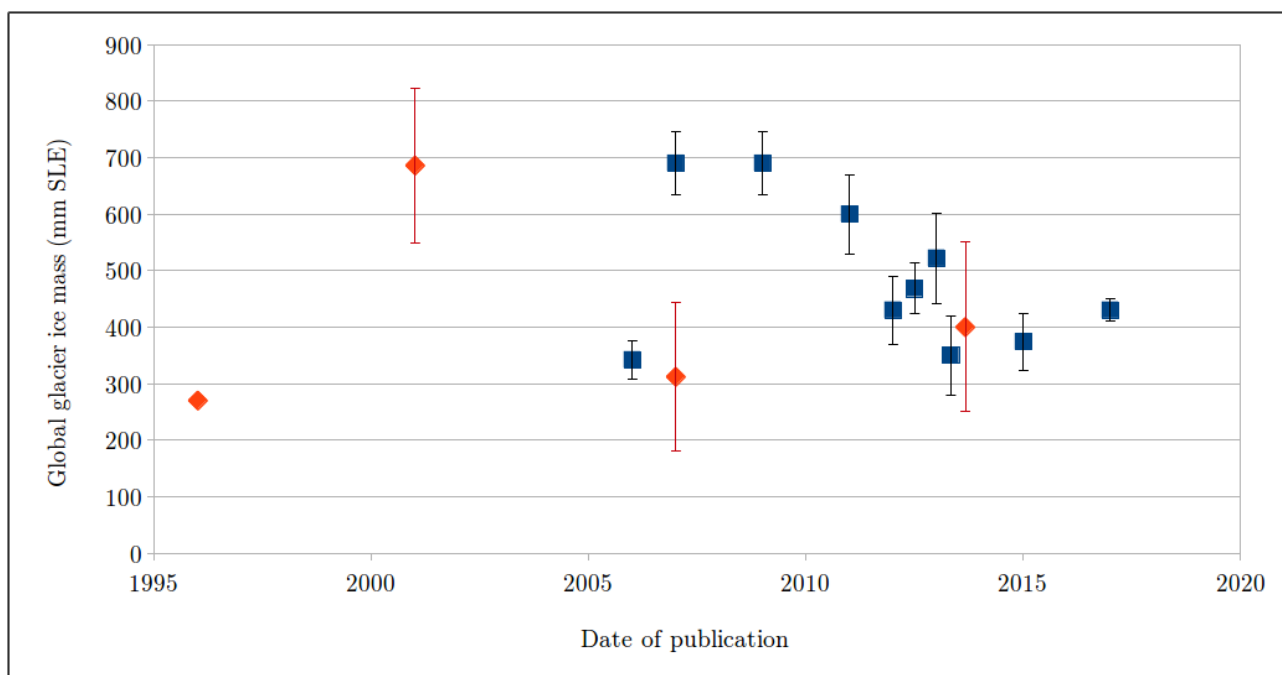
643

644 **2.4.2 Methods**

645 No globally complete observational dataset exists for glacier mass changes (except GRACE
646 estimates, see below). Any calculation of the global glacier contribution to sea-level change has
647 to rely on spatial interpolation or extrapolation or both, or to consider limited knowledge of
648 responses to climate change (due to the heterogeneous spatial distribution of glaciers around

649 the world). Consequently, most observational methods to derive glacier sea-level contribution
650 must extend local observations (in situ or satellite) to a larger region. Thanks to the recent global
651 glacier outline inventory (Randolph Glacier Inventory – RGI – first release in 2012) as well as
652 global climate observations, glacier modeling can now also be used to estimate the contribution
653 of glaciers to sea level (Marzeion et al., 2012, Huss and Hock, 2015, Maussion et al., 2018,
654 subm.). Still, those global modeling methods need to globalize local observations and glacier
655 processes which require fundamental assumptions and simplifications. Only GRACE-based
656 gravimetric estimates are global but they suffer from large uncertainties in retrieval algorithms
657 (signal leakage from hydrology, GIA correction) and coarse spatial resolution, not resolving
658 smaller glacierized mountain ranges or those peripheral to the Greenland ice sheet.

659 DEM differencing method is not yet global, but regional, and can hopefully in the near future
660 be applied globally. This method needs also to convert elevation changes to mass changes
661 (using assumptions on snow and ice densities). In contrast, very detailed glacier surface mass
662 balance and glacier dynamic models are today far from being applicable globally, mainly due
663 to the lack of crucial observations (e.g., meteorological data, glacier surface velocity and
664 thickness) and of computational power for the more demanding theoretical models. However,
665 somewhat simplified approaches are currently developed to make best use of the steadily
666 increasing datasets. Modeling-based estimates suffer also from the large spread in estimates of
667 the actual global glacier ice mass (Figure 8). The mean value is 469 +/- 146 mm SLE, with
668 recent studies converging towards a range of values between 400 and 500 mm SLE global
669 glacier ice mass. But as mentioned above, a part of this ice mass will not contribute to sea level.
670



671 *Fig 8. Evolution of global glacier ice mass estimates from different studies published over the*
 672 *past two decades, based on different observations and methods. The red marks correspond to*
 673 *IPCC reports. We clearly see the most recent publications lead to less scattered results. Note*
 674 *that Antarctica and Greenland peripheral glaciers are taken into account in this figure.*

675

676 2.4.3 Results (trends)

677 Table 3 presents most recent estimates of trends in global glacier mass balances.

678

	1993 – 2016 mm/yr SLE	2005 – 2016 mm/yr SLE
G16		0.70 +- 0.070 ^a
M17	0.68 +- 0.032	0.80 +- 0.048
C17	0.63 +- 0.070	0.75 +- 0.070 ^b
L17		0.84 +- 0.640 ^c
M17-G		0.61 +- 0.070 ^d

679

680 *Table 3: All data are in mm/yr SLE. ^a The time period of G16 is 2002 – 2014. ^b The time period*
 681 *of C17 is 2003 – 2009. ^c The time period of L17 is 2003 – 2009. ^d The time period of M17-G is*
 682 *2002/2005 – 2013/2015 because this value is an average of different estimates.*

683

684 The ensemble mean contribution of glaciers to sea-level rise for the time period 1993 – 2016 is
685 0.65 +/- 0.051 mm/yr SLE and 0.74 +/- 0.18 mm/yr for the time period 2005 – 2016
686 (uncertainties are averaged). Different studies refer to different time periods. However, because
687 of the probable low variability of global annual glacier changes, compared to other components
688 of the sea-level budget, averaging trends for slightly different time periods is appropriate.

689 The main source of uncertainty is that the vast majority of glaciers are unmeasured, which
690 makes interpolation or extrapolation necessary, whether for in situ or satellite measurements,
691 and for glacier modeling. Other main contributions to uncertainty in the ensemble mean stem
692 from methodological differences, such as the downscaling of atmospheric forcing required for
693 glacier modeling, the separation of glacier mass change to other mass change in the spatial
694 gravimetry signal and the derivation of observational estimates of mass change from different
695 raw measurements (e.g. length and volume changes, mass balance measurements and geodetic
696 methods) all with their specific uncertainties.

697

698 **2.5 Greenland**

699 Ice sheets are the largest potential source of future sea level rise (SLR) and represent the largest
700 uncertainty in projections of future sea level. Almost all land ice (~99.5%) is locked in the ice
701 sheets, with a volume in sea level equivalent/SLE terms of 7.4 m for Greenland, and 58.3 m for
702 Antarctica. It has been estimated that approximately 25% to 30% of the total land ice
703 contribution to sea level rise over the last decade came from the Greenland ice sheet (e.g.
704 Dieng et al., 2017, Box and Colgan, 2017).

705 There are three main methods that can be used to estimate the mass balance of the Greenland
706 ice sheet: (1) measurement of changes in elevation of the ice surface over time (dh/dt) either
707 from imagery or altimetry; (2) the mass budget or Input-Output Method (IOM) which involves
708 estimating the difference between the surface mass balance and ice discharge; and (3)
709 consideration of the redistribution of mass via gravity anomaly measurements which only
710 became viable with the launch of GRACE in 2002. Uncertainties due to the GIA correction are
711 small in Greenland compared to Antarctica: on the order of ± 20 Gt/yr mass equivalent (Khan
712 et al., 2016). Prior to 2003, mass trends are reliant on IOM and altimetry. Both techniques have
713 limited sampling in time and/or space for parts of the satellite era (1992-2002) and errors for
714 this earlier period are, therefore, higher (van den Broeke et al., 2016, Hurkmans et al., 2014).

715 The consistency between the three methods mentioned above was demonstrated for Greenland
716 by Sasgen et al. (2012) for the period 2003-2009. Ice sheet wide estimates showed excellent

717 agreement although there was less consistency at a basin scale. We have, therefore, high
 718 confidence and relatively low uncertainties in the mass rates for the Greenland ice sheet in the
 719 satellite era (see also Bamber et al., 2018).

720

721 **2.5.1 Datasets considered for the assessment**

722 This assessment of sea level budget contribution from the Greenland ice sheet considers the
 723 following datasets:

Reference	Time period	Method
Update from Barletta et al. (2013)	2003-2016	GRACE
Groh and Horwath (2016)	2003-2015	GRACE
Update from Luthcke et al. (2013)	2003-2015	GRACE
Update from Sasgen et al. (2012)	2003-2016	GRACE
Update from Schrama et al. (2014)	2003-2016	GRACE
Update from (van den Broeke et al., 2016)	1993-2016	Input/output Method (IOM)
Wiese et al. (2016)	2003-2016	GRACE
Update from Wouters et al. (2008)	2003-2016	GRACE

724 *Table 4. Datasets considered in the Greenland mass balance assessment, as well as covered*
 725 *time span and type of observations.*

726

727 **2.5.2. Methods and analyses**

728 All but one of these datasets are based on GRACE data and therefore provide annual time series
 729 from ~2002 onwards. The one exception uses IOM (van den Broeke et al., 2016) to give an
 730 annual mass time series for a longer time period (1993 onwards).

731 Notwithstanding this, each group has chosen their own approach to estimate mass balance from
 732 GRACE observations. As the aim of this Global Sea Level Budget assessment is to compile
 733 existing results (rather than undertake new analyses), we have not imposed a specific
 734 methodology. Instead, we asked for the contributed datasets to reflect each group's 'best
 735 estimate' of annual trends for Greenland using the method(s) they have published.

736 Greenland contains glaciers and ice caps around the margins of the main ice sheet, often referred
 737 to as peripheral GIC (PGIC), which are a significant proportion of the total mass imbalance
 738 (circa 15-20%) (Bolch et al., 2013). Some studies consider the mass balance of the ice sheets

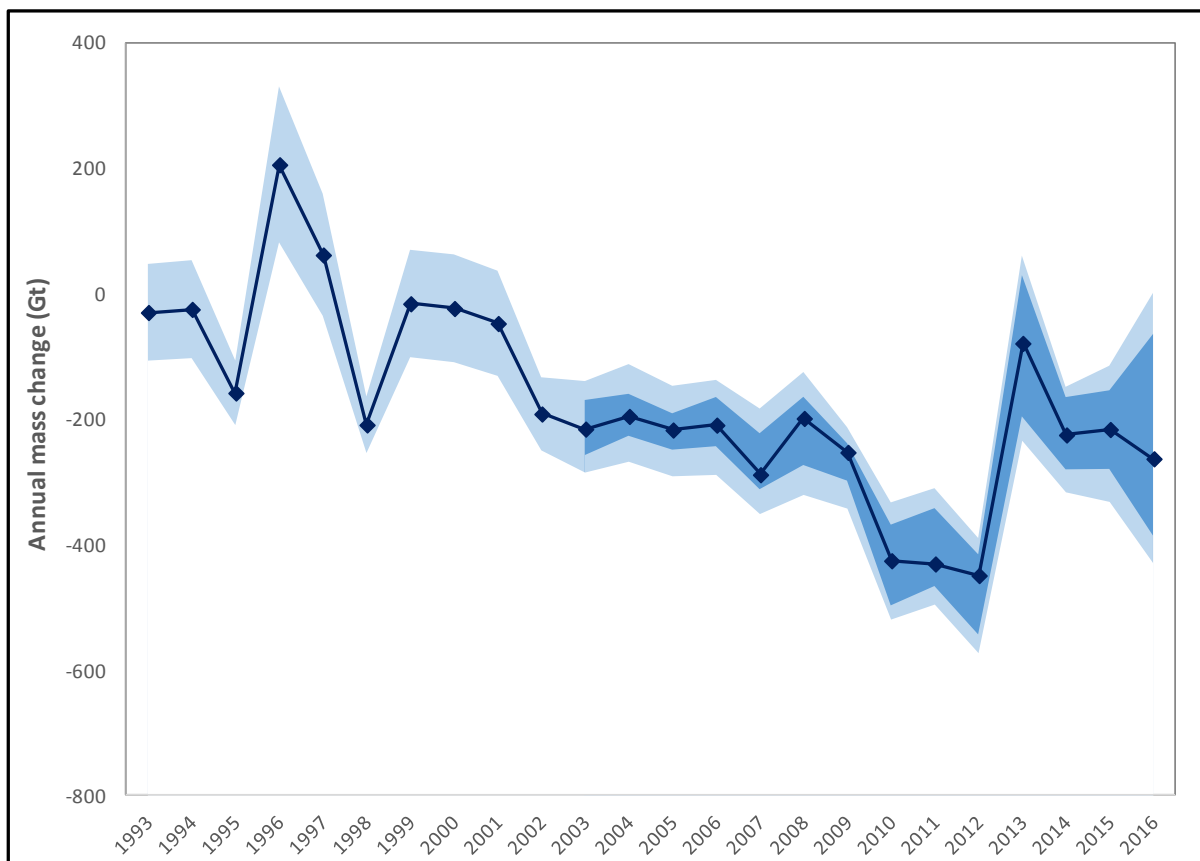
739 and the PGIC separately but there has been, in general, no consistency in the treatment of PGIC
 740 and many studies do not specify if they are included or excluded from the total. The GRACE
 741 satellites have an approximate spatial resolution of 300 km and the large number of studies that
 742 use GRACE, by default, include all land ice within the domain of interest. For this reason, the
 743 results below for Greenland mass trends all include PGIC.

744 From these datasets, for each year from 1993 to 2015 (and 2016 where available), we have
 745 calculated an average change in mass (calculated as the weighted mean based on the stated error
 746 value for each year) and an error term. Prior to 2003, the results are based on just one dataset
 747 (van den Broeke et al., 2016).

748

749 **2.5.3 Results**

750



751

752 *Figure 9. Greenland annual mass change from 1993 to 2016. The medium blue region shows*
 753 *the range of estimates from the datasets listed in Table 1. The lighter blue region shows the*
 754 *range of estimates when stated errors are included, to provide upper and lower bounds. The*
 755 *dark blue line shows the mean mass trend.*

756

757

758

759

Year	Δ mass (Gt/yr)	Error (Gt/yr)	σ (Gt)
1993	-30	76	
1994	-25	77	
1995	-159	51	
1996	205	123	
1997	61	97	
1998	-209	45	
1999	-16	85	
2000	-24	85	
2001	-48	83	
2002	-192	58	
2003	-216	13	28
2004	-196	12	24
2005	-218	13	21
2006	-210	12	29
2007	-289	10	31
2008	-199	11	39
2009	-253	11	21
2010	-426	9	42
2011	-431	9	47
2012	-450	10	41
2013	-80	13	76
2014	-225	13	38
2015	-217	13	48
2016	-263	23	123
Average estimate 1993-2015	-167	54	
Average estimate 1993-2016	-171	53	
Average estimate 2005-2015	-272	11	
Average estimate 2005-2016	-272	13	

760

761 *Table 5. Annual time series of Greenland mass change (GT/yr, negative values mean*
 762 *decreasing mass). Δ mass is calculated as the weighted mean based on the stated error value*
 763 *for each year. The error for each year is calculated as the mean of all stated 1-sigma errors*
 764 *divided by \sqrt{N} where N is the number of datasets available for that year, assuming that the*
 765 *errors are uncorrelated. The standard deviation (σ) is also given to illustrate the level of*
 766 *agreement between datasets for each year when multiple datasets are available (2003*
 767 *onwards).*

768

769 There is generally a good level of agreement between the datasets (Figure 9), and taken together
 770 they provide an average estimate of 171 Gt/yr of ice mass loss (or sea level budget contribution)
 771 from Greenland for the period 1993 to 2016, increasing to 272 Gt/yr for the period 2005 to 2016
 772 (Table 5).

773 All the datasets illustrate the previously documented accelerating mass loss up to 2012 (Rignot
 774 et al., 2011, Velicogna, 2009) . In 2012, the ice sheet experienced exceptional surface melting
 775 reaching as far as the summit (Nghiem et al., 2012) and a record mass loss since, at least 1958,
 776 of over 400 Gt (van den Broeke et al., 2016) . The following years, however, show a reduced
 777 loss (not more than 270 Gt in any year). Inclusion of the years since 2012 in the 2005-2016
 778 trend estimate reduces the overall rate of mass loss acceleration and its statistical significance.
 779 There is greater divergence in the GRACE time series for 2016. We associate this with the
 780 degradation of the satellites as they came towards the end of their mission. For 2005-2012, it
 781 might be inferred that there is a secular trend towards greater mass loss and from 2010-2012
 782 the value is relatively constant. Inter-annual variability in mass balance of the ice sheet is driven,
 783 primarily, by the surface mass balance (i.e. atmospheric weather) and it is apparent that the
 784 magnitude of this year to year variability can be large: exceeding 360 Gt (or 1 mm sea level
 785 equivalent) between 2012 and 2013. Caution is required, therefore, in extrapolating trends from
 786 a short record such as this.

787

788 **2.6 Antarctica**

789 The annual turn over of mass of Antarctica is about 2,200 Gt/yr (over 6 mm/yr of SLE), 5 times
 790 larger than in Greenland (Wessem et al. 2017). In contrast to Greenland, ice and snow melt
 791 have a negligible influence on Antarctica's mass balance which is therefore completely
 792 controlled by the balance between snowfall accumulation in the drainage basins and ice
 793 discharge along the periphery. The continent is also 7 times larger than Greenland, which makes

794 satellite techniques absolutely essential to survey the continent. Interannual variations in
795 accumulation are large in Antarctica, showing decadal to multi-decadal variability, so that many
796 years of data are required to extract trends, and missions limited to only a few years may
797 produce misleading results (e.g. Rignot et al., 2011).

798 As in Greenland, the estimation of the mass balance has employed a variety of techniques,
799 including 1) the gravity method with GRACE since April 2002 until the end of the mission in
800 late 2016; 2) the IOM method using a series of Landsat and Synthetic-Aperture Radar (SAR)
801 satellites for measuring ice motion along the periphery (Rignot et al., 2011), ice thickness from
802 airborne depth radar sounders such as Operation IceBridge (Leuschen et al., 2014), and
803 reconstructions of surface mass balance using regional atmospheric climate models constrained
804 by re-analysis data (RACMO, MAR and others); and 3) radar/laser altimetry method which mix
805 various satellite altimeters and correct ice elevation changes with density changes from firm
806 models. The largest uncertainty in the GRACE estimate in Antarctica is the GIA which is larger
807 than in Greenland and a large fraction of the observed signal. The IOM method compares two
808 large numbers with large uncertainties to estimate the mass balance as the difference. In order
809 to detect an imbalance at the 10% level, surface mass balance and ice discharge need to be
810 estimated with a precision typically of 5 to 7%. The altimetry method is limited to areas of
811 shallow slope, hence is difficult to use in the Antarctic Peninsula and in the deep interior of the
812 Antarctic continent due to unknown variations of the penetration depth of the signal in
813 snow/firn. The only method that expresses the partitioning of the mass balance between surface
814 processes and dynamic processes is the IOM method (e.g. Rignot et al., 2011). The gravity
815 method is an integrand method which does not suffer from the limitations of SMB models but
816 is limited in spatial resolution (e.g. Velicogna et al., 2014). The altimetry method provides
817 independent evidence of changes in ice dynamics, e.g. by revealing rapid ice thinning along the
818 ice streams and glaciers revealed by ice motion maps, as opposed to large scale variations
819 reflecting a variability in surface mass balance (McMillan et al., 2014).

820 All these techniques have improved in quality over time and have accumulated a decade to
821 several decades of observations, so that we are now able to assess the mass balance of the
822 Antarctic continent using methods with reasonably low uncertainties, and multiple lines of
823 evidence as the methods are largely independent, which increases confidence in the results (see
824 recent publication by the IMBIE Team, 2018). There is broad agreement in the mass loss from
825 the Antarctic Peninsula and West Antarctica; most residual uncertainties are associated with
826 East Antarctica as the signal is relatively small compared to the uncertainties, although most
827 estimates tend to indicate a low contribution to sea level (e.g. Shepherd et al., 2012).

828

829 **2.6.1 Datasets considered for the assessment**

830 This assessment considers the following datasets:

831

Reference	Method	2005-2015 SLE Trend (mm/yr)	1993-2015 SLE Trend (mm/yr)
Update from Martín-Español et al. (2016)	Joint inversion GRACE/altimetry /GPS	0.43±0.07	-
Update from Forsberg et al. (2017)	Joint inversion GRACE/CryoSat	0.31±0.02	-
Update from Groh and Horwath (2016)	GRACE	0.32±0.11	-
Update from Luthcke et al. (2013)	GRACE	0.36±0.06	-
Update from Sasgen et al. (2013)	GRACE	0.47±0.07	-
Update from Velicogna et al. (2014)	GRACE	0.33±0.08	-
Update from Wiese et al. (2016)	GRACE	0.39±0.02	-
Update from Wouters et al. (2013)	GRACE	0.41±0.05	-
Update from Rignot et al. 2011	Input/Output method (IOM)	0.46±0.05	0.25±0.1
Update from Schrama et al. (2014); version 1	GRACE ICE6G GIA model	0.47±0.03	
Update from Schrama et al. (2014); version 2	GRACE Updated GIA models	0.33±0.03	

832 *Table 6. Datasets considered in this assessment of the Antarctica mass change, and associated*
833 *trends for the 2005-2015 and 1993-2015 expressed in mm/yr SLE. Positive values mean positive*
834 *contribution to sea level (i.e. sea level rise)*

835

836

837 In Table 6, the negative trend estimate by Zwally et al. (2016) is not added. It is worth noting

838 that including it would only slightly reduce the ensemble mean trend.

839

840
841
842
843
844
845
846
847
848
849
850
851
852
853
854
855
856
857
858
859
860
861
862
863
864
865
866
867
868
869
870
871
872
873

2.6.2 Methods and analyses

The datasets used in this assessment are Antarctica mass balance time series generated using different approaches. Two estimates are a joint inversion of GRACE/altimetry/GPS data (Martín-Español et al., 2016), and GRACE and CryoSat data (Forsberg et al., 2017). Two methods are mascon solutions obtained from the GRACE intersatellite range-rate measurements over equal-area spherical caps covering the Earth's surface (Luthcke et al., 2013; Wiese et al., 2016), three estimates use the GRACE spherical harmonics solutions (Velicogna et al., 2014; Wiese et al., 2016; Wouters et al., 2013) and one gridded GRACE products (Sasgen et al., 2013).

All GRACE time series were provided as monthly time series except for the one using the Martín-Español et al. (2016) method that were provided as annual estimates. In addition, different groups use different GIA corrections, therefore the spread of the trend solutions represents also the error associated to the GIA correction which, in Antarctica, is the largest source of uncertainty. Sasgen et al. (2013) used their own GIA solution (Sasgen et al., 2017), Martín-Español et al. (2016) as well, Luthcke et al., (2013), Velicogna et al. (2014) and Groh and Horwath (2016) used IJ05-R2 (Ivins et al., 2013), Wouter et al. (2013) used Whitehouse et al. (2012), and Wise et al. (2016) used A et al. (2013). In addition, Groh and Horwath (2016) did not include the peripheral glaciers and ice caps, while all other estimates do.

Table 6 shows the Antarctic contribution to sea level during 2005-2015 from the different GRACE solutions, and for the input and output method (IOM). There is a single IOM-based dataset that provides trends for the period 1993-2015 (update of Rignot et al., 2011). For the period 2005-2015, we calculated the annual sea level contribution from Antarctica using GRACE and IOM estimates (Table 7).

As we are interested in evaluating the long-term trend and inter-annual variability of the Antarctic contribution to sea level, for each GRACE datasets available in monthly time series, we first removed the annual and sub-annual components of the signal by applying a 13-month averaging filter and we then used the smoothed time series to calculate to annual mass change. Figure 10 shows the annual sea level contribution from Antarctica calculated from the GRACE-derived estimates and for the Input-Output method. The GRACE mean annual estimates are calculated as the mean of the annual contributions from the different groups, and the associated error calculated as the sum of the spread of the annual estimates and the mean annual error.

874 **2.6.3 Results**

875

876

877

878

879

880

881

882

883

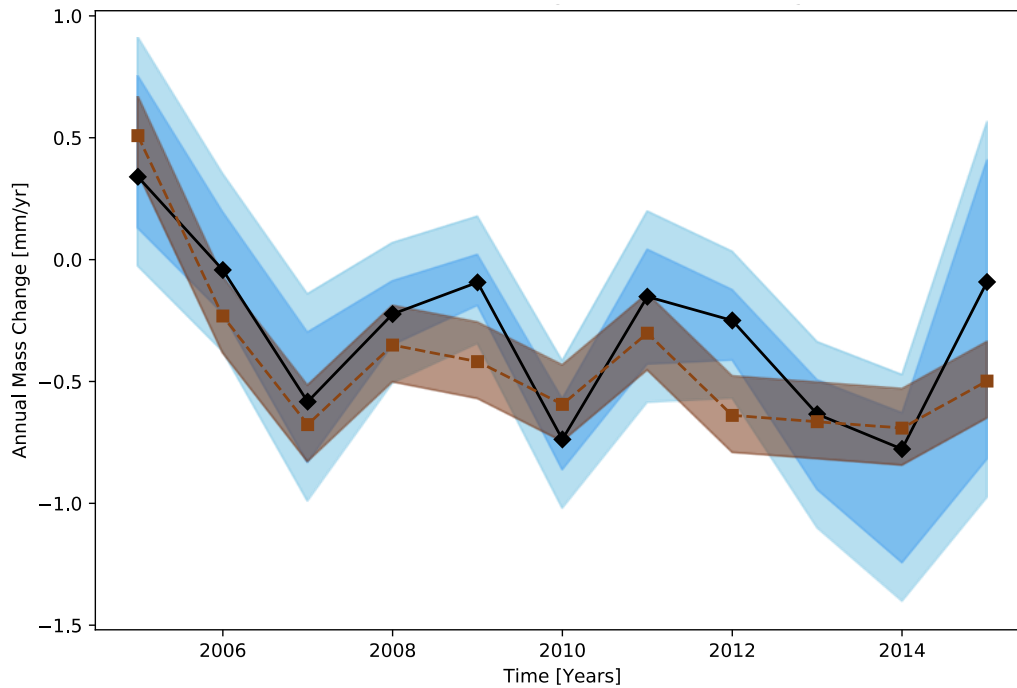
884

885

886

887

888



889 *Figure 10. Antarctic annual sea level contribution during 2005 to 2015. The black squares are*
 890 *the mean annual sea level calculated using the GRACE datasets listed in Table 6. The darker*
 891 *blue band shows the range of estimates from the datasets. The light blue band account for the*
 892 *error in the different GRACE estimates. The brown squares are the annual sea level*
 893 *contribution calculated using the Input-Output method (updated from Rignot et al., 2011), the*
 894 *light brown band is the associated error.*

895

896

Year	GRACE mm/yr SLE	IOM mm/yr SLE	Mean mm/yr SLE
2005	-0.34±0.47	-0.51±0.16	-0.42±0.31
2006	0.04±0.36	0.23±0.16	0.14±0.26
2007	0.58±0.42	0.68±0.16	0.63±0.29
2008	0.22±0.29	0.35±0.16	0.29±0.22
2009	0.09±0.26	0.42±0.16	0.26±0.21
2010	0.74±0.30	0.59±0.16	0.67±0.23
2011	0.15±0.39	0.30±0.16	0.23±0.27

2012	0.25±0.30	0.64±0.16	0.44±0.23
2013	0.63±0.38	0.67±0.16	0.65±0.27
2014	0.78±0.46	0.69±0.16	0.73±0.31
2015	0.09±0.77	0.50±0.16	0.29±0.46
Average estimate 2005-2015	0.38±0.06	0.46±0.05	0.42±0.06

897 *Table 7. Annual sea level contribution from Antarctica during 2005-2015 from GRACE and*
898 *Input-Output method (IOM) calculated as described above and expressed in mm/yr SLE. Also*
899 *shown is the mean of the estimate from the two methods, associated errors are the mean of the*
900 *two estimated errors. Positive values mean positive contribution to sea level (i.e. sea level rise)*

901

902 There is generally broad agreement between the GRACE datasets (Figure 10), as most of the
903 differences between GRACE estimates are caused by differences in the GIA correction. We
904 find a reasonable agreement between GRACE and the IOM estimates although the IOM
905 estimates indicate higher losses. Taken together, these estimates yield an average of 0.42 mm/yr
906 sea level budget contribution from Antarctica for the period 2005 to 2015 (Table 7) and 0.25
907 mm/yr sea level for the time period 1993-2005, where the latter value is based on IOM only.

908 All the datasets illustrate the previously documented accelerating mass loss of Antarctica
909 (Rignot et al., 2011, Velicogna, 2009). In 2005-2010, the ice sheet experienced ice mass loss
910 driven by an increase in mass loss in the Amundsen Sea sector of West Antarctica (Mouginot
911 et al., 2014). The following years showed a reduced increase in mass loss, as colder ocean
912 conditions prevailed in the Amundsen Sea Embayment sector of West Antarctica in 2012-2013
913 which reduced the melting of the ice shelves in front of the glaciers (Dutrieux et al., 2014).
914 Divergence in the GRACE time series is observed after 2015 due to the degradation of the
915 satellites towards the end of the mission.

916 The large inter-annual variability in mass balance in 2005-2015, characteristic of Antarctica,
917 nearly masks out the trend in mass loss, which is more apparent in the longer time series than
918 in short time series. The longer record highlights the pronounced decadal variability in ice sheet
919 mass balance in Antarctica, demonstrating the need for multi-decadal time series in Antarctica,
920 which have been obtained only by IOM and altimetry. The inter-annual variability in mass
921 balance is driven almost entirely by surface mass balance processes. The mass loss of
922 Antarctica, about 200 Gt/yr in recent years, is only about 10% of its annual turn over of mass
923 (2,200 Gt/yr), in contrast with Greenland where the mass loss has been growing rapidly to
924 nearly 100% of the annual turn over of mass. This comparison illustrates the challenge of

925 detecting mass balance changes in Antarctica, but at the same time, that satellite techniques
926 and their interpretation have made tremendous progress over the last 10 years, producing
927 realistic and consistent estimates of the mass using a number of independent methods (Bamber
928 et al., 2018; the IMBIE Team, 2018).

929

930 **2.7 Terrestrial Water Storage**

931 Human transformations of the Earth's surface have impacted the terrestrial water balance,
932 including continental patterns of river flow and water exchange between land, atmosphere and
933 ocean, ultimately affecting global sea level. For instance, massive impoundment of water in
934 man-made reservoirs has reduced the direct outflow of water to the sea through rivers, while
935 groundwater abstractions, wetland and lake storage losses, deforestation and other land use
936 changes have caused changes to the terrestrial water balance, including changing
937 evapotranspiration over land, leading to net changes in land-ocean exchanges (Chao et al., 2008;
938 Wada et al., 2012a,b; Konikow 2011; Church et al., 2013; Doll et al., 2014a,b). Overall, the
939 combined effects of direct anthropogenic processes have reduced land water storage, increasing
940 the rate of sea level rise (SLR) by 0.3-0.5 mm yr⁻¹ during recent decades (Church et al., 2013;
941 Gregory et al., 2013; Wada et al., 2016). Additionally, recent work has shown that climate
942 driven changes in water stores can perturb the rate of sea level change over interannual to
943 decadal time scales, making global land mass budget closure sensitive to varying observational
944 periods (Cazenave et al., 2014; Dieng et al., 2015; Reager et al., 2016; Rietbroek et al., 2016).
945 Here we discuss each of the major component contributions from land, with a summary in Table
946 8, and estimate the net terrestrial water storage (TWS) contribution to sea level.

947

948 ***2.7.1 Direct anthropogenic changes in terrestrial water storage***

949

950 *Water impoundment behind dams*

951 Wada et al. (2016) built on work by Chao et al. (2008) to combine multiple global reservoir
952 storage data sets in pursuit of a quality-controlled global reservoir database. The result is a list
953 of 48064 reservoirs that have a combined total capacity of 7968 km³. The time history of growth
954 of the total global reservoir capacity reflects the history of the human activity in dam building.
955 Applying assumptions from Chao et al. (2008), Wada et al. (2016) estimated that humans have
956 impounded a total of 10,416 km³ of water behind dams, accounting for a cumulative 29 mm
957 drop in global mean sea level. From 1950 to 2000 when global dam-building activity was at its

958 highest, impoundment contributed to the average rate of sea level change at -0.51 mm/year.
959 This was an important process in comparison to other natural and anthropogenic sources of sea
960 level change over the past century, but has now largely slowed due to a global decrease in dam
961 building activity.

962

963 Global groundwater depletion

964 Groundwater currently represents the largest secular trend component to the land water storage
965 budget. The rate of groundwater depletion (GWD) and its contribution to sea level has been
966 subject to debate (Gregory et al., 2013; Taylor et al., 2013). In the IPCC AR4 (Solomon et al.,
967 2007), the contribution of non-frozen terrestrial waters (including GWD) to sea-level variation
968 was not considered due to its perceived uncertainty (Wada, 2016). Observations from GRACE
969 opened a path to monitor total water storage changes including groundwater in data scarce
970 regions (Strassberg et al., 2007; Rodell et al. 2009; Tiwari et al. 2009; Jacob et al., 2012;
971 Shamsudduha et al., 2012; Voss et al., 2013). Some studies have also applied global
972 hydrological models in combination with the GRACE data (see Wada et al., 2016 for a review).
973 Earlier estimates of GWD contribution to sea level range from 0.075 mm yr⁻¹ to 0.30 mm yr⁻¹
974 (Sahagian et al., 1994; Gornitz, 1995, 2001; Foster and Loucks, 2006). More recently, Wada et
975 al. (2012b), using hydrological modelling, estimated that the contribution of GWD to global
976 sea level increased from 0.035 (± 0.009) to 0.57 (± 0.09) mm yr⁻¹ during the 20th century and
977 projected that it would further increase to 0.82 (± 0.13) mm yr⁻¹ by 2050. Döll et al. (2014) used
978 hydrological modeling, well observations, and GRACE satellite gravity anomalies to estimate
979 a 2000–2009 global GWD of 113 km³ yr⁻¹ (0.314 mm yr⁻¹). This value represents the impact of
980 human groundwater withdrawals only and does not consider the effect of climate variability on
981 groundwater storage. A study by Konikow (2011) estimated global GWD to be 145 (± 39) km³
982 yr⁻¹ (0.41 ± 0.1 mm yr⁻¹) during 1991–2008 based on measurements of changes in groundwater
983 storage from in situ observations, calibrated groundwater modelling, GRACE satellite data and
984 extrapolation to unobserved aquifers.

985 An assumption of most existing global estimates of GWD impacts on sea level change is that
986 nearly 100% of the GWD ends up in the ocean. However, groundwater pumping can also
987 perturb regional climate due to land-atmosphere interactions (Lo and Famiglietti, 2013). A
988 recent study by Wada et al. (2016) used a coupled land-atmosphere model simulation to track
989 the fate of water pumped from underground and found it more likely that ~80% of the GWD
990 ends up in the ocean over the long-term, while 20% re-infiltrates and remains in land storage.
991 They estimated an updated contribution of GWD to global SLR ranging from 0.02 (± 0.004)

992 mm yr⁻¹ in 1900 to 0.27 (± 0.04) mm yr⁻¹ in 2000 (Figure 11). This indicates that previous studies
993 had likely overestimated the cumulative contribution of GWD to global SLR during the 20th
994 century and early 21st century by 5-10 mm.

995

996 Land cover and land-use change

997 Humans have altered a large part of the land surface, replacing 33% (Vitousek et al., 1997) or
998 even 41 % (Sterling et al., 2013) of natural vegetation by anthropogenic land cover such as crop
999 fields or pasture. Such land cover change can affect terrestrial hydrology by changing the
1000 infiltration-to-runoff ratio, and can impact subsurface water dynamics by modifying recharge
1001 and increasing groundwater storage (Scanlon et al., 2007). The combined effects of
1002 anthropogenic land cover changes on land water storage can be quite complex. Using a
1003 combined hydrological and water resource model, Bosmans et al. (2017) estimated that land
1004 cover change between 1850 and 2000 has contributed to a discharge increase of 1058 km³ yr⁻¹,
1005 on the same order of magnitude as the effect of human water use. These recent model results
1006 suggest that land-use change is an important topic for further investigation in the future. So far,
1007 this contribution remains highly uncertain.

1008

1009 Deforestation/afforestation

1010 At present, large losses in tropical forests and moderate gains in temperate-boreal forests result
1011 in a net reduction of global forest cover (FAO, 2015; Keenan et al., 2015; MacDicken, 2015;
1012 Sloan and Sayer, 2015). Net deforestation releases carbon and water stored in both biotic tissues
1013 and soil, which leads to sea level rise through three primary processes: deforestation-induced
1014 runoff increases (Gornitz et al., 1997), carbon loss-related decay and plant storage loss, and
1015 complex climate feedbacks (Butt et al., 2011; Chagnon and Bras, 2005; Nobre et al., 2009;
1016 Shukla et al., 1990; Spracklen et al., 2012). Due to these three causes, and if uncertainties from
1017 the land-atmospheric coupling are excluded, a summary by Wada et al. (2016) suggests that the
1018 current net global deforestation leads to an upper-bound contribution of ~ 0.035 mm/yr SLE.

1019

1020 Wetland degradation

1021 Wetland degradation contributes to sea level primarily through (i) direct water drainage or
1022 removal from standing inundation, soil moisture, and plant storage, and (ii) water release from
1023 vegetation decay and peat combustion. Wada et al. (2016) consider a recent wetland loss rate
1024 of 0.565% yr⁻¹ since 1990 (Davidson, 2014) and a present global wetland area of 371 mha
1025 averaged from three databases: Matthews natural wetlands (Matthews and Fung, 1987),

1026 ISLSCP (Darras, 1999), and DISCover (Belward et al., 1999; Loveland and Belward, 1997).
1027 They assume a uniform 1-meter depth of water in wetlands (Milly et al., 2010), to estimate a
1028 contribution of recent global wetland drainage to sea level of 0.067 mm/yr. Wada et al. (2016)
1029 apply a wetland area and loss rate as used for assessing wetland water drainage, to determine
1030 the annual reduction of wetland carbon stock since 1990, if completely emitted, releases water
1031 equivalent to 0.003–0.007 mm yr⁻¹ SLE. Integrating the impacts of wetland drainage, oxidation
1032 and peat combustion, Wada et al. (2016) suggest that the recent global wetland degradation
1033 results in an upper bound of 0.074 mm/yr SLE.

1034

1035 Lake storage changes

1036 Lakes store the greatest mass of liquid water on the terrestrial surface (Oki and Kanae, 2006),
1037 yet, because of their “dynamic” nature (Sheng et al., 2016; Wang et al., 2012), their overall
1038 contribution to sea level remains uncertain. In the past century, perhaps the greatest contributor
1039 in global lake storage was the Caspian Sea (Milly et al., 2010), where the water level exhibits
1040 substantial oscillations attributed to meteorological, geological, and anthropogenic factors
1041 (Ozyavas et al., 2010, Chen et al., 2017). Assuming the lake level variation kept pace with
1042 groundwater changes (Sahagian et al., 1994), the overall contribution of the Caspian Sea,
1043 including both surface and groundwater storage variations through 2014, has been about 0.03
1044 mm yr⁻¹ SLE since 1900, 0.075 (±0.002) mm yr⁻¹ since 1995, or 0.109 (±0.004) mm yr⁻¹ since
1045 2002. Additionally, between 1960 and 1990, the water storage in the Aral Sea Basin declined
1046 at a striking rate of 64 km³ yr⁻¹, equivalent to 0.18 mm yr⁻¹ SLE (Sahagian, 2000; Sahagian et
1047 al., 1994; Vörösmarty and Sahagian, 2000) due mostly to upstream water diversion for
1048 irrigation (Perera, 1993), which was modeled by Pokhrel et al. (2012) to be ~500 km³ during
1049 1951–2000, equivalent to 0.03 mm yr⁻¹ SLE. Dramatic decline in the Aral Sea continued in the
1050 recent decade, with an annual rate of 6.043 (±0.082) km³ yr⁻¹ measured from 2002 to 2014
1051 (Schwatke et al., 2015). Assuming that groundwater drainage has kept pace with lake level
1052 reduction (Sahagian et al., 1994), the Aral Sea has contributed 0.0358 (±0.0003) mm yr⁻¹ to the
1053 recent sea level rise.

1054

1055

1056 Water cycle variability

1057 Natural changes in the interannual to decadal cycling of water can have a large effect on the
1058 apparent rate of sea level change over decadal and shorter time periods (Milly et al., 2003;
1059 Lettenmaier and Milly, 2009; Llovel et al., 2010). For instance, ENSO-driven modulations of

1060 the global water cycle can be important in decadal-scale sea level budgets and can mask
 1061 underlying secular trends in sea level (Cazenave et al., 2014, Nerem et al., 2018).

1062 Sea level variability due to climate-driven hydrology represents a super-imposed variability on
 1063 the secular rates of global mean sea level rise. While this term can be large and is important in
 1064 the interpretation of the sea level record, it is arguably the most difficult term in the land water
 1065 budget to quantify.

1066

1067

1068

1069

1070

1071

1072

1073

1074

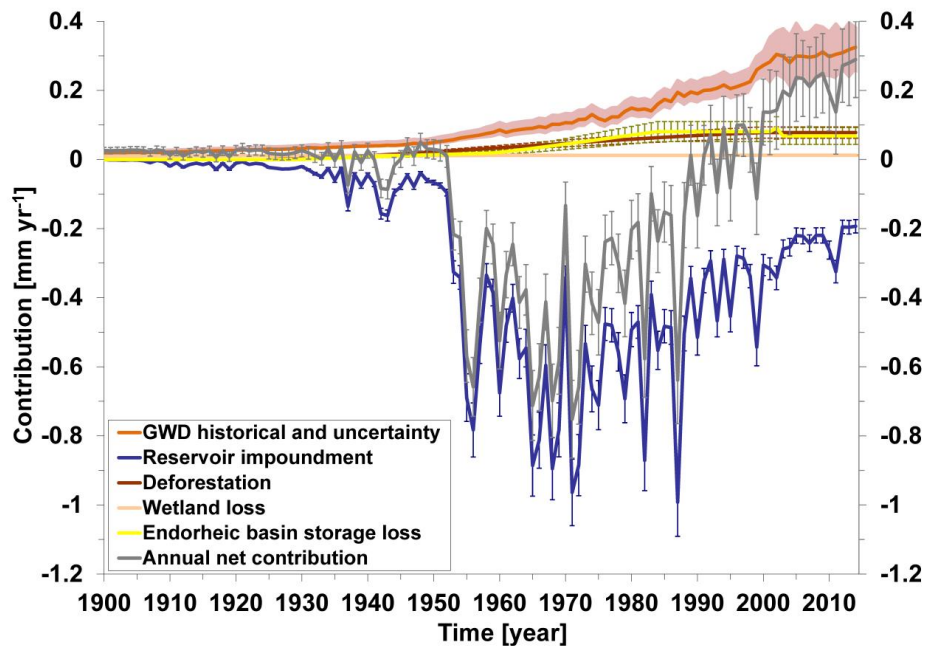
1075

1076

1077

1078

1079



1080

1080 *Figure 11: Time series of the estimated annual contribution of terrestrial water storage change*
 1081 *to global sea-level over the period 1900-2014 (rates in mm yr⁻¹ SLE) (modified from Wada et*
 1082 *al., 2016).*

1083

1084 **2.7.2. Net terrestrial water storage**

1085

1086 GRACE-based estimates

1087

1088

1089

1090

1091

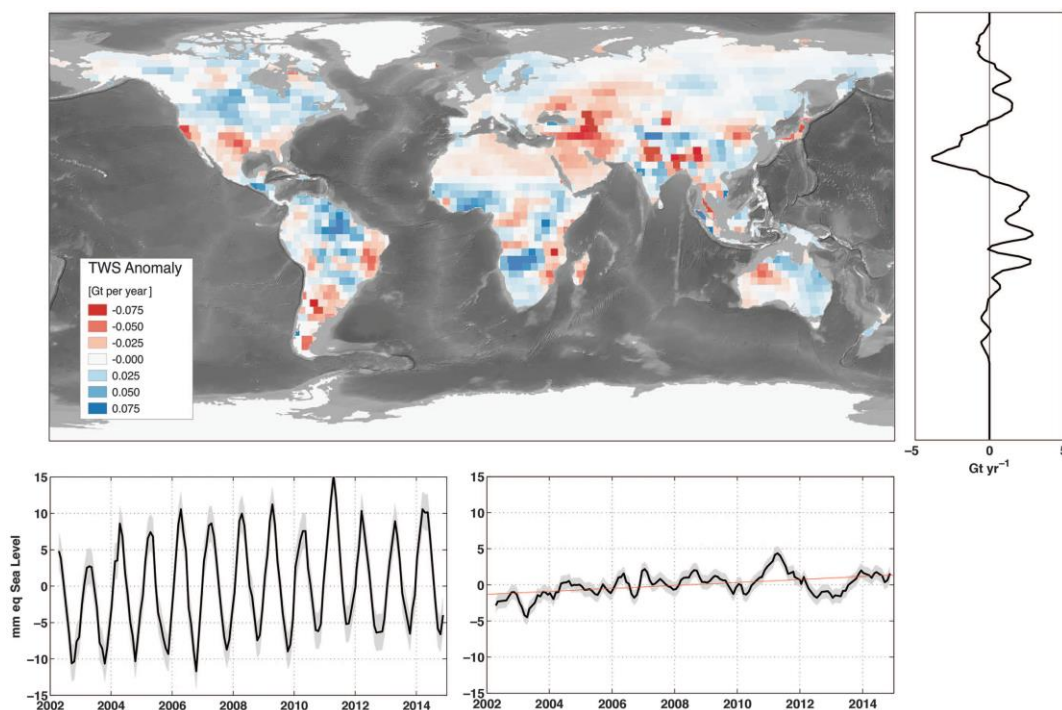
1092

1093

1094

Measurements of non-ice-sheet continental land mass from GRACE satellite gravity have been presented in several recent studies (Jensen et al., 2013, Rietbroek et al., 2016; Reager et al., 2016, Scanlon et al., 2018), and can be used to constrain a global land mass budget. Note that these ‘top-down’ estimates contain both climate-driven and direct anthropogenic driven effects, which makes them most useful in assessing the total impact of land water storage changes and closing the budget of all contributing terms. GRACE observations, when averaged over the whole land domain following Reager et al. (2016), indicate a total TWS change (including glaciers) over the 2002-2014 study period of approximately $+0.32 \pm 0.13$ mm year⁻¹ sea level

1095 equivalent (i.e., ocean gaining mass). Global mountain glaciers have been estimated to lose
 1096 mass at a rate of $0.65 \pm 0.09 \text{ mm yr}^{-1}$ (e.g. Gardner et al., 2013; Reager et al., 2016) during
 1097 that period, such that a mass balance indicates that global glacier-free land gained water at a
 1098 rate of $-0.33 \pm 0.16 \text{ mm yr}^{-1}$ SLE (i.e., ocean losing mass; Figure 12). A roughly similar estimate
 1099 was found from GRACE using glacier free river basins globally ($-0.21 \pm 0.09 \text{ mm/yr}$) (Scanlon
 1100 et al., 2018). Thus, the GRACE-based net TWS estimates suggest a negative sea level
 1101 contribution from land over the GRACE period (Table 8). However, mass change estimate from
 1102 GRACE incorporates uncertainty from all potential error sources that arise in processing and
 1103 post-processing of the data, including from the GIA model, and from the geocenter and mean
 1104 pole corrections.



1119 *Figure 12: An example of trends in land water storage from GRACE observations, April 2002*
 1120 *to November 2014. Glaciers and ice sheets are excluded. Shown are the global map (gigatons*
 1121 *per year), zonal trends, and full time series of land water storage (in mm yr^{-1} SLE). Following*
 1122 *methods details in Reager et al., (2016), GRACE shows a total gain in land water storage*
 1123 *during the 2002-2014 period, corresponding to a sea level trend of $-0.33 \pm 0.16 \text{ mm yr}^{-1}$ SLE*
 1124 *(modified from Reager et al., 2016). These trends include all human-driven and climate-driven*
 1125 *processes in Table 1, and can be used to close the land water budget over the study period.*

1126

1127 Estimates based on global hydrological models

1128 Global land water storage can also be estimated from global hydrological models (GHMs)
 1129 and global land surface models. These compute water, or water and energy balances, at the

1130 Earth surface, yielding time variations of water storage in response to prescribed atmospheric
 1131 data (temperature, humidity and wind) and the incident water and energy fluxes from the
 1132 atmosphere (precipitation and radiation). Meteorological forcing is usually based on
 1133 atmospheric model reanalyses. Model uncertainties result from several factors. Recent work
 1134 has underlined the large differences among different state-of-the-art precipitation datasets
 1135 (Beck et al., 2017) with large impacts on model results at seasonal (Schellekens et al., 2017)
 1136 and longer time scales (Felfelani et al., 2017). Another source of uncertainty is the treatment
 1137 of subsurface storage in soils and aquifers, as well as dynamic changes in storage capacity
 1138 due to representation of frozen soils and permafrost, the complex effects of dynamic
 1139 vegetation, atmospheric vapor pressure deficit estimation and an insufficiently deep soil
 1140 column. A recent study by Scanlon et al. (2018) compared water storage trends from five
 1141 global land surface models and two global hydrological models to GRACE storage trends,
 1142 and found that models estimated the opposite trend in net land water storage to GRACE over
 1143 the 2002 – 2014 period. These authors attributed this discrepancy to model deficiencies, in
 1144 particular soil depth limitations. These combined error sources are responsible for a range of
 1145 storage trends across models of approximately 0.5 ± 0.2 mm/yr SLE. In terms of global land
 1146 average, model differences can cause up to ~ 0.4 mm/yr SLE uncertainty.

1147
 1148
 1149
 1150
 1151
 1152
 1153

Estimate Terrestrial Water Storage contribution to sea level		2002-2014/15 (mm/yr) SLE (Positive values mean sea level rise)
Human contributions by component		
Ground water depletion	<i>Wada et al. (2016)</i>	0.30 (± 0.1)
Reservoir impoundment	<i>Wada et al. (2017)</i>	-0.24 (± 0.02)
Deforestation (after 2010)	<i>Wada et al. (2017)</i>	0.035
Wetland loss (after 1990)	<i>Wada et al. (2017)</i>	0.074
Endorheic basin storage loss Caspian Sea	<i>Wada et al. (2017)</i>	0.109 (± 0.004)

Aral Sea	<i>Wada et al. (2017)</i>	0.036 (\pm 0.0003)
Aggregated human intervention (sum of above)	<i>Scanlon et al. (2018)</i>	0.15 to 0.24
Hydrological model-based estimates		
WGHM model (<i>natural variability plus human intervention; P. Döll, personal communication</i>)		0.15 +/- 0.14
ISBA-TRIP model (<i>natural variability only ; Decharme et al., 2016</i>) + <i>human intervention from Wada et al. (2016) (from Dieng et al., 2017)</i>		0.23 +/- 0.10
GRACE-based estimates of total land water storage (not including glaciers) (<i>Reager et al., 2016; Rietbroek et al., 2016; Scanlon et al., 2018</i>)		
		-0.20 to -0.33 (\pm 0.09 - 0.16)

1154

1155 *Table 8. Estimates of TWS components due to human intervention and net TWS based on*
1156 *hydrological models and GRACE*

1157

1158

1159 **2.7.3 Synthesis**

1160 Based on the different approaches to estimate the net land water storage contribution, we
1161 estimate that corresponding sea level rate ranges from -0.33 to 0.23 mm/yr during the period of
1162 2002-2014/15 due to water storage changes (Table 8). According to GRACE, the net TWS
1163 change (i.e. not including glaciers) over the period 2002-2014 shows a negative contribution to
1164 sea level of -0.33 mm/yr and -0.21 mm/yr by Reager et al. (2016) and Scanlon et al. (2018)
1165 respectively. Such a negative signal is not currently reproduced by hydrological models which
1166 estimate slightly positive trends over the same period (see Table 8). It is to be noted however
1167 that looking at trends only over periods of the order of a decade may not be appropriate due the
1168 strong interannual variability of TWS at basin and global scales. For example, Figure 5 from
1169 Scanlon et al. (2018) (see also Figure S9 from their Supplementary Material), that compares
1170 GRACE TWS and model estimates over large river basins over 2002-2014, clearly show that
1171 the discrepancies between GRACE and models occur at the end of the record for the majority
1172 of basins. This is particularly striking for the Amazon basin (the largest contributor to TWS),
1173 for which GRACE and models agree reasonably well until 2011, and then depart significantly,
1174 with GRACE TWS showing strongly positive trend since then, unlike models. Such a
1175 divergence at the end of the record is also noticed for several other large basins (see Scanlon et
1176 al., Figure S9 SM). No clear explanation can be provided yet, even though one may questions
1177 the quality of the meteorological forcing used by hydrological models for the recent years. But
1178 this calls for some caution when comparing GRACE and models on the basis of trends only

1179 because of the dominant interannual variability of the TWS component. Much more work is
1180 needed to understand differences among models, and between models and GRACE. Of all
1181 components entering in the sea level budget, the TWS contribution currently appears as the
1182 most uncertain one.

1183

1184 **2.8 Glacial Isostatic Adjustment**

1185 The Earth's dynamic response to the waxing and waning of the late-Pleistocene ice sheets is
1186 still causing isostatic disequilibrium in various regions of the world. The accompanying slow
1187 process of GIA is responsible for regional and global fluctuations in relative and absolute sea
1188 level, 3D crustal deformations and changes of the Earth's gravity field (for a review, see Spada,
1189 2017). To isolate the contribution of current climate change, geodetic observations must be
1190 corrected for the effects of GIA (King et al., 2010). These are obtained by solving the "Sea
1191 Level Equation" (Farrell and Clark 1976, Mitrovica and Milne 2003). The sea level can be
1192 expressed as $S=N-U$, where S is the rate of change of sea-level relative to the solid Earth, N is
1193 the geocentric rate of sea-level change, and U is the vertical rate of displacement of the solid
1194 Earth. The sea level equation accounts for solid Earth deformational, gravitational and
1195 rotational effects on sea level, which are sensitive to the Earth's mechanical properties and to
1196 the melting chronology of continental ice. Forward GIA modelling, based on the solution of the
1197 sea level equation, provides predictions of unique spatial patterns (or *fingerprints*, see Plag and
1198 Juettner, 2001) of relative and geocentric sea-level change (e.g., Milne et al. 2009, Kopp et al.
1199 2015). During the last decades, the two fundamental components of GIA modelling have been
1200 progressively constrained from the observed history of relative sea level during the Holocene
1201 (see e.g., Lambeck and Chappell 2001, Peltier 2004). In the context of climate change, the
1202 importance of GIA has been recognised in the mid 1980s, when the awareness of global sea-
1203 level rise stimulated the evaluation of the isostatic contribution to tide gauge observations (see
1204 Table 1 in Spada and Galassi 2012). Subsequently, GIA models have been applied to the study
1205 of the pattern of sea level change from satellite altimetry (Tamisiea 2011), and since 2002 to
1206 the study of the gravity field variations from GRACE. Our primary goal here is to analyse GIA
1207 model outputs that have been used to infer global mean sea level change and ice sheet volume
1208 change from geodetic datasets during the altimetry era. These outputs are the sea-level
1209 variations detected by satellite altimetry across oceanic regions (n), the ocean mass change (w)
1210 and the modern ice sheets mass balance from GRACE. We also discuss the GIA correction that
1211 needs to be applied to GRACE-based land water storage changes. The GIA correction applied

1212 to tide gauge-based sea level observations at the coastlines is not discussed here. Since GIA
 1213 evolves on time scales of millennia (e.g., Turcotte and Schubert, 2014), the rate of change of
 1214 all the isostatic signals in can be considered constant on the time scale of interest.

1215

1216 **2.8.1 GIA correction to altimetry-based sea level**

1217 Unlike tide gauges, altimeters directly sample the sea surface in a geocentric reference frame.
 1218 Nevertheless, GIA contributes significantly to the rates of absolute sea-level change observed
 1219 over the “altimetry era”, which require a correction N_{gia} that is obtained by solving the SLE
 1220 (e.g., Spada 2017). As discussed in detail by Tamisiea (2011), N_{gia} is sensitive to the assumed
 1221 rheological profile of the Earth and to the history of continental glacial ice sheets. The variance
 1222 of N_{gia} over the surface of the oceans is much reduced, being primarily determined by the change
 1223 of the Earth’s gravity potential, apart from a spatially uniform shift. As discussed by Spada and
 1224 Galassi (2016), the GIA contribution N_{gia} is strongly affected by variations in the centrifugal
 1225 potential associated with Earth rotation, whose fingerprint is dominated by a spherical harmonic
 1226 contribution of degree $l=2$ and order $m=\pm 1$. Since N_{gia} has a smooth spatial pattern, the global
 1227 the GIA correction to altimetry data can be obtained by simply subtracting its average $n = \langle$
 1228 $N_{gia} \rangle$ over the ocean sampled by the altimetry missions. The computation of the GIA
 1229 contribution N_{gia} has been the subject of various investigations, based on different GIA models.
 1230 The estimate by Peltier (2001) of n equals -0.30 mm/yr, based on the ICE-4G (VM2) GIA
 1231 model. Such a value has been adopted in the majority of studies estimating the GMSL rise from
 1232 altimetry. Since n appears to be small compared to the global mean sea-level rise from altimetry
 1233 (~ 3 mm/yr), a more precise evaluation has not been of concern until recently. However, it is
 1234 important to notice that n is of comparable magnitude as the GMSL trend uncertainty, currently
 1235 estimated to ~ 0.3 mm/yr (see sub section 2.2). In Table 9a, we summarize the values of n
 1236 according to works in the literature where various GIA model models and averaging methods
 1237 have been employed. Based on values in Table 9a for which a standard deviation is available,
 1238 the average of n (weighted by the inverse of associated errors), assumed to represent the best
 1239 estimate, is $n = (-0.29 \pm 0.02)$ mm/yr where the uncertainty corresponds to 2σ .

1240

1241 **2.8.2 GIA correction to GRACE-based ocean mass**

1242 GRACE observations of present-day gravity variations are sensitive to GIA, due to the sheer
 1243 amount of rock material that is transported by GIA throughout the mantle and the resulting
 1244 changes in surface topography, especially over the formerly glaciated areas. The continuous
 1245 change in the gravity field results in a nearly linear signal in GRACE observations. Since the

1246 gravity field is determined by global mass redistribution, GIA models used to correct GRACE
 1247 data need to be global as well, especially when the region of interest is represented by all ocean
 1248 areas. To date, the only global ice reconstruction publicly available is provided by the
 1249 University of Toronto. Their latest product, named ICE-6G, has been published and distributed
 1250 in 2015 (Peltier et al., 2015); note that the ice history has been simultaneously constrained with
 1251 a specific Earth model, named VM5a. During the early period of the GRACE mission, the
 1252 available Toronto model was ICE-5G (VM2) (Peltier, 2004). However, different groups have
 1253 independently computed GIA model solutions based on the Toronto ice history reconstruction,
 1254 by using different implementations of GIA codes and somehow different Earth models. The
 1255 most widely used model is the one by Paulson et al. (2007), later updated by A et al. (2013).
 1256 Both studies use a deglaciation history based on ICE-5G, but differ for the viscosity profile of
 1257 the mantle: A et al. use a 3D compressible Earth with VM2 viscosity profile and a PREM-based
 1258 elastic structure used by Peltier (2004), whereas Paulson et al. (2007) use an incompressible
 1259 Earth with self-gravitation, and a Maxwell 1-D multi-layer mantle. Over most of the oceans,
 1260 the GIA signature is much smaller than over the continents. However, once integrated over the
 1261 global ocean, the signal w due to GIA is about -1 mm/yr of equivalent sea level change
 1262 (Chambers et al., 2010), which is of the same order of magnitude as the total ocean mass change
 1263 induced by increased ice melt (Leuliette and Willis, 2011). The main uncertainty in the GIA
 1264 contribution to ocean mass change estimates, apart from the general uncertainty in ice history
 1265 and Earth mechanical properties, originates from the importance of changes in the orientation
 1266 of the Earth's rotation axis (Chambers et al., 2010, Tamisiea, 2011). Different choices in
 1267 implementing the so-called "rotational feedback" lead to significant changes in the resulting
 1268 GIA contribution to GRACE estimates. The issue of properly accounting from rotational effects
 1269 has not been settled yet (Mitrovica et al., 2005, Peltier and Luthcke, 2009, Mitrovica and Wahr,
 1270 2011, Martinec and Hagedoorn, 2014). Table 9b summarises the values of the mass-rate GIA
 1271 contribution w according to the literature, where various models and averaging methods are
 1272 employed. The weighed average of the values in Table 9b for which an assessment of the
 1273 standard deviation is available, is $w = (-1.44 \pm 0.36)$ mm/yr (the uncertainty is 2σ), which we
 1274 assume to represent the preferred estimate.

1275

1276 ***2.8.3 GIA correction to GRACE-based terrestrial water storage***

1277 As discussed in the previous section, the GIA correction to apply to GRACE over land is
 1278 significant, especially in regions formerly covered by the ice sheets (Canada and Scandinavia).
 1279 Over Canada, GIA models significantly differ. This is illustrated in Figure 13 that shows

1280 difference between two models of GIA correction to GRACE over land, the A et al. (2013) and
 1281 Peltier et al. (2009) models. We see that over the majority of the land areas, differences are
 1282 small, except over north Canada, in particular around the Hudson Bay, where differences larger
 1283 than +/- 20 mm/yr SLE are noticed. This may affect GRACE-based TWS estimates over
 1284 Canadian river basins.

1285

1286

1287

1288

1289

1290

1291

1292

1293

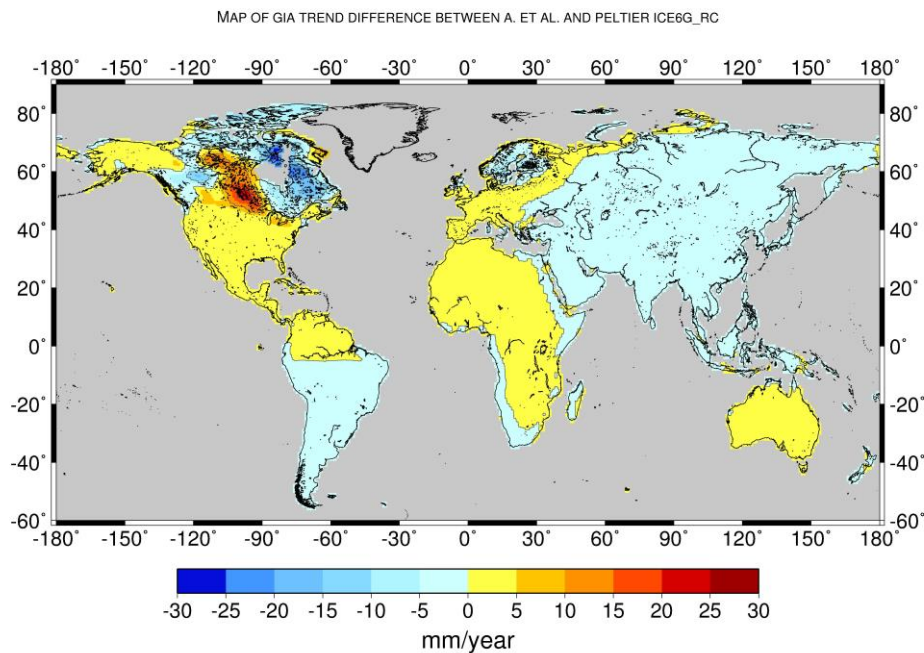
1294

1295

1296

1297

1298



1299 *Figure 13: Difference map between two models of GIA correction to GRACE over land: A et*
 1300 *al. (2013) minus Peltier et al. (2015) models. Unit in mm/yr SLE.*

1301

1302 When averaged over the whole land surface as done in some studies to estimate the combined
 1303 effect of land water storage and glacier melting from GRACE (e.g., Reager et al., 2015; see
 1304 section 2.7), the GIA correction ranges from ~ 0.5 to 0.7 mm/yr (in mm/yr SLE). Values for
 1305 different GIA models are given in Table 9c.

1306

1307 **2.8.4 GIA correction to GRACE-based ice sheet mass balance**

1308 The GRACE gravity field observations allow the determination of mass balances of ice sheets
 1309 and large glacier systems with an accuracy similar or superior to the input-output method or
 1310 satellite laser and radar altimetry (Shepherd et al., 2012). However, GRACE ice-mass balances
 1311 rely on successfully separating and removing the apparent mass change related to GIA. While
 1312 the GIA correction is small compared to the mass balance for Greenland ice sheet (ca. < 10%),
 1313 its magnitude and uncertainty in Antarctica is of the order of the ice-mass balance itself (e.g.

1314 Martín-Español et al., 2016). Particularly for today's glaciated areas, GIA remains poorly
 1315 resolved due to the sparsity of data constraints, leading to large uncertainties in the climate
 1316 history, the geometry and retreat chronology of the ice sheet, as well as the Earth structure. The
 1317 consequences are ambiguous GIA predictions, despite fitting the same observational data.
 1318 There are two principal approaches towards resolving GIA underneath the ice sheets. Empirical
 1319 estimates can be derived making use of the different sensitivities of satellite observations to ice-
 1320 mass changes and GIA (e.g. Riva et al., 2009, Wu et al., 2010). Alternatively, GIA can be
 1321 modelled numerically by forcing an Earth model with a fixed ice retreat scenario (e.g., Peltier
 1322 2009, Whitehouse et al., 2012) or with output from a thermodynamic ice sheet model (Gomez
 1323 et al., 2013, Konrad et al., 2015). Values of GIA-induced apparent mass change for Greenland
 1324 and Antarctica as listed in the literature should be applied with caution (Table 9d) when
 1325 applying them to GRACE mass balances. Each of these estimates may rely on a different
 1326 GRACE post-processing strategy and may differ in the approach used for solving the
 1327 gravimetric inverse problem (mascon analysis, forward-modelling, averaging kernels). Of
 1328 particular concern is the modelling and filtering of the pole tide correction caused by the
 1329 rotational variations related to GIA, affecting coefficients of harmonic degree $l=2$ and order
 1330 $m=\pm 1$. As mentioned above, agreement on the modelling of the rotational feedback has not
 1331 been reached within the GIA community. Furthermore, the pole tide correction applied during
 1332 the determination gravity-field solutions differs between the GRACE processing centres and
 1333 may not be consistent with the GIA correction listed. This inconsistency may introduce a
 1334 significant bias in the ice-mass balance estimates (e.g. Sasgen et al., 2013, Supplementary
 1335 Material). Wahr et al. (2015) presented recommendations on how to treat the pole tides in
 1336 GRACE analysis. However, a systematic inter-comparison of the GIA predictions in terms of
 1337 their low-degree coefficients and their consistency with the GRACE processing standards still
 1338 need to be done.

1339

1340 Table 9. *Estimated contributions of GIA to the rate of absolute sea level change observed by*
 1341 *altimetry (a), to the rate of mass change observed by GRACE over the global oceans (b), to the*
 1342 *rate of mass change observed by GRACE over land (c), and to Greenland and Antarctic ice*
 1343 *sheets (d), during the altimetry era. The GIA corrections are expressed in mm/yr SLE except*
 1344 *over Greenland and Antarctica where values are given in Gt/yr (ice mass equivalent). Most of*
 1345 *the GIA contributions are expressed as a value \pm one standard deviation; a few others are given*
 1346 *in terms of a plausible range, for some the uncertainties are not specified.*

1347

(a) GIA correction to absolute sea level measured by altimetry

<i>Reference</i>	<i>GIA</i> <i>(mm/yr)</i>	<i>Notes</i>
Peltier (2009) (Table 3)	-0.30 ± 0.02 -0.29 ± 0.03 -0.28 ± 0.02	Average of 3 groups of 4 values obtained by variants of the analysis procedure, using ICE-5G(VM2), over a global ocean, in the range of latitudes 66°S to 66°N and 60°S to 60°N, respectively.
Tamisiea (2011) (Figure 2)	-0.15 to -0.45 -0.20 to -0.50	Simple average over the oceans for a range of estimates obtained varying the Earth model parameters, over a global ocean and between latitudes 66°S and 66°N.
Huang (2013) (Table 3.6)	-0.26 ± 0.07 -0.27 ± 0.08	Average from an ensemble of 14 GIA models over a global ocean and between latitude from 66°S to 66°N.
Spada (2017) (Table 1)	-0.32 ± 0.08	Based on four runs of the Sea Level Equation solver SELEN (Spada and Stocchi, 2007) using model ICE-5G(VM2), with different assumptions in solving the SLE.

(b) GIA contribution to GRACE mass-rate of change over the oceans

<i>Reference</i>	<i>GIA</i> <i>(mm/yr SLE)</i>	<i>Notes</i>
Peltier (2009) (Table 3)	-1.60 ± 0.30	Average of values from 12 corrections for variants of the analysis procedure, using ICE-5G (VM2).
Chambers (2010) (Table 1)	-1.45 ± 0.35	Average over the oceans for a range of estimates produced by varying the Earth models.
Tamisiea (2011) (Figures 3 and 4)	-0.5 to -1.9 -0.9 to -1.5	Ocean average of a range of estimates varying the Earth model, and based on a restricted set, respectively.
Huang (2013) (Table 3.7)	-1.31 ± 0.40 -1.26 ± 0.43	Average from an ensemble of 14 GIA models over a global ocean and between latitude from 66°S to 66°N, respectively.

(c) GIA contribution to GRACE-based terrestrial water storage change

Reference *GIA correction (mm/yr SLE)*
(without Greenland, Antarctica, Iceland,
Svalbard, Hudson Bay and Black Sea

A et al. (2013)	0.63
Peltier ICE5G	0.68
Peltier ICE6G_rc	0.71
ANU_ICE6G	0.53

(d) GIA contribution to GRACE mass-rate of the ice sheets

<i>Reference</i>	<i>Greenland</i>	
	<i>GIA</i> <i>(Gt/yr)</i>	<i>Notes</i>
Simpson et al. (2009) ^f	-3 ± 12^m	Thermodynamic sheet / solid Earth model, 1D (uncoupled); constrained by geomorphology; inversion results in Sutterley <i>et al.</i> (2014).
Peltier (2009) (ICE-5G) ^g	-4^f	Ice load reconstruction / solid Earth model, 1D (ICE-5G / similar to VM2); Greenland component of ICE-5G (13 Gt/yr) + Laurentide component of ICE-5G (-17 Gt/yr); inversion results in Khan <i>et al.</i> 2016, Discussion.
Khan <i>et al.</i> (2016) (GGG-1D) ^r	15 ± 10^f	Ice load reconstruction / solid Earth model, 1D (uncoupled); constrained with geomorphology & GPS; Greenland component (+32 Gt/yr) + Laurentide component of ICE-5G (-17 Gt/yr); inversion results in Khan <i>et al.</i> (2016), Discussion.
Fleming <i>et al.</i> (2004) ^r (Green1)	3^f	Ice load reconstruction / solid Earth model, 1D (uncoupled); constrained with geomorphology; Greenland component (+ 20 Gt/yr) + Laurentide component of ICE-

5G (-17 Gt/yr); inversion in Sasgen *et al.* (2012, supplement).

Wu *et al.* (2010)^g -69 ± 19^m Joint inversion estimate based on GPS, satellite laser ranging, and very long baseline interferometry, and bottom pressure from ocean model output; inversion results in Sutterley *et al.* (2014).

Antarctica

<i>Reference</i>	<i>GIA (Gt/yr)</i>	<i>Notes</i>
Whitehouse <i>et al.</i> (2012) (W12a) ^r	60 ⁿ	Thermodynamic sheet / solid Earth model, 1D (uncoupled); constrained by geomorphology; inversion results in Shepherd <i>et al.</i> 2012, supplement (Fig. S8).
Ivins <i>et al.</i> (2013) (IJ05_R2) ^r	40-65 ⁿ	Ice load reconstruction / solid Earth model, 1D; constrained by geomorphology and GPS uplift rates; Ivins <i>et al.</i> 2013; inversion results in Shepherd <i>et al.</i> 2012, Supplement (Fig. S8).
Peltier (2009) (ICE-5G) ^g	140-180 ⁿ	Ice load reconstruction / solid Earth model ICE-5G(VM2); constrained by geomorphology; inversion results in Shepherd <i>et al.</i> 2012, supplement (Fig. S8).
Argus <i>et al.</i> (2014) (ICE-6G) ^g	107 ⁿ	Ice load reconstruction / solid Earth model ICE-6G(VM5a); constrained by geomorphology and GPS; theory recently corrected by Purcell <i>et al.</i> 2016; inversion results in Argus <i>et al.</i> (2014), conclusion 7.8.
Sasgen <i>et al.</i> (2017) (REGINA) ^r	55 ± 22^f	Joint inversion estimate based on GRACE, altimetry, GPS and viscoelastic response functions; lateral heterogeneous Earth model parameters; inversion results in Sasgen <i>et al.</i> (2017), Table 1.

Gunter <i>et al.</i> (2014) (G14) ^r	ca. 64 ± 40 ^a (multimodel uncert.)	Joint inversion estimate based on GRACE, altimetry, GPS and regional climate model output; conversion of uplift to mass using average rock density; inversion results in, Gunter <i>et al.</i> (2014) Table 1.
Martin-Español <i>et al.</i> (2016) (RATES) ^r	55 ± 8 $45 \pm 7^*$	Joint inversion estimate based on GRACE, altimetry, GPS and regional climate model output; inversion results in Sasgen <i>et al.</i> (2017), * is improved for GIA of smaller spatial scales; inversion results in Martin-Español <i>et al.</i> (2016), Fig. 6.

1348
1349 ^r regional model; ^g global model; ^m mascon inversion; ^f forward modelling inversion; ^a averaging
1350 kernel inversion; ⁿ inversion method not specified.
1351

1352 The GRACE-based ocean mass, Antarctica mass and terrestrial water storage changes are
1353 much model dependent. As these GIA corrections cannot be assessed from independent
1354 information, they represent a large source of uncertainties to the sea level budget components
1355 based on GRACE.

1356

1357 **2.9 Ocean mass change from GRACE**

1358

1359 Since 2002, GRACE satellite gravimetry has provided a revolutionary means for
1360 measuring global mass change and redistribution at monthly intervals with unprecedented
1361 accuracy, and offered the opportunity to directly estimate ocean mass change due to water
1362 exchange between the ocean and other components of the Earth (e.g., ice sheets, mountain
1363 glaciers, terrestrial water). GRACE time-variable gravity data have been successfully applied
1364 in a series of studies of ice mass balance of polar ice sheets (e.g., Velicogna and Wahr, 2006;
1365 Luthcke *et al.*, 2006) and mountain glaciers (e.g., Tamisiea *et al.*, 2005; Chen *et al.*, 2007) and
1366 their contributions to global sea level change. GRACE data can also be used to directly study
1367 long-term oceanic mass change or non-steric sea level change (e.g., Willis *et al.*, 2008; Leuliette
1368 *et al.*, 2009; Cazenave *et al.*, 2009), and provide a unique opportunity to study interannual or
1369 long-term TWS change and its potential impacts on sea level change (Richey *et al.*, 2015;
1370 Reager *et al.*, 2016).

1371 GRACE time-variable gravity data can be used to quantify ocean mass change from three
 1372 different main approaches. One is through measuring ice mass balance of polar ice sheets and
 1373 mountain glaciers and variations of TWS, and their contributions to the GMSL (e.g., Velicogna
 1374 and Wahr, 2005; Schrama et al., 2014). The second approach is to directly quantify ocean mass
 1375 change using ocean basin mask (kernel) (e.g., Chambers et al., 2004; Llovel et al., 2010;
 1376 Johnson and Chambers, 2013). In the ocean basin kernel approach, coastal ocean areas within
 1377 certain distance (e.g., 300 or 500 km) from the coast are excluded, in order to minimize
 1378 contaminations from mass change signal over the land (e.g., glacial mass loss and TWS
 1379 change). The third approach solves mass changes on land and over ocean at the same time via
 1380 forward modeling (e.g., Chen et al., 2013; Yi et al., 2015). The forward modeling is a global
 1381 inversion to reconstruct the “true” mass change magnitudes over land and ocean with
 1382 geographical constraint of locations of the mass change signals, and can help effectively reduce
 1383 leakage between land and ocean (Chen et al., 2015).

1384

1385 Estimates of ocean mass changes from GRACE are subject to a number of major error
 1386 sources. These include : (1) leakage errors from the larger signals over ice sheets and land
 1387 hydrology due to GRACE’s low spatial resolution (of at least a few to several hundred km) and
 1388 the need of coastal masking, (2) spatial filtering of GRACE data to reduce spatial noise, (3)
 1389 errors and biases in geophysical model corrections (e.g., GIA, atmospheric mass) that need to
 1390 be removed from GRACE observations to isolate oceanic mass change and/or polar ice sheets
 1391 and mountain glaciers mass balance, and (4) residual measurement errors in GRACE gravity
 1392 measurements, especially those associated with GRACE low-degree gravity changes. In
 1393 addition, how to deal with the absent degree-1 terms, i.e., geocenter motion in GRACE gravity
 1394 fields, is expected to affect estimates of GRACE-based oceanic mass rates and ice mass
 1395 balances.

1396

Data sources	Time Period	Ocean mass trends (mm/yr)
Chen et al. (2013) (A13 GIA)	2005.01- 2011.12	1.80 ± 0.47
Johnson and Chambers (2013) (A13 GIA)	2003.01- 2012.12	1.80 ± 0.15

Purkey et al. (2014) (A13 GIA)	2003.01- 2013.01	1.53 ± 0.36
Dieng et al. (2015a) (Paulson07 GIA)	2005.01- 2012.12	1.87 ± 0.11
Dieng et al. (2015b) (Paulson07 GIA)	2005.01- 2013.12	2.04 ± 0.08
Yi et al. (2015) (A13 GIA)	2005.01- 2014.07	2.03 ± 0.25
Rietbroek et al. (2016)	2002.04- 2014.06	1.08 ± 0.30
Chambers et al. (2017)	2005.0 – 2015.0	2.11 ± 0.36

1397 *Table 10. Recently published (since 2013) estimates of GRACE-based ocean mass rates*
1398 *(GIA corrected). Most of the listed studies use either the A13 (A et al., 2013) or Paulson07*
1399 *(Paulson et al., 2007) GIA model.*

1400

1401

1402 With a different treatment of the GRACE land-ocean signal leakage effect through global
1403 forward modeling, Chen et al. (2013) estimated ocean mass rates using GRACE RL05 time-
1404 variable gravity solutions over the period 2005-2011, and showed that the ocean mass change
1405 contributes to 1.80 ± 0.47 mm/yr (over the same period), which is significantly larger than
1406 previous estimates over about the same period. Yi et al. (2015) further confirmed that correct
1407 calibration of GRACE data and appropriate treatment of GRACE leakage bias are critical to
1408 improve the accuracy of GRACE estimated ocean mass rates. Table 10 summarizes different
1409 estimates of GRACE ocean mass rates. The uncertainty estimates of the listed studies (Table
1410 10) are computed from different methods, with different considerations of error sources into
1411 the error budget, and represent different confidence levels.

1412

1413 As demonstrated in Chen et al. (2013), different treatments of just the degree-2 spherical
1414 harmonics of GRACE gravity solution alone can lead to substantial differences in GRACE
1415 estimated ocean mass rates (ranging from 1.71 to 2.17 mm/yr). Similar estimates from GRACE
1416 gravity solutions from different data processing centers can also be different. In the meantime,
1417 long-term degree-1 spherical harmonics variation, representing long-term geocenter motion and

1418 neglected in some of the previous studies (due to the lack of accurate observations) are also
1419 expected to have non-negligible effect on GRACE derived ocean mass rates (Chen et al., 2013).
1420 Different methods for computing ocean mass change using GRACE data may also lead to
1421 different estimates (Chen et al., 2013; Johnson and Chambers, 2013, Jensen et al., 2013).

1422 To help better understand the potential and uncertainty of GRACE satellite gravimetry in
1423 quantification of the ocean mass rate, Table 11 provides a comparison of GRACE-estimated
1424 ocean mass rates over the period January 2005 to December 2016 based on different GRACE
1425 data products and different data processing methods, including the CSR, GFZ and JPL GRACE
1426 RL05 spherical harmonic solutions (i.e., the so-called GSM solutions), and CSR, JPL, and
1427 GSFC mascon solutions (the available GSFC mascons only cover the period up to July 2016).
1428 The three GRACE GSM results (CSR, GFZ, and JPL) are updates from Johnson and Chambers
1429 (2013), with degree-2 zonal term replaced by satellite laser ranging results (Cheng and Ries,
1430 2012), geocenter motion from Swenson et al. (2008), GIA model from A et al. (2013), an
1431 averaging kernel with a land mask that extends out 300 km, and no destriping or smoothing, as
1432 described in Johnson and Chambers (2013). An update of GRACE ocean mass rate from Chen
1433 et al. (2013) is also included for comparisons, which is based on the CSR GSM solutions using
1434 forward modeling (a global inversion approach), with similar treatments of the degree-2 zonal
1435 term, geocenter motion, and GIA effects.

1436 The JPL mascon ocean mass rate is computed from all mascon grids over the ocean, and
1437 the GSFC mascon ocean mass rate is computed from all ocean mascons, with the
1438 Mediterranean, Black and Red Seas excluded. A coastline resolution improvement (CRI)
1439 filter is already applied in the JPL mascons to reduce leakage (Wiese et al., 2016), and in both
1440 the GSFC and JPL mascon solutions, the ocean and land are separately defined (Luthcke et al.,
1441 2013; Watkins et al., 2015). For the CSR mascon results, an averaging kernel with a land mask
1442 that extends out 200 km is applied to reduced leakage (Chen et al., 2017). Similar treatments or
1443 corrections of degree-2 zonal term, geocenter motion, and GIA effects are also applied in the
1444 three mascon solutions. When solving GRACE mascon solutions, the GRACE GAD fields
1445 (representing ocean bottom pressure changes, or combined atmospheric and oceanic mass
1446 changes) have been added back to the mascon solutions. To correctly quantify ocean mass
1447 change using GRACE mascon solutions, the means of the GAD fields over the oceans, which
1448 represents mean atmospheric mass changes over the ocean (as ocean mass is conserved in the
1449 GAD fields) need to be removed from GRACE mascon solutions. The removal of GAD average
1450 over the ocean in GRACE mascon solutions has very minor or negligible effect (of ~ 0.02

1451 mm/yr) on ocean mass rate estimates, but is important for studying GMSL change at seasonal
1452 time scales.

1453 Over the 12-year period (2005-2016), the three GRACE GSM solutions show pretty
1454 consistent estimates of ocean mass rate, in the range of 2.3 to 2.5 mm/yr. Greater differences
1455 are noticed for the mascon solutions. The GSFC mascons show the largest rate of 2.61mm/yr.
1456 The CSR and JPL mascon solutions show relatively smaller ocean mass rates of 1.76 and 2.02
1457 mm/yr, respectively, over the studied period. Based on the same CSR GSM solutions, the
1458 forward modeling and basin kernel estimates agree reasonably well (2.52 vs. 2.44 mm/yr). In
1459 addition to the degree-2 zonal term, geocenter motion, and GIA correction, the degree-2, order-
1460 1 spherical harmonics of the current GRACE RL05 solutions are affected by the definition of
1461 the reference mean pole in GRACE pole tide correction (Wahr et al., 2015). This mean pole
1462 correction, excluded in all estimates listed in Table 11 (for fair comparison), is estimated to
1463 contribute ~ -0.11 mm/yr to GMSL. How to reduce errors from the different sources play a
1464 critical role in estimating ocean mass change from GRACE time-variable gravity data.

1465

1466

Data sources	Ocean mass trend (mm/yr)
GSM CSR Forward Modeling (update from Chen et al., 2013)	2.52±0.17
GSM CSR (update from Johnson and Chambers, 2013)	2.44±0.15
GSM GFZ (update from Johnson and Chambers, 2013)	2.30±0.15
GSM JPL (update from Johnson and Chambers, 2013)	2.48±0.16
Mascon CSR (200 km)	1.76±0.16
Mascon JPL	2.02±0.16
Mascon GSFC (update from Luthcke et al., 2013)	2.61±0.16
Ensemble mean	2.3 ± 0.19

1467 *Table 11. Ocean mass trends (in mm/yr) estimated from GRACE for the period January 2005*
1468 *– December 2016 (the GSFC mascon solutions cover up to July 2016). The uncertainty is based*
1469 *on 2 times the sigma of least-squares fitting.*

1470

1471 GRACE satellite gravimetry has brought a completely new era for studying global ocean
1472 mass change. Owing to the extended record of GRACE gravity measurements (now over 15
1473 years), improved understanding of GRACE gravity data and methods for addressing GRACE
1474 limitations (e.g., leakage and low-degree spherical harmonics), and improved knowledge of
1475 background geophysical signals (e.g., GIA), GRACE-derived ocean mass rates from different

1476 studies in recent years show clearly increased consistency (Table 11). Most of the results agree
 1477 well with independent observations from satellite altimeter and Argo floats, although the
 1478 uncertainty ranges are still large. The GRACE Follow-On (FO) mission has been launched in
 1479 May 2018. The GRACE and GRACE-FO together are expected to provide at least over two (or
 1480 even three) decades of time-variable gravity measurements. Continuous improvements of
 1481 GRACE data quality (in future releases) and background geophysical models are also expected,
 1482 which will help improve the accuracy GRACE observed ocean mass change.

1483 For the sea level budget assessment over the GRACE period, we will use the ensemble mean.

1484

1485 **3. Sea Level Budget results**

1486 In section 2, we have presented the different terms of the sea level budget equation, mostly
 1487 based on published estimates (and in some cases, from their updates). We now use them to
 1488 examine the closure of the sea level budget. For all terms, we only consider ensemble mean
 1489 values.

1490

1491 **3.1 Entire altimetry era (1993-Present)**

1492

1493 *3.1.1 Trend estimates over 1993-Present*

1494 Because it is now clear that the GMSL and some components are accelerating (e.g., Nerem et
 1495 al., 2018), we propose to characterize the long term variations of the time series by both a trend
 1496 and an acceleration. We start looking at trends. Table 12 gathers the trends estimated in section
 1497 2. The end year is not always the same for all components (see section 2). Thus the word
 1498 ‘present’ means either 2015 or 2016 depending on the component. As no trend estimate is
 1499 available for the entire altimetry era for the terrestrial water storage contribution, we do not
 1500 consider this component. The residual trend (GMSL minus sum of components trend) may then
 1501 provide some constraint on the TWS contribution.

1502

1503

Component	Trends (mm/yr) 1993-Present
1. GMSL (TOPEX-A drift corrected)	3.07 +/- 0.37
2. Thermosteric sea level (full depth)	1.3 +/- 0.4
3. Glaciers	0.65 +/- 0.15

4. Greenland	0.48 +/- 0.10
5. Antarctica	0.25 +/- 0.10
6. TWS	/
7. Sum of components (without TWS→ 2.+3.+4.+5.)	2.7 +/- 0.23
8. GMSL minus sum of components (without TWS)	0.37 +/- 0.3

1504

1505 *Table 12: Trend estimates for individual components of the sea level budget, sum of components*
1506 *and GMSL minus sum of components over 1993-present. Uncertainties of the sum of*
1507 *components and residuals represent rooted mean squares of components errors, assuming that*
1508 *errors are independent.*
1509

1510 Results presented in Table 12 are discussed in detail in section 4.

1511

1512 **3.1.2 Acceleration**

1513 The GMSL acceleration estimated in section 2.2 using Ablain et al. (2017b)'s TOPEX-A drift
1514 correction amounts to 0.10 mm/yr² for the 1993-2017 time span. This value is in good
1515 agreement with Nerem et al. (2018) estimate (of 0.084 +/- 0.025 mm/yr²) over nearly the same
1516 period, after removal of the interannual variability of the GMSL. In Nerem et al. (2018),
1517 acceleration of individual components are also estimated as well as acceleration of the sum of
1518 components. The latter agrees well with the GMSL acceleration. Here we do not estimate the
1519 acceleration of the component ensemble means because time series are not always available.
1520 We leave this for a future assessment.

1521

1522 **3.2 GRACE and Argo period (2005- Present)**

1523

1524 **3.2.1 Sea level budget using GRACE-based ocean mass**

1525 If we consider the ensemble mean trends for the GMSL, thermosteric and ocean mass compents
1526 given in sections 2.2, 2.3 and 2.9 over 2005-present, we find agreement (within error bars)
1527 between the observed GMSL (3.5 +/- 0.2 mm/yr) and the sum of Argo-based thermosteric plus
1528 GRACE-based ocean mass (3.6 +/- 0.4 mm/yr) (see Table 13). The residual (GMSL minus sum
1529 of components) trend amounts to -0.1 mm/yr. Thus in terms of trends, the sea level budget
1530 appears closed over this time span within quoted uncertainties.

1531

1532 **3.2.2 Trend estimates over 2005-Present from estimates of individual contributions**

1533

1534 Table 13 gathers trends of individual components of the sea level budget over 2005-present, as
 1535 well sum of components and residuals (GMSL minus sum of components) trend. As for the
 1536 longer period, ensemble mean values are considered for each component.

1537

Component	Trend (mm/yr) 2005- Present
1. GMSL	3.5 +/- 0.2
2. Thermosteric sea level (full depth)	1.3 +/- 0.4
3. Glaciers	0.74 +/- 0.1
4. Greenland	0.76 +/- 0.1
5. Antarctica	0.42 +/- 0.1
6. TWS from GRACE (mean of Reager et al. and Scanlon et al.)	-0.27 +/- 0.15
7. Sum of components (2.+3.+4.+5.+6.)	2.95 +/- 0.21
8. Sum of components (thermosteric full depth + GRACE-based ocean mass)	3.6 +/- 0.4
9. GMSL minus sum of components (including GRACE-based TWS → 2.+3.+4.+5.+6.)	0.55 +/- 0.3
10. GMSL minus sum of components (without GRACE-based TWS → 2.+3.+4.+5.)	0.28 +/- 0.2
11. GMSL minus sum of components (thermosteric full depth + GRACE-based ocean mass)	-0.1 +/- 0.3

1538

1539 *Table 13: Trend estimates for individual components of the sea level budget, sum of components*
 1540 *and GMSL minus sum of components over 2005-present.*

1541

1542 As for Table 12, the results presented in Table 13 are discussed in detail in section 4.

1543

1544

1545

1546

1547

1548 **3.2.3 Year-to-year budget over 2005-Present using GRACE-based ocean mass**

1549

1550 We now examine the year-to-year sea level and mass budgets. Table 14 provides annual mean
 1551 values for the ensemble mean GMSL, GRACE-based ocean mass and Argo-based thermosteric
 1552 component. The components are expressed as anomalies and their reference is arbitrary. So to
 1553 compare with the GMSL, a constant offset for all years was applied to the thermosteric and
 1554 ocean mass annual means. The reference year (where all values are set to zero) is 2003.

1555

1556

1557

Year	Ensemble mean GMSL mm	Sum of components mm	GMSL minus sum of components mm
2005	7.00	8.78	-0.78
2006	10.25	10.78	-0.53
2007	10.51	11.35	-0.85
2008	15.33	15.07	0.25
2009	18.78	18.88	-0.10
2010	20.64	20.53	0.11
2011	20.91	21.38	-0.48
2012	31.10	29.33	1.77
2013	33.40	33.87	-0.47
2014	36.65	36.22	0.43
2015	46.34	45.69	0.65

1558

1559 *Table 14. Annual mean values for the ensemble means GMSL and sum of components (GRACE-*
 1560 *based ocean mass and Argo-based thermosteric, full depth). Constant offset applied to the sum*
 1561 *of components. The reference year (where all values are set to zero) is 2003.*

1562

1563 Figure 14 shows the sea level budget over 2005-2015 in terms of annual bar chart using values
 1564 given in Table 14. It compares for years 2005 to 2016 the annual mean GMSL (blue bars) and

1565 annual mean sum of thermosteric and GRACE-based ocean mass (red bars). Annual residuals
 1566 are also shown (green bars). These are either positive or negative depending on years. The trend
 1567 of these annual residuals is estimated to 0.135 mm/yr.

1568 In Figure 15 is also shown the annual sea level budget over 2005-2015 but now using the
 1569 individual components for the mass terms. As we have no annual estimates for TWS, we ignore
 1570 it, so that the total mass includes only glaciers, Greenland and Antarctica. The annual residuals
 1571 thus include the TWS component in addition to the missing contributions (e.g., deep ocean
 1572 warming). For years 2006 to 2011, the residuals are negative, an indication of a negative TWS
 1573 to sea level as suggested by GRACE results (Reager et al., 2016, Scanlon et al., 2018). But as
 1574 of 2012, the residuals become positive and on average over 2005-2015, the residual trend
 1575 amounts +0.28 mm/yr, a value larger than when using GRACE ocean mass.

1576 Finally, Figure 16 presents the mass budget. It compares annual GRACE-based ocean mass to
 1577 the sum of the mass components, without TWS as in Figure 15. The residual trends over 2005-
 1578 2015 time span is 0.14 mm/yr. It may dominantly represent the TWS contribution. From one
 1579 year to another residuals can be either positive or negative, suggesting important interannual
 1580 variability in the TWS or even in the deep ocean.

1581

1582

1583

1584

1585

1586

1587

1588

1589

1590

1591

1592

1593

1594

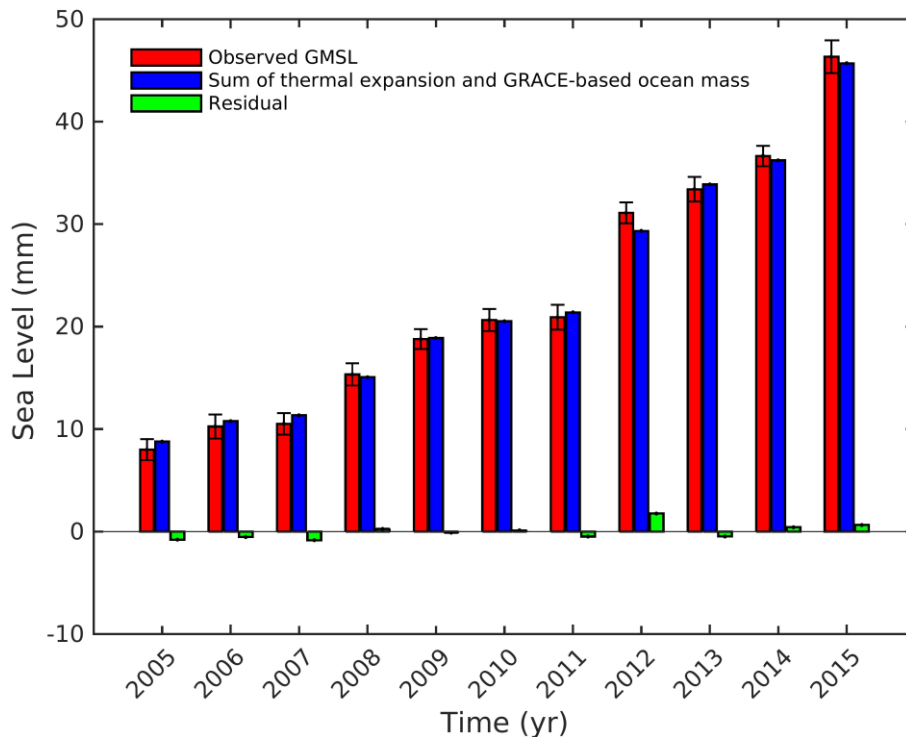
1595

1596

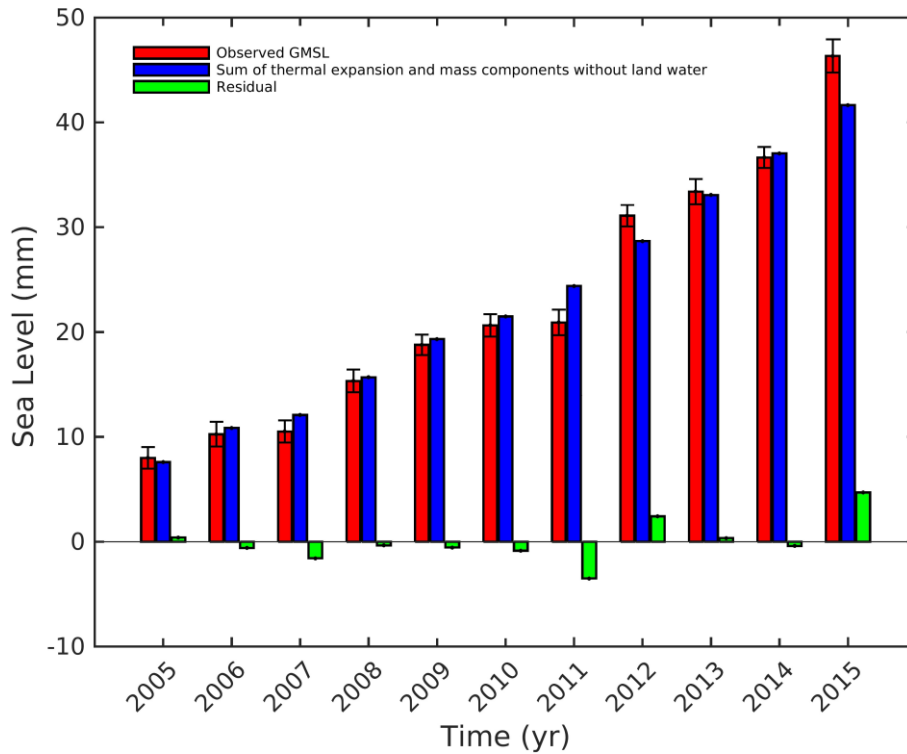
1597

1598

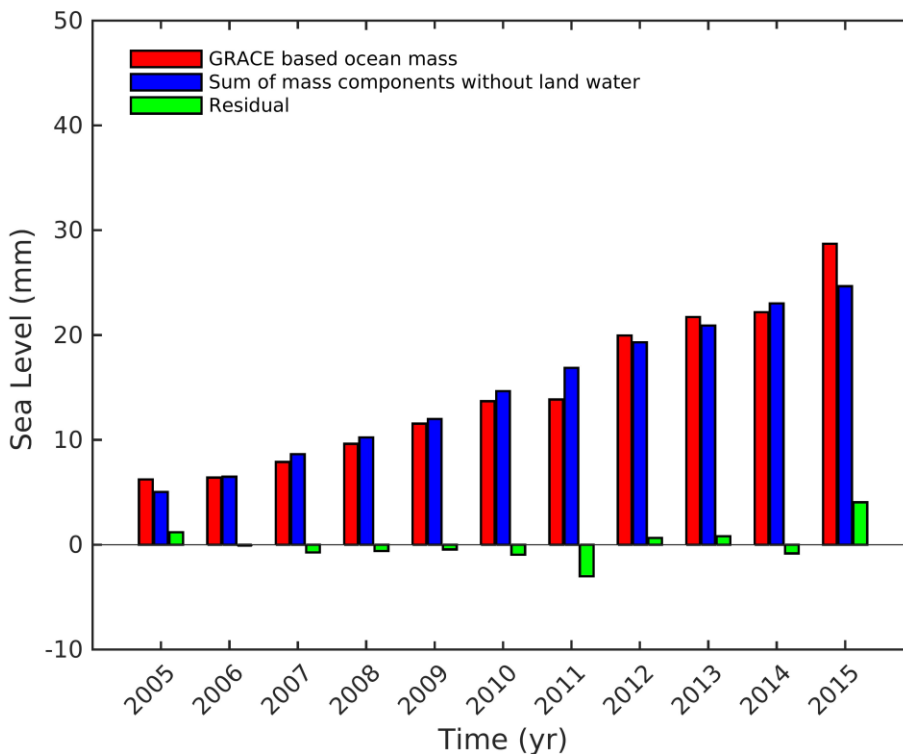
1599



1600 *Figure 14: Annual sea level (blue bars) and sum of thermal expansion (full depth) and GRACE*
 1601 *ocean mass component (red bars). Black vertical bars are associated uncertainties. Annual*
 1602 *residuals (green bars) are also shown.*



1622 *Figure 15: Annual global mean sea level (blue bars) and sum components without TWS (full*
 1623 *depth thermal expansion+ glaciers + Greenland + Antarctica) (red bars). Black vertical bars*
 1624 *are associated uncertainties. Annual residuals (green bars) are also shown.*



1639
1640
1641
1642
1643
1644

Figure 16: Annual GRACE-based ocean mass (red bars) and sum components without TWS (full depth thermal expansion+ glaciers + Greenland + Antarctica) (blue bars). Annual residuals (green bars) are also shown.

1645 **4. Discussion**

1646 The results presented in section 2 for the components of the sea level budget are based on
1647 syntheses of the recently published literature. When needed, the time series have been updated.
1648 In section 3, we considered ensemble means for each component to average out random errors
1649 of individual estimates. We examined the closure/non closure of the sea level budget using
1650 these ensemble mean values, for 2 periods: 1993-present and 2005-present (Argo and GRACE
1651 period). Because of the lack of observation-based TWS estimate for the 1993-present time span,
1652 we compared the observed GMSL trend to the sum of components excluding TWS. We found
1653 a positive residual trend of 0.37 ± 0.3 mm/yr, supposed to include the TWS contribution, plus
1654 other imperfectly known contributions (deep ocean warming) and data errors.

1655 For the 2005-present time span, we considered both GRACE-based ocean mass and sum of
1656 individual mass components, allowing us to also look at the mass budget. For TWS, as
1657 discussed in section 2.7, GRACE provides a negative trend contribution to sea level over the
1658 last decade (i.e., increase on water storage on land) attributed to internal natural variability
1659 (Reager et al., 2016), unlike hydrological models that lead to a small (possibly not significantly
1660 different from zero) positive contribution to sea level over the same period . Assuming that
1661 GRACE observations are perfect, such discrepancies could be attributed to the inability of
1662 models to correctly account for uncertainties in meteorological forcing and inadequate
1663 modeling of soil storage capacity (see discussion in section 2.7). However, when looking at
1664 the sea level budget over the GRACE time span and using the GRACE-based TWS, we find a
1665 rather large positive residual trend (> 0.5 mm/yr) that needs to be explained. Since GRACE-
1666 based ocean mass is supposed to represent all mass terms, one may want to attribute this residual
1667 trend to an additional contribution of the deep ocean to the abyssal contribution already taken
1668 into account here, but possibly underestimated because of incomplete monitoring by current
1669 observing systems. If such a large positive contribution from the deep ocean (meaning ocean
1670 warming) is real (which is unlikely, given the high implied heat storage), this has to be
1671 confirmed by independent approaches e.g., using ocean reanalyses, and eventually model-based
1672 and top-of-the-atmosphere estimates of the Earth Energy Imbalance.

1673 In addition to mean trends over the period, we also looked at the annual budget for all years
1674 starting in 2005. For most components, annual mean values are provided during the Argo-
1675 GRACE era, except for the terrestrial water storage component. However, the sea level budget
1676 based on GRACE ocean mass (plus ocean thermal expansion; Figure 14) includes the TWS
1677 contribution. As shown in Figure 14, yearly residuals are small, suggesting near closure of the
1678 sea level budget. The residual trend amounts to 0.13 mm/yr. It could be interpreted as an
1679 additional deep ocean contribution not accounted by the SIO estimate (see section 2.3).
1680 However, when looking at Figure 14, we note that yearly residuals are either positive or
1681 negative, an indication of interannual variability that can hardly be explained by a deep ocean
1682 contribution. The residual trend derived from the difference (GMSL minus sum of components)
1683 (Table 13) amounts -0.1 ± 0.3 mm/yr, suggesting a sea level budget closed within 0.3 mm/yr
1684 over 2005-present, with no substantial deep ocean contribution.

1685 Figure 16 compares GRACE ocean mass to the sum of mass components (excluding TWS, for
1686 the reasons mentioned above). In principle, this mass budget may provide a constraint on the
1687 TWS contribution. The corresponding residual trend amounts to 0.14 mm/yr over the GRACE
1688 period, a value that disagrees with the above quote GRACE-based TWS estimates. However, it
1689 is worth noting that the GRACE-based TWS trend is much dependent on the considered time
1690 span because of the strong interannual variability; a recent study by Palanisamy et al. (in
1691 preparation), based on 347 land river basins, found zero GRACE-based TWS trend over 2005-
1692 2015. Given the remaining data uncertainties, any robust conclusion can hardly be reached so
1693 far. That being said, more work is needed to clarify the sign discrepancy between GRACE-
1694 based and model-based TWS estimates.

1695

1696 **5. Concluding Remarks**

1697 As mentioned in the introduction, the global mean sea level budget has been the object of
1698 numerous previous studies, including successive IPCC assessments of the published literature.
1699 What is new in the effort presented here, is that it involves the international community
1700 currently studying present-day sea level and its components. Moreover, it relies on a large
1701 variety of datasets derived from different space-based and in situ observing systems. Near
1702 closure of the sea level budget as reported here over the GRACE and Argo era suggests that no
1703 large systematic errors affect these independent observing systems, including the satellite
1704 altimetry system. Study of the sea level budget allows improved understanding of the different
1705 processes causing sea level rise, such as ocean warming and land ice melt. When accuracy

1706 increases, it will offer an integrative view of the response of the Earth system to natural &
1707 anthropogenic forcing and internal variability, and provide an independent constraint on the
1708 current Earth Energy Imbalance. Validation of climate models against observations is another
1709 important application of this kind of assessment (e.g., Slangen et al., 2017).

1710 However, important uncertainties still remain, that affect several terms of the budget; for
1711 exemple the GIA correction applied to GRACE data over Antarctica or the net land water
1712 storage contribution to sea level. The latter results from a variety of factors but is dominated by
1713 ground water pumping and natural climate variability. Both terms are still uncertain and
1714 accurately quantifying them remains a challenge.

1715 Several ongoing international projects related to sea level should provide in the near future
1716 improved estimates of the components of the sea level budget. This is the case, for exemple, of
1717 the ice sheet mass balance inter-comparison exercise (IMBIE, 2nd assessment), a community
1718 effort supported by NASA (National Aeronautics and Space Administration) and ESA,
1719 dedicated to reconcile satellite measurements of ice sheet mass balance (The IMBIE Team,
1720 2018). This is also the case for the ongoing ESA Sea level Budget Closure project (Horwath et
1721 al., 2018) that uses a number of space-based Essential Climate Variables (ECVs) reprocessed
1722 during the last few years in the context of the ESA Climate Change Initiative project. The
1723 recently launched GRACE follow-on mission will lengthen the current mass component time
1724 series, with hopefully increased precision and resolution. Finally, the deep Argo project, still in
1725 an experimental phase, will provide important information on the deep ocean heat content in
1726 the coming years. Availability of this new data set will be open new insight on the total
1727 thermosteric component of the sea level budget, allowing constraining other missing or poorly
1728 known contributions, from the evaluation of the budget.

1729 The sea level budget assessment discussed here essentially relies on trend estimates. But annual
1730 budget estimates have been proposed for the first time over the GRACE-Argo era. It is planned
1731 to provide updates of the global sea level budget every year, as done for more than a decade for
1732 the global carbon budget (Le Queré et al., 2018). In the next assessments, updates of all
1733 components will be considered, accounting for improved evaluation of the raw data, improved
1734 processing and corrections, use of ocean reanalyses, etc. Need for additional information where
1735 gaps exist should also be considered. As a closing remark, study of the sea level budget in terms
1736 of time series, not just trends as done here, will be required.

1737 **List of authors and affiliations:**

1738 Anny Cazenave (LEGOS, France & ISSI, Switzerland), Benoit Meyssignac (LEGOS, France);
 1739 Michael Ablain (CLS, France), Jonathan Bamber (U. Bristol, UK), Valentina Barletta (DTU-
 1740 SPACE, Denmark), Brian Beckley (SGT Inc./NASA GSFC, USA), Jérôme Benveniste
 1741 (ESA/ESRIN, Italy), Etienne Berthier (LEGOS, France), Alejandro Blazquez (LEGOS,
 1742 France), Tim Boyer (NOAA, USA), Denise Caceres (Goethe U., Germany), Don Chambers
 1743 (U. South Florida, USA), Nicolas Champollion (U. Bremen, Germany), Ben Chao (IES-AS,
 1744 Taiwan), Jianli Chen (U. Texas, USA), Lijing Cheng (IAP-CAS, China), John A. Church (U.
 1745 New South Wales, Australia), Stephen Chuter (U. Bristol, UK), J. Graham Cogley (Trent U.,
 1746 Canada), Soenke Dangendorf (U. Siegen, Germany), Damien Desbruyères (IFREMER,
 1747 France), Petra Döll (Goethe U., Germany), Catia Domingues (CSIRO, Australia), Ulrike Falk
 1748 (U. Bremen, Germany), James Famiglietti (JPL/Caltech, USA), Luciana Fenoglio-Marc (U.
 1749 Bonn, Germany), Rene Forsberg (DTU-SPACE, Denmark), Gaia Galassi (U. Urbino, Italy),
 1750 Alex Gardner (JPL/Caltech, USA), Andreas Groh (TU-Dresden, Germany), Benjamin
 1751 Hamlington (Old Dominion U., USA), Anna Hogg (U. Leeds, UK), Martin Horwath (TU-
 1752 Dresden, Germany), Vincent Humphrey (ETHZ, Switzerland), Laurent Husson (U. Grenoble,
 1753 France), Masayoshi Ishii (MRI-JMA, Japan), Adrian Jaeggi (U. Bern, Switzerland), Svetlana
 1754 Jevrejeva (NOC, UK), Gregory Johnson (NOAA/PMEL, USA), Jürgen Kusche (U. Bonn,
 1755 Germany), Kurt Lambeck (ANU, Australia & ISSI, Switzerland), Felix Landerer (JPL/Caltech,
 1756 USA), Paul Leclercq (UIO, Norway), Benoit Legresy (CSIRO, Australia), Eric Leuliette
 1757 (NOAA, USA), William Llovel (LEGOS, France), Laurent Longuevergne (U. Rennes, France),
 1758 Bryant D. Loomis (NASA GSFC, USA), Scott B. Luthcke (NASA GSFC, USA), Marta
 1759 Marcos (UIB, Spain), Ben Marzeion (U. Bremen, Germany), Chris Merchant (U. Reading, UK),
 1760 Mark Merrifield (UCSD, USA), Glenn Milne (U. Ottawa, Canada), Gary Mitchum (U. South
 1761 Florida, USA), Yara Mohajerani (UCI, USA), Maeva Monier (Mercator-Ocean, France), Steve
 1762 Nerem (U. Colorado, USA), Hindumathi Palanisamy (LEGOS, France), Frank Paul (UZH,
 1763 Switzerland), Begoña Perez (Puertos del Estados, Spain), Christopher G. Piecuch (WHOI,
 1764 USA), Rui M. Ponte (AER inc., USA), Sarah G. Purkey (SIO/UCSD, USA), John T. Reager
 1765 (JPL/Caltech, USA), Roelof Rietbroek (U. Bonn, Germany), Eric Rignot (UCI and JPL, USA),
 1766 Riccardo Riva (TUDELFT, The Netherlands), Dean H. Roemmich (SIO/UCSD USA), Louise
 1767 Sandberg Sørensen (DTU-SPACE, Denmark), Ingo Sasgen (AWI, Germany), E.J.O. Schrama
 1768 (TUDELFT, The Netherlands), Sonia I. Seneviratne (ETHZ, Switzerland), C.K. Shum (Ohio
 1769 State U., USA), Giorgio Spada (U. Urbino, Italy), Detlef Stammer (U. Hamburg, Germany),
 1770 Roderic van de Wal (U. Utrecht, The Netherlands), Isabella Velicogna (UCI and JPL, USA),

1771 Karina von Schuckmann (Mercator-Océan, France), Yoshihide Wada (U. Utrecht, The
1772 Netherlands), Yiguo Wang (NERSC/BCCR, Norway), Christopher Watson (U. Tasmania,
1773 Australia), David Wiese (JPL/Caltech, USA), Susan Wijffels (CSIRO, Australia), Richard
1774 Westaway (U. Bristol, UK), Guy Woppelmann (U. La Rochelle, France), Bert Wouters (U.
1775 Utrecht, The Netherlands)

1776

1777 **Acknowledgements and author contributions:**

1778 This community assessment was initiated by A. Cazenave and B. Meyssignac as a contribution
1779 to the Grand Challenge ‘Regional Sea Level and Coastal Impacts’ of the World Climate
1780 Research Programme (WCRP). The results presented in this paper were prepared by 9 different
1781 teams dedicated to the various terms of the sea level budget (i.e., altimetry-based sea level, tide
1782 gauges, thermal expansion, glaciers, Greenland, Antarctica, terrestrial water storage, glacial
1783 isostatic adjustment, ocean mass from GRACE). Thanks to the team leaders (in alphabetic
1784 order), M. Ablain, J. Bamber, N. Champollion, J. Chen, C. Domingues, S. Jevrejeva, J.T.
1785 Reager, K. von Schuckmann, G. Spada, I. Velicogna and R. van de Wal, who interacted with
1786 their team members, collected all needed information, provided a synthesized assessment of the
1787 literature and when needed, updated the published results. The coordinators A.C. and B.M.
1788 collected those materials and prepared a first draft of the manuscript, but all authors contributed
1789 to its refinement and to the discussion of the results. Special thanks are addressed to J.
1790 Benveniste, E. Berthier, G. Cogley, J. Church, G. Johnson (PMEL Contribution Number 4776),
1791 B. Marzeion, F. Paul, R. Ponte, and E. Schrama for improving the successive versions of the
1792 manuscript, and to H. Palanisamy for providing all figures presented in section 3.

1793 The views, opinions, and findings contained in this paper are those of the authors and should
1794 not be construed as an official NOAA, U.S. Government or other institutions position, policy,
1795 or decision.

1796 We are grateful to the anonymous reviewer for his/her thorough comments that helped to
1797 improve the manuscript.

1798

1799 **References**

- 1800 1. A G., Chambers, D. P., Calculating trends from GRACE in the presence of large
 1801 changes in continental ice storage and ocean mass. *Geophys. J. Int.*, pp. 272,
 1802 doi:10.1111/j.1365-246X.2008.04012.x, 2008.
- 1803 2. A G., Wahr J. and Zhong S., Computations of the viscoelastic response of a 3-D
 1804 compressible Earth to surface loading: an application to Glacial Isostatic Adjustment in
 1805 Antarctica and Canada, *Geophysical Journal International*, 192.2, 557-572, 2013.
- 1806 3. Ablain M., A. Cazenave, G. Valladeau, and S. Guinehut, “A New Assessment of the
 1807 Error Budget of Global Mean Sea Level Rate Estimated by Satellite Altimetry over
 1808 1993–2008.” *Ocean Science*, doi:10.5194/os-5-193-2009, 2009.
- 1809 4. Ablain, M., S. Philipps, M. Urvoy, N. Tran, and N. Picot, “Detection of Long-Term
 1810 Instabilities on Altimeter Backscatter Coefficient Thanks to Wind Speed Data
 1811 Comparisons from Altimeters and Models.” *Marine Geodesy* 35 (sup1):258–75,
 1812 doi:10.1080/01490419.2012.718675, 2012.
- 1813 5. Ablain M., A. Cazenave, G. Larnicol, M. Balmaseda, P. Cipollini, Y. Faugère, M. J.
 1814 Fernandes, et al., “Improved Sea Level Record over the Satellite Altimetry Era (1993–
 1815 2010) from the Climate Change Initiative Project.” *Ocean Science*, doi:10.5194/os-11-
 1816 67-2015, 2015.
- 1817 6. Ablain M., J. F. Legeais, P. Prandi, M. Marcos, L. Fenoglio-Marc, H. B. Dieng, J.
 1818 Benveniste, and A. Cazenave, “Satellite Altimetry-Based Sea Level at Global and
 1819 Regional Scales.” *Surveys in Geophysics*, doi:10.1007/s10712-016-9389-8, 2017a.
- 1820 7. Ablain M., R. Jugier, L. Zawadki, and N. Taburet, “The TOPEX-A Drift and Impacts
 1821 on GMSL Time Series.” AVISO Website. October 2017.
 1822 https://meetings.aviso.altimetry.fr/fileadmin/user_upload/tx_ausycslseminar/files/Poster_OSTST17_GMSL_Drift_TOPEX-A.pdf, 2017b.
- 1823 8. Abraham J. P., et al., A review of global ocean temperature observations: Implications
 1824 for ocean heat content estimates and climate change, *Rev. Geophys.*, 51, 3, 450-483,
 1825 doi:10.1002/rog.20022, 2013.
- 1826 9. Adrian R et al., Lakes as sentinels of climate change *Limnology and Oceanography*
 1827 54:2283-2297 doi:10.4319/lo.2009.54.6_part_2.2283, 2009.
- 1828 10. Ahmed M, Sultan M, Wahr J, Yan E, The use of GRACE data to monitor natural and
 1829 anthropogenic induced variations in water availability across Africa *Earth-Science*
 1830 *Reviews* 136:289-300, 2014.
- 1831 11. Argus D.F. Peltier, W. R., Drummond, R., The Antarctica component of postglacial
 1832 rebound model ICE-6G_C (VM5a) based on GPS positioning, exposure age dating of
 1833 ice thicknesses, and relative sea level histories. *Geophysical Journal International* 198,
 1834 1, 537-563, 2014.
- 1835 12. Armentano TV, Menges ES, Patterns of Change in the Carbon Balance of Organic Soil-
 1836 Wetlands of the Temperate Zone *J Ecol*, 74:755-774, doi:10.2307/2260396, 1986.
- 1837 13. Awange J.L., Sharifi M.A., Ogonda G., Wickert J., Grafarend E.W., Omulo M., The
 1838 falling Lake Victoria water level: GRACE, TRIMM and CHAMP satellite analysis of
 1839 the lake basin, *Water Resources Management* 22:775-796, 2008.
- 1840 14. Bahr, D. and Radic, V., Significant contribution to total mass from very small glaciers,
 1841 *The Cryosphere*, 6, 763-770, 2012.
- 1842 15. Bahr, D., Pfeffer, W., Sassolas, C. and Meier, M., Response time of glaciers as a
 1843 function of size and mass balance: 1. Theory, *Journal of Geophysical Research: Solid*
 1844 *Earth*, 103, 9777-9782, 1998.
- 1845 16. Balmaseda M.A., K. Mogensen, A. Weaver (2013b). Evaluation of the ECMWF Ocean
 1846 Reanalysis ORAS4. *Q. J. R. Meteorol. Soc.*, doi:10.1002/qj.2063, 2013.
- 1847

- 1848 17. Bamber J.L., R.M. Westaway, B. Marzeion and B. Wouters, The land ice contribution
 1849 to sea level during the satellite era, *Environ. Res. Lett.*, 13, 063008, [doi:10.1088/1748-](https://doi.org/10.1088/1748-9326/aac2f0)
 1850 [9326/aac2f0](https://doi.org/10.1088/1748-9326/aac2f0), 2018.
- 1851 18. Barletta, V. R., Sørensen, L. S. & Forsberg, R. Scatter of mass changes estimates at
 1852 basin scale for Greenland and Antarctica, *The Cryosphere*, 7, 1411-1432, 2013.
- 1853 19. Barnett, T.P.. The estimation of “global” sea level change: A problem of uniqueness.
 1854 *J. Geophys. Res.*, 89 (C5), 7980-7988, 1984.
- 1855 20. Beck, H. E., van Dijk, A. I., de Roo, A., Dutra, E., Fink, G., Orth, R., & Schellekens, J.,
 1856 Global evaluation of runoff from 10 state-of-the-art hydrological models. *Hydrology*
 1857 *and Earth System Sciences*, 21, 6, 2881, 2017.
- 1858 21. Becker M, Llovel W, Cazenave A, Güntner A, Crétaux J-F, Recent hydrological
 1859 behavior of the East African great lakes region inferred from GRACE, satellite altimetry
 1860 and rainfall observations, *C. R. Geosci* 342:223-233, 2010.
- 1861 22. Beckley, B. D., P. S. Callahan, D. W. Hancock, G. T. Mitchum, and R. D. Ray. “On the
 1862 ‘Cal-Mode’ Correction to TOPEX Satellite Altimetry and Its Effect on the Global Mean
 1863 Sea Level Time Series.” *Journal of Geophysical Research, C: Oceans* 122 (11):8371–
 1864 84. <https://doi.org/10.1002/2017jc013090>, 2017.
- 1865 23. Belward AS, Estes JE, Kline KD, The IGBP-DIS global 1-km land-cover data set
 1866 DISCover: A project overview *Photogrammetric Engineering and Remote Sensing*
 1867 65:1013-1020, 1999.
- 1868 24. Bindoff, N., J. Willebrand, V. Artale, et al., Observations: Oceanic climate and sea level.
 1869 In *Climate Change 2007: The Physical Science Basis; Contribution of Working Group*
 1870 *I to the Fourth Assessment Report of the Intergovernmental Panel on Climate Change*.
 1871 Edited by S. Solomon, D. Qin, M. Manning, et al., 386–432. Cambridge, UK, and New
 1872 York: Cambridge Univ. Press, 2007.
- 1873 25. Boening, C., J. K. Willis, F. W. Landerer, R. S. Nerem, and J. Fasullo, The 2011 La
 1874 Niña: So strong, the oceans fell, *Geophys. Res. Lett.*, 39(19), n/a-n/a,
 1875 [doi:10.1029/2012GL053055](https://doi.org/10.1029/2012GL053055), 2012.
- 1876 26. Bosmans, J. H. C., van Beek, L. P. H., Sutanudjaja, E. H., and Bierkens, M. F. P.:
 1877 Hydrological impacts of global land cover change and human water use, *Hydrol. Earth*
 1878 *Syst. Sci.* 21, 5603–5626, doi.org/10.5194/hess-21-5603-2017, 2017.
- 1879 27. Boyer, T., C. Domingues, S. Good, G. C. Johnson, J. M. Lyman, M. Ishii, V. Gouretski,
 1880 J., Antonov, N. Bindoff, J. Church, R. Cowley, J. Willis, and S. Wijffels. 2015.
 1881 Sensitivity of global ocean heat content estimates to mapping methods, XBT bias
 1882 corrections, and baseline climatology, *Journal of Climate*, 29, 4817–4842,
 1883 [doi:10.1175/JCLI-D-15-0801.1](https://doi.org/10.1175/JCLI-D-15-0801.1), 2016.
- 1884 28. Bredehoeft, J. D., The water budget myth revisited: why hydrogeologists model?,
 1885 *Ground Water*, 40, 340–345, [doi:10.1111/j.1745-6584.2002.tb02511.x](https://doi.org/10.1111/j.1745-6584.2002.tb02511.x), 2002.
- 1886 29. Butt N, de Oliveira PA, Costa MH, Evidence that deforestation affects the onset of the
 1887 rainy season in Rondonia, Brazil *Journal of Geophysical Research-Atmospheres* 116:
 1888 D11120 [doi:10.1029/2010jd015174](https://doi.org/10.1029/2010jd015174), 2011.
- 1889 30. Bolch, T., Sandberg Sørensen, L., Simonsen, S. B., Mölg, N., Machguth, H., Rastner,
 1890 P. & Paul, F. Mass loss of Greenland's glaciers and ice caps 2003–2008 revealed from
 1891 ICESat laser altimetry data. *Geophysical Research Letters*, 40, 875-881, 2013.
- 1892 31. Box, J. E. & Colgan, W. T., Sea level rise contribution from Arctic land ice: 1850-2100.
 1893 Snow, Water, Ice and Permafrost in the Arctic (SWIPA) 2017. Oslo, Norway: Arctic
 1894 Monitoring and Assessment Programme (AMAP), 2017.
- 1895 32. Brun, F., Berthier, E., Wagnon, P., Kääb, A. and Treichler, D., A spatially resolved
 1896 estimate of High Mountain Asia mass balances from 2000 to 2016, *Nature Geoscience*,
 1897 2017.

- 1898 33. Cao, G., C. Zheng, B. R. Scanlon, J. Liu, and W. Li, Use of flow modeling to assess
 1899 sustainability of groundwater resources in the North China Plain, *Water Resour. Res.*,
 1900 49, doi:10.1029/2012WR011899, 2013.
- 1901 34. Calafat, F.M., Chambers, D.P., and M.N. Tsimplis. On the ability of global sea level
 1902 reconstructions to determine trends and variability. *J. Geophys. Res.*, 119, 1572-1592,
 1903 2014.
- 1904 35. Cazenave, A., Dominh, K., Guinehut, S., Berthier, E., Llovel, W., Ramillien, G., Ablain,
 1905 M., and Larnicol, G., 2009. Sea level budget over 2003–2008: A reevaluation from
 1906 GRACE space gravimetry, satellite altimetry and Argo, *Glob. Planet. Change* **65**:83–
 1907 88, doi:10.1016/j.gloplacha.2008.10.004, 2009.
- 1908 36. Cazenave, A., Llovel, W., Contemporary Sea Level Rise, *Annu. Rev. Mar. Sci.* 2:145–
 1909 73, 10.1146/annurev-marine-120308-081105, 2010.
- 1910 37. Cazenave, A., Champollion, N., Paul, F. and Benveniste, J. Integrative Study of the
 1911 Mean Sea Level and Its Components, *Space Science Series of ISSI - Spinger*, 416 pp,
 1912 vol 58., 2017.
- 1913 38. Cazenave, A, H.B. Dieng, B. Meyssignac, K. von Schuckmann, B. Decharme, and E.
 1914 Berthier. “The Rate of Sea-Level Rise.” *Nature Climate Change* 4 (5):358–61.
 1915 <https://doi.org/10.1038/nclimate2159>, 2014.
- 1916 39. Chagnon FJF, Bras RL (2005) Contemporary climate change in the Amazon
 1917 *Geophysical Research Letters* 32:L13703 doi:10.1029/2005gl022722, 2005.
- 1918 40. Chao, B. F., Y. H. Wu, and Y. S. Li, Impact of artificial reservoir water impoundment
 1919 on global sea level, *Science*, 320, 212-214, doi:10.1126/science.1154580, 2008.
- 1920 41. Cheema, M. J., W. W. Immerzeel, and W. G. Bastiaanssen, Spatial quantification of
 1921 groundwater abstraction in the irrigated Indus basin, *Ground Water*, 52, 25-36,
 1922 doi:10.1111/gwat.12027, 2014.
- 1923 42. Chambers, D. P., J. Wahr, M. E. Tamisiea, and R. Steven Nerem, Reply to Comments
 1924 by Peltier et al., 2012 (“Concerning the Interpretation of GRACE Time Dependent
 1925 Gravity Observations and the Influence Upon them of Rotational Feedback in Glacial
 1926 Isostatic Adjustment.”) *J. Geophys. Res.*, 117, doi: 10.1029/2012JB009441, 2012.
- 1927 43. Chambers, D. P., Wahr, J., Tamisiea, M. E., and Nerem, R. S., Ocean mass from
 1928 GRACE and glacial isostatic adjustment. *Journal of Geophysical Research (Solid*
 1929 *Earth)*, 115(B14): L11415, doi:10.1029/2010JB007530, 2010.
- 1930 44. Chambers, D. P., A. Cazenave, N. Champollion, H. Dieng, W. Llovel, R. Forsberg, K.
 1931 von Schuckmann, and Y. Wada, Evaluation of the Global Mean Sea Level Budget
 1932 between 1993 and 2014, *Surv. Geophys.* 38, 309-327, doi: 10.1007/s10712-016-9381-
 1933 3, 2017.
- 1934 45. Chen, Xianyao, Xuebin Zhang, John A. Church, Christopher S. Watson, Matt A. King,
 1935 Didier Monselesan, Benoit Legresy, and Christopher Harig. “The Increasing Rate of
 1936 Global Mean Sea-Level Rise during 1993–2014.” *Nature Climate Change* **7**, 492–95.
 1937 <https://doi.org/10.1038/nclimate3325>, 2017.
- 1938 46. Chen, J. L., Wilson, C. R., and Tapley, B. D., Contribution of ice sheet and mountain
 1939 glacier melt to recent sea level rise, *Nature Geoscience*, doi: 10.1038/NGEO1829, 2013.
- 1940 47. Chen, J. L., Wilson, C. R., Tapley, B. D., Blankenship, D. D., and Ivins, E. R.,
 1941 Patagonia Icefield Melting Observed by GRACE, *Geophys. Res. Lett.*, Vol. 34, No. 22,
 1942 L22501, 10.1029/2007GL031871, 2007.
- 1943 48. Chen, J. L., Wilson, C. R., Tapley, B. D., Save, H., and Cretaux, J.-F., Long-term and
 1944 seasonal Caspian Sea level change from satellite gravity and altimeter
 1945 measurements. *Journal of Geophysical Research (Solid Earth)*, 122:2274–2290,
 1946 doi:10.1002/2016JB013595, 2017.

- 1947 49. Chen, J. L., C. R. Wilson, and B. D. Tapley (2010), The 2009 exceptional Amazon flood
 1948 and interannual terrestrial water storage change observed by GRACE, *Water Resour.*
 1949 *Res.*, 46, W12526, doi:10.1029/2010WR009383.
- 1950 50. Chen, J., J. S. Famiglietti, B. R. Scanlon, and M. Rodell, Groundwater Storage Changes:
 1951 Present Status from GRACE Observations, *Surveys in Geophysics*, 37, 397–417,
 1952 doi:10.1007/s10712-015-9332-4, 2017.
- 1953 51. Cheng, M.K., and Ries, J.R., Monthly estimates of C20 from 5 SLR satellites based on
 1954 GRACE RL05 models, GRACE Technical Note 07, The GRACE Project, Center for
 1955 Space Research, University of Texas at Austin, 2012.
- 1956 52. Cheng L., Trenberth K., Fasullo J., Boyer T., Abraham J. and Zhu J., Improved
 1957 estimates of ocean heat content from 1960-2015, *Science Advances*, 3, e1601545, 2017.
- 1958 53. Choblet, G., Husson, L., Bodin, T., Probabilistic surface re- construction of coastal sea
 1959 level rise during the twentieth century *J. Geophys. Res.*, 119, 9206-9236, 2014.
- 1960 54. Church, J. et al., Sea level change, in Stocker, T. et al. (eds.) *Climate Change 2013: The*
 1961 *Physical Science Basis. Contribution of Working Group I to the Fifth Assessment*
 1962 *Report of the Intergovernmental Panel on Climate Change* (Cambridge University
 1963 Press, Cambridge, United Kingdom and New York, NY, USA), 2013.
- 1964 55. Church, John, Jonathan Gregory, Neil White, Skye Platten, and Jerry Mitrovica.
 1965 “Understanding and Projecting Sea Level Change.” *Oceanography* 24 (2):130–43.
 1966 <https://doi.org/10.5670/oceanog.2011.33>, 2011.
- 1967 56. Church, J. A., and N. J. White. A 20th century acceleration in global sea-level rise,
 1968 *Geophys. Res. Lett.*, 33, L01602, doi:10.1029/2005GL024826, 2006.
- 1969 57. Church, J. A., and N. J. White, Sea-Level Rise from the Late 19th to the Early 21st
 1970 Century, *Surveys in Geophysics*, 32(4-5), 585-602, doi:10.1007/s10712-011-9119-1.,
 1971 2011.
- 1972 58. Ciais P et al., Carbon and other biogeochemical cycles. In: Stocker TF et al. (eds)
 1973 *Climate change 2013: the physical science basis. Contribution of working group I to the*
 1974 *fifth assessment report of the Intergovernmental Panel on Climate Change.* Cambridge
 1975 University Press, Cambridge, United Kingdom and New York, NY, USA, pp 465-570,
 1976 2013.
- 1977 59. Cretaux JF et al., SOLS: A lake database to monitor in the Near Real Time water level
 1978 and storage variations from remote sensing data *Adv Space Res* 47:1497-1507
 1979 doi:10.1016/j.asr.2011.01.004, 2011.
- 1980 60. Cogley, J., Geodetic and direct mass-balance measurements: comparison and joint
 1981 analysis, *Annals of Glaciology*, 50, 96-100, 2009.
- 1982 61. Couhert, Alexandre, Luca Cerri, Jean-François Legeais, Michael Ablain, Nikita P.
 1983 Zelensky, Bruce J. Haines, Frank G. Lemoine, William I. Bertiger, Shailen D. Desai,
 1984 and Michiel Otten. “Towards the 1mm/y Stability of the Radial Orbit Error at Regional
 1985 Scales.” *Advances in Space Research: The Official Journal of the Committee on Space*
 1986 *Research* 55 (1):2–23. <https://doi.org/10.1016/j.asr.2014.06.041>, 2015.
- 1987 62. Dangendorf, S., M. Marcos, A. Müller, E. Zorita, R. Riva, K. Berk, and J. Jensen,
 1988 Detecting anthropogenic footprints in sea level rise. *Nature Communications*, 6, 7849,
 1989 2015.
- 1990 63. Dangendorf, Sönke, Marta Marcos, Guy Wöppelmann, Clinton P. Conrad, Thomas
 1991 Frederikse, and Riccardo Riva. “Reassessment of 20th Century Global Mean Sea
 1992 Level Rise.” *Proceedings of the National Academy of Sciences* 114 (23):5946–51.
 1993 <https://doi.org/10.1073/pnas.1616007114>, 2017.
- 1994 64. Davaze, L., Rabatel, A., Arnaud, Y., Sirguey, P., Six, D., Letreguilly, A. and Dumont,
 1995 M., Monitoring glacier albedo as a proxy to derive summer and annual mass balances
 1996 from optical remote-sensing data, *The Cryosphere*, 12, 271-286, 2018.

- 1997
1998
1999
2000
2001
2002
2003
2004
2005
2006
2007
2008
2009
2010
2011
2012
2013
2014
2015
2016
2017
2018
2019
2020
2021
2022
2023
2024
2025
2026
2027
2028
2029
2030
2031
2032
2033
2034
2035
2036
2037
2038
2039
2040
2041
2042
2043
2044
2045
2046
65. Darras S, IGBP-DIS wetlands data initiative, a first step towards identifying a global delineation of wetlands. IGBP-DIS Office, Toulouse, France, 1999.
 66. Davidson NC, How much wetland has the world lost? Long-term and recent trends in global wetland area *Marine and Freshwater Research* 65:934-941 doi:10.1071/Mf14173, 2014.
 67. DeAngelis, A., F. Dominguez, Y. Fan, A. Robock, M. D. Kustu, and D. Robinson, Evidence of enhanced precipitation due to irrigation over the Great Plains of the United States, *J. Geophys. Res.*, 115, D15115, doi:10.1029/2010JD013892, 2010.
 68. Decharme B., R. Alkama, F. Papa, S. Faroux, H. Douville and C. Prigent, Global off-line evaluation of the ISBA-TRIP flood model, *Climate Dynamics*, 38, 1389-1412, doi:10.1007/s00382-011-1054-9, 2012.
 69. Decharme, B., Brun, E., Boone, A., Delire, C., Le Moigne, P., and Morin, S. (2016), Impacts of snow and organic soils parameterization on northern Eurasian soil temperature profiles simulated by the ISBA land surface model, *The Cryosphere*, 10, 853-877, doi:10.5194/tc-10-853-2016.
 70. Dieng, H. B., N. Champollion, A. Cazenave, Y. Wada, E. Schrama, and B. Meyssignac, Total land water storage change over 2003-2013 estimated from a global mass budget approach, *Environ. Res. Lett.*, 10, 124010, doi:10.1088/1748-9326/10/12/124010, 2015a.
 71. Dieng, H. B., Cazenave, A., von Schuckmann, K., Ablain, M., and Meyssignac, B., 2015b. Sea level budget over 2005-2013: missing contributions and data errors. *Ocean Science*, 11:789-802, doi:10.5194/os-11-789-2015, 2015b.
 72. Dieng, H. B., Palanisamy, H., Cazenave, A., Meyssignac, B., and von Schuckmann, K., The Sea Level Budget Since 2003: Inference on the Deep Ocean Heat Content. *Surveys in Geophysics*, 36:209-229, doi:10.1007/s10712-015-9314-6, 2015c.
 73. Dieng, H.B., A.Cazenave, B.Meyssignac, M.Ablain, New estimate of the current rate of sea level rise from a sea level budget approach, *Geophysical Research Letters*, 44, doi:10.1002/2017GL073308, 2017.
 74. Döll, P., H. Hoffmann-Dobrev, F. T. Portmann, S. Siebert, A. Eicker, M. Rodell, and G. Strassberg, Impact of water withdrawals from groundwater and surface water on continental water storage variations, *J. Geodyn.*, 59-60, 143-156, doi:10.1016/j.jog.2011.05.001, 2012.
 75. Döll, P., M. Fritsche, A. Eicker, and S. H. Mueller, Seasonal water storage variations as impacted by water abstractions: Comparing the output of a global hydrological model with GRACE and GPS observations, *Surv. Geophys.*, doi:10.1093/gji/ggt485, 2014a.
 76. Döll, P., H. Müller Schmied, C. Schuh, F. T. Portmann, and A. Eicker, Global-scale assessment of groundwater depletion and related groundwater abstractions: Combining hydrological modeling with information from well observations and GRACE satellites, *Water Resour. Res.*, 50, 5698-5720, doi:10.1002/2014WR015595, 2014b.
 77. Döll, P., H. Douville, A. Güntner, H. Müller Schmied, and Y. Wada, Modelling freshwater resources at the global scale: Challenges and prospects, *Surv. Geophys.*, 37, 195-221, Special Issue: ISSI Workshop on Remote Sensing and Water Resources, 2017.
 78. Domingues C, Church J, White N, Gleckler PJ, Wijffels SE, et al. 2008. Improved estimates of upper ocean warming and multidecadal sea level rise. *Nature* 453:1090-93, doi:10.1038/nature07080, 2008.
 79. Douglas B., Global sea level rise, *Journal of Geophysical Research: Oceans* 96(C4):6981-6992, 1991.
 80. Douglas B., Global sea rise: a redetermination, *Surveys in Geophysics* 18(2-3):279-292, 1997.

- 2047 81. Douglas, B.C., Sea level change in the era of recording tide gauges, in *Sea Level Rise,*
 2048 *History and Consequences*, pp. 37–64, eds Douglas, B.C., Kearney, M.S. &
 2049 Leatherman, S.P., Academic Press, San Diego, CA, 2001.
- 2050 82. Durack P., Gleckler, P., Landerer, F., and Taylor, K., Quantifying underestimates of
 2051 long-term upper-ocean warming, *Nature Climate Change* 4, 999–1005, doi:10.1038/
 2052 nclimate2389, 2014.
- 2053 83. Dutrioux P et al., Strong sensitivity of Pine Island ice shelf melting to climatic
 2054 variability, *Science* 343(6167), 2014.
- 2055 84. Escudier et al., Satellite radar altimetry: principle, accuracy and precision, in ‘Satellite
 2056 altimetry over oceans and land surfaces, D.L Stammer and A. Cazenave eds., 617
 2057 pages, CRC Press, Taylor and Francis Group, Boca Raton, New York, London, ISBN:
 2058 13: 978-1-4987-4345-7, 2018.
- 2059 85. Famiglietti, J. S., The global groundwater crisis, *Nature Clim. Change*, 4, 945-948,
 2060 doi:10.1038/nclimate2425, 2014.
- 2061 86. FAO, Global forest resources assessment 2015: how have the world's forests changed?
 2062 Rome, 2015.
- 2063 87. Farinotti, D. et al. (2017). How accurate are estimates of glacier ice thickness ?, *The*
 2064 *Cryosphere*, 11, 949-970, 2017.
- 2065 88. Farrell W., Clark J., On postglacial sea level, *Geophysical Journal International*
 2066 46.3:647-667, 1976.
- 2067 89. Fasullo, J. T., C. Boening, F. W. Landerer, and R. S. Nerem, Australia's unique influence
 2068 on global sea level in 2010–2011, *Geophys. Res. Lett.*, 40, 4368–4373,
 2069 doi:10.1002/grl.50834, 2013.
- 2070 90. Felfelani, F., Wada, Y., Longuevergne, L., & Pokhrel, Y. N., Natural and human-
 2071 induced terrestrial water storage change: A global analysis using hydrological models
 2072 and GRACE. *Journal of Hydrology*, 553, 105-118, 2017.
- 2073 91. Feng, W., M. Zhong, J.-M. Lemoine, R. Biancale, H.-T. Hsu, and J. Xia, Evaluation of
 2074 groundwater depletion in North China using the Gravity Recovery and Climate
 2075 Experiment (GRACE) data and ground-based measurements, *Water Resour. Res.*, 49,
 2076 2110–2118, doi:10.1002/wrcr.20192, 2013.
- 2077 92. Fleming K., Lambeck K., Constraints on the Greenland Ice Sheet since the Last Glacial
 2078 Maximum from sea-level observations and glacial-rebound models, *Quaternary Science*
 2079 *Reviews*23(9), 1053-1077, 2004.
- 2080 93. Forsberg, R., Sørensen, L. & Simonsen, S: Greenland and Antarctica Ice Sheet Mass
 2081 Changes and Effects on Global Sea Level. *Surveys in Geophysics*, 38, 89.
 2082 doi:10.1007/s10712-016-9398-7, 2017.
- 2083 94. Foster, S. and D. P. Loucks (eds.), *Non-Renewable Groundwater Resources: A*
 2084 *guidebook on socially-sustainable management for water-policy makers*, IHP-VI, Series
 2085 on Groundwater No. 10, UNESCO, Paris, France, 2006.
- 2086 95. Frederikse et al, A consistent sea-level reconstruction and its budget on basin and
 2087 global scales over 1958-2014, *Journal of Climate*, [https://doi.org/10.1175/JCLI-D-17-](https://doi.org/10.1175/JCLI-D-17-0502.1)
 2088 [0502.1](https://doi.org/10.1175/JCLI-D-17-0502.1), 2017.
- 2089 96. Frey, H., Machguth, H., Huss, M., Huggel, C., Bajracharaya, S., Bolch, T., Kulkarni,
 2090 A., Linsbauer, A., Salzmann, N. and Stoffel, M., Estimating the volume of glaciers in
 2091 the Himalayan-Karakoram region using different methods, *The Cryosphere*, 2014.
- 2092 97. Gardner, A.S., G. Moholdt, J.G. Cogley, B. Wouters, A.A. Arendt, J. Wahr, E. Berthier,
 2093 R. Hock, W.T. Pfeffer, G. Kaser, S.R.M. Ligtenberg, T.Bolch, M.J. Sharp, J.O. Hagen,
 2094 M.R. van den Broeke, and F. Paul, A reconciled estimate of glacier contributions to sea
 2095 level rise: 2003 to 2009. *Science*, 340, 852-857, doi:10.1126/science.1234532, 2013.

- 2096 98. Gleick, P. H., Global Freshwater Resources: Soft-Path Solutions for the 21st Century,
2097 *Science*, 302, 1524-1528, doi:10.1126/science.1089967, 2003.
- 2098 99. Golytsyn GS, Panin GN, Once more on the water level changes of the Caspian Sea
2099 *Vestnik Akademii Nauk SSSR* 9:59-63 (in Russian), 1989.
- 2100 100. Gomez N., Pollard D., Mitrovica J.X., A 3-D coupled ice sheet–sea level model
2101 applied to Antarctica through the last 40 ky, *Earth and Planetary Science Letters* 384,
2102 88-99, 2013.
- 2103 101. Gornitz V, Rosenzweig C, Hillel D, Effects of anthropogenic intervention in the
2104 land hydrologic cycle on global sea level rise *Global and Planetary Change* 14:147-161
2105 doi:10.1016/s0921-8181(96)00008-2, 1997.
- 2106 102. Gornitz, V., Sea-level rise: A review of recent past and near-future trends. *Earth*
2107 *Surf. Process. Landforms*, 20, 7–20. doi: 10.1002/esp.3290200103, 1995.
- 2108 103. Gornitz, V., In *Sea Level Rise: History and Consequences*, Douglas, B. C., M.
2109 S. Kearney, and S. P. Leatherman (eds.), 97-119, Academic Press, San Diego, CA, USA,
2110 2001.
- 2111 104. Gornitz, V., Lebedeff, S. and Hansen, J., Global sea level trend in the past
2112 century, *Science*, 215, 1611–1614, 1982.
- 2113 105. Gouretski, V. and K. Peter Koltermann. How much is the ocean really warming?
2114 *Geophysical Research Letters*, 34, L01610, doi:10.1029/2006GL027834, 2007.
- 2115 106. Gregory, J. M., and J. A. Lowe. Predictions of global and regional sea-level rise
2116 using AOGCMs with and without flux adjustment. *Geophys. Res. Lett.*, **27**, 3069–3072,
2117 2000..
- 2118 107. Gregory, J. M., N. J. White, J. A. Church, M. F. P. Bierkens, J. E. Box, M. R.
2119 van den Broeke, J. G. Cogley, X. Fettweis, E. Hanna, P. Huybrechts, L. F. Konikow, P.
2120 W. Leclercq, B. Marzeion, J. Oerlemans, M. E. Tamisiea, Y. Wada, L. M. Wake, R. S.
2121 W. van de Wal, Twentieth-Century Global-Mean Sea Level Rise: Is the Whole Greater
2122 than the Sum of the Parts?. *J. Climate*, 26, 4476–4499, doi:10.1175/JCLI-D-12-00319.1,
2123 2013.
- 2124 108. Grinsted, A., An estimate of global glacier volume, *The Cryosphere*, 7, 141–151,
2125 2013.
- 2126 109. Groh, A., & Horwath, M., The method of tailored sensitivity kernels for GRACE
2127 mass change estimates. *Geophysical Research Abstracts*, 18, EGU2016-12065, 2016.
- 2128 110. Gunter B.C., Didova O., Riva R.E.M., Ligtenberg S.R.M., Lenaerts J.T.M., King
2129 M.A., Van den Broeke M.R., Urban T., and others, Empirical estimation of present-day
2130 Antarctic glacial isostatic adjustment and ice mass change, *The Cryosphere* 8(2), 743-
2131 760, 2014.
- 2132 111. Haeberli, W. and Linsbauer, A., Brief communication: global glacier volumes
2133 and sea level; small but systematic effects of ice below the surface of the ocean and of
2134 new local lakes on land, *The Cryosphere*, 7, 817-821, 2013.
- 2135 112. Hamlington, B. D., R. R. Leben, R. S. Nerem, W. Han, and K.-Y. Kim,
2136 Reconstructing sea level using cyclostationary empirical orthogonal functions, *J.*
2137 *Geophys. Res.*, 116, C12015, doi:10.1029/2011JC007529, 2011.
- 2138 113. Hamlington, B.D., Thompson, P., Hammond, W.C., Blewitt, G., and R.D.
2139 Ray, Assessing the impact of vertical land motion on twentieth century global mean
2140 sea level estimates, *Journal of Geophysical Research: Oceans*, 121(7), 4980-4993. doi:
2141 10.1002/2016JC011747, 2016.
- 2142 114. Hay, Carling C., Eric Morrow, Robert E. Kopp, and Jerry X. Mitrovica.
2143 “Probabilistic Reanalysis of Twentieth-Century Sea-Level Rise.” *Nature* 517, 7535,
2144 481–84, doi:10.1038/nature14093, 2015.
- 2145 115. Henry, O., M. Ablain, B. Meyssignac, A. Cazenave, D. Masters, S. Nerem, and

- 2146 G. Garric. “Effect of the Processing Methodology on Satellite Altimetry-Based Global
2147 Mean Sea Level Rise over the Jason-1 Operating Period.” *Journal of Geodesy* 88, 4,
2148 351-361, doi: 10.1007/s00190-013-0687-3, 2014.
- 2149 116. Horwath, M., Novotny K, Cazenave, A., Palanisamy, H., Marzeion, B., Paul,
2150 F., Döll, P., Cáceres, D., Hogg, A., Shepherd, A., Forsberg, R., Sørensen, L., Barletta,
2151 V.R., Andersen, O.B., Rannald, H., Johannessen, J., Nilsen, J.E., Gutknecht, B.D.,
2152 Merchant, Ch.J., MacIntosh, C.R., von Schuckmann, K., *ESA Climate Change Initiative*
2153 *(CCI) Sea Level Budget Closure (SLBC_cci) Sea Level Budget Closure Assessment*
2154 *Report D3.1. Version 1.0, 2018.*
- 2155 117. Hosoda, S., T. Ohira and T. Nakamura. A monthly mean dataset of global
2156 oceanic temperature and salinity derived from Argo float observations. JAMSTEC Rep.
2157 Res. Dev., Volume 8, November 2008, 47–59, 2008.
- 2158 118. Khan, S. A., Sasgen, I., Bevis, M., Van Dam, T., Bamber, J. L., Wahr, J., Willis,
2159 M., Kjær, K. H., Wouters, B., Helm, V., Csatho, B., Fleming, K., Bjørk, A. A.,
2160 Aschwanden, A., Knudsen, P. & Munneke, P. K., Geodetic measurements reveal
2161 similarities between post–Last Glacial Maximum and present-day mass loss from the
2162 Greenland ice sheet. *Science Advances*, 2, 2016.
- 2163 119. Huang, Z., Y. Pan, H. Gong, P. J. Yeh, X. Li, D. Zhou, and W. Zhao,
2164 Subregional-scale groundwater depletion detected by GRACE for both shallow and
2165 deep aquifers in North China Plain, *Geophys. Res. Lett.*, 42, 1791–1799. doi:
2166 10.1002/2014GL062498, 2015.
- 2167 120. Huang Z., The Role of glacial isostatic adjustment (GIA) process on the
2168 determination of present-day sea level rise, Report n° 505, Geodetic Science, The Ohio
2169 State University, 2013.
- 2170 121. Huntington TG, Can we dismiss the effect of changes in land-based water
2171 storage on sea-level rise? *Hydrological Processes* 22:717-723 doi:10.1002/hyp.7001,
2172 2008.
- 2173 122. Hurkmans, R. T. W. L., Bamber, J. L., Davis, C. H., Joughin, I. R.,
2174 Khvorostovsky, K. S., Smith, B. S. & Schoen, N., Time-evolving mass loss of the
2175 Greenland Ice Sheet from satellite altimetry. *The Cryosphere*, 8, 1725-1740, 2014.
- 2176 123. Huss, M. and Hock, R., A new model for global glacier change and sea-level
2177 rise, *Front Earth Science*, 2015.
- 2178 124. IMBIE Team (the), Mass balance of the Antarctic ice sheet from 1992 to 2017,
2179 *Nature*, 558, 219-222, doi:10.1038/s41586-018-0179-y, 2018.
- 2180 125. Ishii, M., and M. Kimoto, Reevaluation of Historical Ocean Heat Content
2181 Variations with Time-varying XBT and MBT Depth Bias Corrections. *Journal of*
2182 *Oceanography* 65 (3) (June 1): 287–299. doi:10.1007/s10872-009-0027-7., 2009.
- 2183 126. Ivins, E. R., T. S. James, J. Wahr, E. J. O Schrama, F. W. Landerer, and K. M.
2184 Simon, Antarctic contribution to sea level rise observed by GRACE with improved GIA
2185 correction, *J. Geophys. Res. Solid Earth*, 118, 3126–3141, doi:10.1002/jgrb.50208,
2186 2013.
- 2187 127. Jacob, T., J. Wahr, W. T. Pfeffer, and S. Swenson, Recent contributions of
2188 glaciers and ice caps to sea level rise, *Nature* 482, 514–518, doi:10.1038/nature10847,
2189 2012.
- 2190 128. Jensen, L., R. Rietbroek, and J. Kusche, Land water contribution to sea level
2191 from GRACE and Jason-1 measurements, *J. Geophys. Res. Oceans*, 118, 212–226,
2192 doi:10.1002/jgrc.20058, 2013.
- 2193 129. Jevrejeva S et al.. Nonlinear trends and multi-year cycle in sea level records,
2194 *Journal of Geophysical Research*, 111, 2005JC003229, 2006.
- 2195 130. Jevrejeva, S., J. C. Moore, A. Grinsted, A. P. Matthews, and G. Spada, “Trends

- 2196 and Acceleration in Global and Regional Sea Levels since 1807.” *Global and Planetary*
 2197 *Change* 113:11–22. <https://doi.org/10.1016/j.gloplacha.2013.12.004>, 2014.
- 2198 131. Johannesson, T., Raymond, C. and Waddington, E., Time-Scale for Adjustment
 2199 of Glaciers to Changes in Mass Balance, *Journal of Glaciology*, 35, 355-369, 1989.
- 2200 132. Johnson, G. C. and Chambers, D. P., Ocean bottom pressure seasonal cycles and
 2201 decadal trends from GRACE Release-05: Ocean circulation implications, *J. Geophys.*
 2202 *Res. Oceans*, 118, 4228–4240, doi:10.1002/jgrc.20307, 2013.
- 2203 133. Johnson, G. C., and A. N. Birnbaum. 2017. As El Niño builds, Pacific Warm
 2204 Pool expands, ocean gains more heat. *Geophysical Research Letters*, 44, 438-445,
 2205 doi:10.1002/2016GL071767, 2017.
- 2206 134. Khan, S. A., Sasgen, I., Bevis, M., Van Dam, T., Bamber, J. L., Wahr, J., Willis,
 2207 M., Kjær, K. H., Wouters, B., Helm, V., Csatho, B., Fleming, K., Bjørk, A. A.,
 2208 Aschwanden, A., Knudsen, P. and Munneke, P. K., Geodetic measurements reveal
 2209 similarities between post–Last Glacial Maximum and present-day mass loss from the
 2210 Greenland ice sheet. *Science Advances*, 2., 2016.
- 2211 135. Kääh, A., Treichler, D., Nuth, C. and Berthier, E., Brief communication:
 2212 contending estimates of 2003–2008 glacier mass balance over the Pamir–Karakoram–
 2213 Himalaya, *The Cryosphere*, 9, 557–564, 2015.
- 2214 136. Kaser, G., Cogley, J., Dyurgerov, M., Meier, M. and Ohmura, A., Mass balance
 2215 of glaciers and ice caps: Consensus estimates for 1961-2004, *Geophysical Research*
 2216 *Letters*, 33, L19501, 2006.
- 2217 137. Keenan RJ, Reams GA, Achard F, de Freitas JV, Grainger A, Lindquist E.,
 2218 Dynamics of global forest area: Results from the FAO Global Forest Resources
 2219 Assessment 2015 *Forest Ecol Manag* 352:9-20 doi:10.1016/j.foreco.2015.06.014,
 2220 2015.
- 2221 138. Kemp, A. C., B. Horton, J. P. Donnelly, M. E. Mann, M. Vermeer, and S.
 2222 Rahmstorf, Climate related sea level variations over the past two millennia. *PNAS*
 2223 108.27: 11017–11022, 2011.
- 2224 139. Khatiwala S, Primeau F, Hall T., Reconstruction of the history of anthropogenic
 2225 CO2 concentrations in the ocean *Nature* 462:346-U110 doi:10.1038/nature08526, 2009.
- 2226 140. King M.A., Altamimi Z., Boehm J., Bos M., Dach R., Elosegui P., and others,
 2227 Improved constraints on models of glacial isostatic adjustment: a review of the
 2228 contribution of ground-based geodetic observations, *Surveys in geophysics* 31(5):465,
 2229 2010.
- 2230 141. Klige RK, Myagkov MS, Changes in the water regime of the Caspian Sea, *Geol.*
 2231 *Journal* 27:299-307, 1992.
- 2232 142. Konikow, L. F., Contribution of global groundwater depletion since 1900 to sea-
 2233 level rise, *Geophys. Res. Lett.*, 38, L17401, doi:10.1029/2011GL048604, 2011.
- 2234 143. Konrad H., Sasgen I., Pollard D., Klemann V., Potential of the solid-Earth
 2235 response for limiting long-term West Antarctic Ice Sheet retreat in a warming climate,
 2236 *Earth and Planetary Science Letters* 432, 254-264, 2015.
- 2237 144. Kopp R.E., Hay C.C., Little C.M., Mitrovica J.X., Geographic variability of sea-
 2238 level change, *Current Climate Change Reports* 1(3):192, 2015.
- 2239 145. Kustu, M., Y. Fan, and A. Robock, Large-scale water cycle perturbation due to
 2240 irrigation pumping in the US High Plains: A synthesis of observed streamflow changes,
 2241 *J. Hydrol.*, 390, 222–244, doi:10.1016/j.jhydrol.2010.06.045, 2010.
- 2242 146. Kustu, M. D., Y. Fan, and M. Rodell, Possible link between irrigation in the U.S.
 2243 High Plains and increased summer streamflow in the Midwest, *Water Resour. Res.*, 47,
 2244 W03522, doi:10.1029/2010WR010046, 2011.
- 2245 147. Lambeck K, Chappell J., *Science* 292(5517):679, 2001.

- 2246 148. Lambeck K., Sea-level change from mid-Holocene to recent time: An Australian
 2247 example with global implications, In: Ice Sheets, Sea Level and the Dynamic Earth, JX
 2248 Mitrovica and LLA Vermeersen, Eds., Geodynamics Series, 29:33-50, 2002.
- 2249 149. Lambeck K. et al., Paleoenvironmental records, geophysical modelling and
 2250 reconstruction of sea level trends and variability on centennial and longer time scales,
 2251 *In Understanding sea level rise and variability*, JA Church et al ed., Wiley-Blackwell,
 2252 2010.
- 2253 150. Leclercq, P., Oerlemans, J. and Cogley, J., Estimating the glacier contribution to
 2254 sea-level rise for the period 1800–2005, *Surveys in Geophysics*, 32, 519–535, 2011.
- 2255 151. Legeais, J-F, Michaël Ablain, Lionel Zawadzki, Hao Zuo, Johnny A.
 2256 Johannessen, Martin G. Scharffenberg, Luciana Fenoglio-Marc, et al., “An Accurate
 2257 and Homogeneous Altimeter Sea Level Record from the ESA Climate Change
 2258 Initiative.” *Earth System Science Data Discussions*, 1–35, [doi:10.5194/essd-2017-116](https://doi.org/10.5194/essd-2017-116),
 2259 2018.
- 2260 152. Lehner, B., C. Reidy Liermann, C. Revenga, C. Vörösmarty, B. Fekete, P.
 2261 Crouzet, P. Döll, M. Endejan, K. Frenken, J. Magome, C. Nilsson, J. C. Robertson, R.
 2262 Rödel, N. Sindorf, and D. Wisser, High-resolution mapping of the world's reservoirs
 2263 and dams for sustainable river-flow management, *Fron. Ecol. Environ.*, 9, 494-502,
 2264 [doi:10.1890/100125](https://doi.org/10.1890/100125), 2011.
- 2265 153. Le Queré et al., Global Carbon Budget 2017, *Earth Syst. Sci. Data*, 10, 405-448,
 2266 2018, doi.org/10.5194/essd-10-405-2018, 2018.
- 2267 154. Lettenmaier, D. P., and P. C. D. Milly, Land waters and sea level, *Nat. Geosci.*,
 2268 2, 452-454, [doi:10.1038/ngeo567](https://doi.org/10.1038/ngeo567), 2009.
- 2269 155. Leuliette, E. W., and Miller, L., Closing the sea level rise budget with altimetry,
 2270 Argo, and GRACE, *Geophys. Res. Lett.*, 36, L04608, [doi:10.1029/2008GL036010](https://doi.org/10.1029/2008GL036010),
 2271 2009.
- 2272 156. Leuliette, E.W., and Willis, J.K., Balancing the sea level budget, *Oceanography*
 2273 24 (2): 122–129, [doi:10.5670/oceanog.2011.32](https://doi.org/10.5670/oceanog.2011.32), 2011.
- 2274 157. Leuschen, C.: IceBridge Geolocated Radar Echo Strength Profiles, Boulder,
 2275 Colorado, NASA DAAC at the National Snow and Ice Data Center,
 2276 <http://dx.doi.org/10.5067/FAZTWP500V70>, last access: 15 June 2014
- 2277 158. Levitus S., J.I. Antonov, T.P. Boyer, O.K. Baranova, H.E. Garcia, R.A.
 2278 Locarnini, A.V. Mishonov, J.R. Reagan, D. Seidov, E.S. Yarosh and M.M. Zweng,
 2279 World ocean heat content and thermosteric sea level change (0-2000 m), 1955-2010,
 2280 *Geophys. Res. Lett.*, 39, L10603, [doi:10.1019/2012GL051106](https://doi.org/10.1019/2012GL051106), 2012.
- 2281 159. Llovel, W., J. K. Willis, F. W. Landerer, and I. Fukumori, Deep-ocean
 2282 contribution to sea level and energy budget not detectable over the past decade, *Nature*
 2283 *Clim. Change* 4, 1031–1035, [doi:10.1038/nclimate2387](https://doi.org/10.1038/nclimate2387), 2014.
- 2284 160. Llovel, W., M. Becker, A. Cazenave, J.-F. Crétaux, and G. Ramillien, *C. R.*
 2285 *Geosci.* 342, 179–188, [doi:10.1016/j.crte.2009.12.004](https://doi.org/10.1016/j.crte.2009.12.004), 2010.
- 2286 161. Lo, M.-H., and J. S. Famiglietti, Irrigation in California’s Central Valley
 2287 strengthens the southwestern U.S. water cycle, *Geophys. Res. Lett.*, 40,
 2288 [doi:10.1002/grl.50108](https://doi.org/10.1002/grl.50108), 2013.
- 2289 162. Loriaux, T. and Casassa, G., Evolution of glacial lakes from the Northern
 2290 Patagonia Icefield and terrestrial water storage in a sea-level rise context, *Global and*
 2291 *Planetary Change*, 102, 33-40, 2013.
- 2292 163. Lovel TR, Belward AS, The IGBP-DIS global 1 km land cover data set,
 2293 DISCover: first results *International Journal of Remote Sensing* 18:3291-3295, 1997.
- 2294 164. Luthcke, S. B., Sabaka, T. J., Loomis, B. D., Arendt, A. A., McCarthy, J. J., and
 2295 Camp, J., Antarctica, Greenland and Gulf of Alaska land-ice evolution from an iterated

- 2296 GRACE global mascon solution. *Journal of Glaciology*, 59:613–631,
 2297 doi:10.3189/2013JoG12J147, 2013.
- 2298 165. Luthcke, S. B., Zwally, H. J., Abdalati, W., Rowlands, D. D., Ray, R. D., Nerem,
 2299 R. S., Lemoine, F. G., McCarthy, J. J., and Chinn, D. S., Recent Greenland Ice Mass
 2300 Loss by Drainage System from Satellite Gravity Observations. *Science*, 314:1286–
 2301 1289, doi:10.1126/science.1130776, 2006.
- 2302 166. Luthcke, S. B., Sabaka, T., Loomis, B., Arendt, A., McCarthy, J. & Camp, J.,
 2303 Antarctica, Greenland and Gulf of Alaska land-ice evolution from an iterated GRACE
 2304 global mascon solution. *Journal of Glaciology*, 59, 613-631, 2013.
- 2305 167. Lyman, J. M., S. A. Godd, V. V. Gouretski, et al., Robust warming of the global
 2306 upper ocean. *Nature* 465:334–337, 2010.
- 2307 168. MacDicken KG, Global Forest Resources Assessment, What, why and how?
 2308 *Forest Ecol Manag* 352:3-8 doi:10.1016/j.foreco.2015.02.006, 2015.
- 2309 169. Martín-Español, A., Zammit-Mangion, A., Clarke, P. J., Flament, T., Helm, V.,
 2310 King, M. A., and Wouters, B., Spatial and temporal Antarctic Ice Sheet mass trends,
 2311 glacio-isostatic adjustment, and surface processes from a joint inversion of satellite
 2312 altimeter, gravity, and GPS data. *Journal of Geophysical Research: Earth*
 2313 *Surface*, 121(2), 182-200, 2016.
- 2314 170. Martinec Z., Hagedoorn J., The rotational feedback on linear-momentum balance
 2315 in glacial isostatic adjustment, *Geophysical Journal International* 199, 3, 1823-1846,
 2316 2014.
- 2317 171. Merrifield MA et al., An anomalous recent acceleration of global sea level rise.
 2318 *J. Clim.* 22: 5772–5781. doi:10.1175/2009JCLI2985.1., 2009.
- 2319 172. Meyssignac B., M. Becker, W. Llovel, and A. Cazenave, An Assessment of
 2320 Two-Dimensional Past Sea Level Reconstructions Over 1950–2009 Based on Tide-
 2321 Gauge Data and Different Input Sea Level Grids, *Surveys in Geophysics*,
 2322 doi:10.1007/s10712-011-9171-x, 2011.
- 2323 173. Milne G.A., Gehrels W.R., Hughes C.W., Tamisiea M.E., Identifying the causes
 2324 of sea-level change, *Nature Geoscience* 2.7:471, 2009.
- 2325 174. Mitrovica J.X., Milne G.A., On the origin of late Holocene sea-level highstands
 2326 within equatorial ocean basins, *Quaternary Science Reviews* 21, 20-22, 2179-2190,
 2327 2002.
- 2328 175. Mitrovica J.X., Milne G.A., On post-glacial sea level: I. General theory,
 2329 *Geophysical Journal International* 154, 2, 253, 2003.
- 2330 176. Mitrovica J.X., Wahr J., Matsuyama I., Paulson A., The rotational stability of an
 2331 ice-age earth, *Geophysical Journal International*, 161.2, 491-506, 2005.
- 2332 177. Mitrovica J.X., Wahr J., Ice age Earth rotation, *Annual Review of Earth and*
 2333 *Planetary Sciences* 39, 577-616, 2011.
- 2334 178. Marzeion, B., Jarosch, A., Hofer, M., Past and future sea-level change from the
 2335 surface mass balance of glaciers, *The Cryosphere*, 6, 1295–1322, 2012.
- 2336 179. Marzeion, B., Cogley, J., Richter, K. and Parkes, D., Attribution of global
 2337 glacier mass loss to anthropogenic and natural causes, *Science*, 345, 919–92, 2014.
- 2338 180. Marzeion, B., Champollion, N., Haeberli, W., Langley, K., Leclercq, P. and
 2339 Paul, F., Observation-Based Estimates of Global Glacier Mass Change and Its
 2340 Contribution to Sea-Level Change, *Surveys in Geophysics*, 28, 105-130, 2017.
- 2341 181. Marzeion, B., Kaser, G., Maussion, F. and Champollion, N., Limited influence
 2342 of climate change mitigation on short-term glacier mass loss, *Nature Climate Change*,
 2343 doi:[10.1038/s41558-018-0093-1](https://doi.org/10.1038/s41558-018-0093-1), 2018.
- 2344 182. Masters, D., R. S. Nerem, C. Choe, E. Leuliette, B. Beckley, N. White, and M.
 2345 Ablain., “Comparison of Global Mean Sea Level Time Series from TOPEX/Poseidon,

- 2346 Jason-1, and Jason-2.” *Marine Geodesy* 35 (sup1):20–41.
 2347 <https://doi.org/10.1080/01490419.2012.717862>, 2012.
- 2348 183. Matthews E, Fung I, Methane emission from natural wetlands: Global
 2349 distribution, area, and environmental characteristics of sources *Global Biogeochemical*
 2350 *Cycles* 1:61-86, 1987.
- 2351 184. Matthews GVT, *The Ramsar Convention on wetlands: its history and*
 2352 *development*. Ramsar Convention Bureau, Gland, Switzerland, 1993.
- 2353 185. Maussion, F, Butenko, A., Eis, J., Fourteau, K., Jarosch, A., Landmann, J.,
 2354 Oesterle, J., Recinos, B., Rothenpieler, T., Vlug, A., Wild, C. and Marzeion; B., *The*
 2355 *Open Global Glacier Model (OGGM) v1.0, subm. to The Cryosphere*, 2018.
- 2356 186. McMillan M. et al. Increased ice losses from Antarctica detected by Cryosat-2,
 2357 *Geophys. Res. Lett.*, 41(11), 3899-3905, 2014.
- 2358 187. Meherhomji VM, Probable Impact of Deforestation on Hydrological Processes
 2359 *Climatic Change* 19:163-173 doi:10.1007/Bf00142223, 1991.
- 2360 188. Micklin PP, *The Aral Crisis - Introduction to the Special Issue Post-Sov Geogr*
 2361 *33:269-282*, 1992.
- 2362 189. Milly P. C. D. et al., Terrestrial water-storage contributions to sea-level rise and
 2363 variability , in *Understanding Sea-Level Rise and Variability:226-255*, 2010.
- 2364 190. Milly, P. C. D., A. Cazenave, and M. C. Gennero, Contribution of climate-driven
 2365 change in continental water storage to recent sea-level rise. *Proc. Natl. Acad. Sci.*, 100,
 2366 13158–13161, 2003.
- 2367 191. Mitra S, Wassmann R, Vlek PLG, An appraisal of global wetland area and its
 2368 organic carbon stock *Curr Sci India* 88:25-35, 2005.
- 2369 192. Mitsch WJ, Gosselink JG, *Wetlands*, 2nd ed. Van Nostrand Reinhold, New
 2370 York, 1993.
- 2371 193. Mouginot J., E. Rignot, B. Scheuchl, Sustained increase in ice discharge from
 2372 the Amundsen Sea Embayment, West Antarctica, from 1973 to 2013, *Geophys. Res.*
 2373 *Lett.* 41, 1576-1584, 2014.
- 2374 194. Natarov, S. I., M. A. Merrifield, J. M. Becker, and P. R. Thompson, Regional
 2375 influences on reconstructed global mean sea level, *Geophys. Res. Lett.*, 44, 3274-
 2376 3282, 2017.
- 2377 195. Nerem, R. S., D. P. Chambers, C. Choe, and G. T. Mitchum. “Estimating Mean
 2378 Sea Level Change from the TOPEX and Jason Altimeter Missions.” *Marine Geodesy*
 2379 33 (sup1):435–46. <https://doi.org/10.1080/01490419.2010.491031>, 2010.
- 2380 196. Nerem R.S., Beckley B.D., Fasullo J., Hamlington B.D., Masters D. and
 2381 Mitchum G.T., Climate Change Driven Accelerated Sea Level Rise Detected In The
 2382 Altimeter Era, *PNAS*, 2018.
- 2383 197. Nghiem, S., Hall, D., Mote, T., Tedesco, M., Albert, M., Keegan, K., Shuman,
 2384 C., Digirolamo, N. & Neumann, G., The extreme melt across the Greenland ice sheet in
 2385 2012. *Geophysical Research Letters*, 39, 2012.
- 2386 198. Nobre P, Malagutti M, Urbano DF, de Almeida RAF, Giarolla E, Amazon
 2387 Deforestation and Climate Change in a Coupled Model Simulation *J Climate* 22:5686-
 2388 5697 doi:10.1175/2009jcli2757.1, 2009.
- 2389 199. Oki, T. and S. Kanae, Global hydrological cycles and world water resources,
 2390 *Science*, 313, 1068-1072, doi:10.1126/science.1128845, 2006.
- 2391 200. Ozyavas A, Khan SD, Casey JF, A possible connection of Caspian Sea level
 2392 fluctuations with meteorological factors and seismicity *Earth Planet Sc Lett* 299:150-
 2393 158 doi:10.1016/j.epsl.2010.08.030, 2010.
- 2394 201. Pala, C., Once a Terminal Case, the North Aral Sea Shows New Signs of Life,
 2395 *Science*, 312, 183, doi:10.1126/science.312.5771.183, 2006.

- 2396 202. Pala, C., In Northern Aral Sea, Rebound Comes With a Big Catch, *Science*, 334,
2397 303, doi:10.1126/science.334.6054.303, 2011.
- 2398 203. Palmer M. et al., 2016.
- 2399 204. Paul, F., Huggel, C. and Käab, Combining satellite multispectral image data and
2400 a digital elevation model for mapping of debris-covered glaciers, *Remote Sensing of*
2401 *Environment*, 89, 510–518, 2004.
- 2402 205. Paulson, A., Zhong, S., and Wahr, J., Inference of mantle viscosity from GRACE
2403 and relative sea level data. *Geophysical Journal International*, 171:497–508,
2404 doi:10.1111/j.1365-246X.2007.03556.x, 2007.
- 2405 206. Peltier W.R., Global glacial isostatic adjustment and modern instrumental
2406 records of relative sea level history, in: B.C. Douglas, M.S. Kearney, S.P. Leatherman
2407 (Eds.), *Sea-Level Rise: History and Consequences*, vol. 75, Academic Press, San Diego,
2408 2001, pp. 65–95.
- 2409 207. Peltier W.R., Luthcke S.B., On the origins of Earth rotation anomalies: New
2410 insights on the basis of both “paleogeodetic” data and Gravity Recovery and Climate
2411 Experiment (GRACE) data, *Journal of Geophysical Research: Solid Earth* 114,
2412 B11405, 2009.
- 2413 208. Peltier W.R., Global glacial isostasy and the surface of the ice-age Earth: the
2414 ICE-5G (VM2) model and GRACE, *Annual Review of Earth and Planetary Sciences*
2415 32, 111, 2004.
- 2416 209. Peltier W.R., Argus D.F., Drummond R., Space geodesy constrains ice age
2417 terminal deglaciation: The global ICE-6G_C (VM5a) model, *Journal of Geophysical*
2418 *Research: Solid Earth* 120, 1, 450-487, 2015.
- 2419 210. Peltier W.R., Closure of the budget of global sea level rise over the GRACE era:
2420 the importance and magnitudes of the required corrections for global glacial isostatic
2421 adjustment. *Quaternary Science Reviews*, 28, 1658-1674, 2009.
- 2422 211. Peltier, W. R., R. Drummond, and K. Roy, Comment on "Ocean mass from
2423 GRACE and glacial isostatic adjustment" by D. P. Chambers et al. *Journal of*
2424 *Geophysical Research-Solid Earth*, **117**, B11403, 2012.
- 2425 212. Perera J, A Sea Turns to Dust *New Sci* 140:24-27, 1993.
- 2426 213. Pfeffer, W., Arendt, A., Bliss, A., Bolch, T., Cogley, J., Gardner, A., Hagen, J.-
2427 O., Hock, R., Kaser, G., Kienholz, C., Miles, E., Moholdt, G., Mölg, N., Paul, F., Radić,
2428 V., Rastner, P., Raup, B., Rich, J. and Sharp, M., The Randolph Glacier Inventory: a
2429 globally complete inventory of glaciers., *Journal of Glaciology*, 60, 537–552, 2014.
- 2430 214. Plag H.P., Juettner H.U., Inversion of global tide gauge data for present-day ice
2431 load changes, *Memoirs of National Institute of Polar Research* 54:301, 2001.
- 2432 215. Pokhrel, Y. N., N. Hanasaki, P. J.-F. Yeh, T. Yamada, S. Kanae, and T. Oki,
2433 Model estimates of sea level change due to anthropogenic impacts on terrestrial water
2434 storage, *Nat. Geosci.*, 5, 389–392, doi:10.1038/ngeo1476, 2012.
- 2435 216. Pokhrel, Y. N., S. Koirala, P. J.-F. Yeh, N. Hanasaki, L. Longuevergne, S.
2436 Kanae, and T. Oki, Incorporation of groundwater pumping in a global Land Surface
2437 Model with the representation of human impacts, *Water Resour. Res.*, 51, 78–96,
2438 doi:10.1002/2014WR015602, 2015.
- 2439 217. Postel, S. L., Pillar of Sand: Can the Irrigation Miracle Last? W.W. Norton, New
2440 York USA, ISBN 0-393-31937-7, 1999.
- 2441 218. Purcell A.P., Tregoning P., Dehecq A., An assessment of the ICE6G_C (VM5a)
2442 glacial isostatic adjustment model, *Journal of Geophysical Research: Solid Earth* 121,
2443 5, 3939-3950, 2016.

- 2444 219. Purkey, S. G., Johnson, G. C., and Chambers, D. P., Relative contributions of
 2445 ocean mass and deep steric changes to sea level rise between 1993 and 2013, *J. Geophys.*
 2446 *Res. Oceans*, 119, 7509–7522, doi:10.1002/2014JC010180, 2014.
- 2447 220. Purkey, S., and G. C. Johnson, Warming of global abyssal and deep southern
 2448 ocean waters between the 1990s and 2000s: Contributions to global heat and sea level
 2449 rise budget, *J. Clim.*, 23, 6336–6351, doi:10.1175/2010JCLI3682.1, 2010.
- 2450 221. Radic, V. and Hock, R., Regional and global volumes of glaciers derived from
 2451 statistical upscaling of glacier inventory data, *Journal of Geophysical Research Earth*
 2452 *Surface*, 115, F01010, 2010.
- 2453 222. Radic, V. and Hock, R., Regionally differentiated contribution of mountain
 2454 glaciers and ice caps to future sea-level rise, *Nature Geoscience*, 4, 91-94, 2011.
- 2455 223. Ramillien G, Frappart F, Seoane L, Application of the regional water mass
 2456 variations from GRACE Satellite Gravimetry to large-scale water management in
 2457 Africa *Remote Sensing* 6:7379-7405, 2014.
- 2458 224. Ray, R.D. and B.C. Douglas, Experiments in reconstructing twentieth-century
 2459 sea levels, *Prog. Oceanogr.* 91, 495–515, 2011.
- 2460 225. Reager, J. T., Gardner, A. S., Famiglietti, J. S., Wiese, D. N., Eicker, A., & Lo,
 2461 M. H., A decade of sea level rise slowed by climate-driven hydrology. *Science*,
 2462 351(6274), 699-703, doi:10.1126/science.aad8386, 2016.
- 2463 226. Reager, J. T., Thomas, B. F., and Famiglietti, J. S., River basin flood potential
 2464 inferred using GRACE gravity observations at several months lead time. *Nature*
 2465 *Geoscience*, 7:588–592, doi:10.1038/ngeo2203, 2014.
- 2466 227. Rhein, M., S.R. Rintoul, S. Aoki, E. Campos, D. Chambers, R.A. Feely, S.
 2467 Gulev, G.C. Johnson, S.A. Josey, A. Kostianoy, C. Mauritzen, D. Roemmich, L.D.
 2468 Talley and F. Wang: Observations: Ocean. In: *Climate Change 2013: The Physical*
 2469 *Science Basis. Contribution of Working Group I to the Fifth Assessment Report of the*
 2470 *Intergovernmental Panel on Climate Change* [Stocker, T.F., D. Qin, G.-K. Plattner, M.
 2471 Tignor, S.K. Allen, J. Boschung, A. Nauels, Y. Xia, V. Bex and P.M. Midgley (eds.)].
 2472 Cambridge University Press, Cambridge, United Kingdom and New York, NY, USA.,
 2473 2013.
- 2474 228. Richey, A. S., B. F. Thomas, M.-H. Lo, J. T. Reager, J. S. Famiglietti, K. Voss,
 2475 S. Swenson, and M. Rodell, Quantifying renewable groundwater stress with GRACE,
 2476 *Water Resour. Res.*, 51, 5217–5238, doi:10.1002/2015WR017349, 2015.
- 2477 229. Rietbroek, R., Brunnabend, S.-E., Kusche, J. and Schröter, J., Resolving sea
 2478 level contributions by identifying fingerprints in time-variable gravity and altimetry, *J.*
 2479 *Geodyn.*, 59-60, 72-81, 2012.
- 2480 230. Rietbroek, R., Brunnabend, S.-E., Kusche, J., Schröter, J., and Dahle, C.,
 2481 Revisiting the contemporary sea-level budget on global and regional scales.
 2482 *Proceedings of the National Academy of Sciences*, 113(6):1504–1509,
 2483 doi:10.1073/pnas.1519132113, 2016.
- 2484 231. Rignot, E. J., I. Velicogna, M. R. van den Broeke, A. J. Monaghan, and J. T. M.
 2485 Lenaerts, Acceleration of the contribution of the Greenland and Antarctic ice sheets to
 2486 sea level rise, *Geophys. Res. Lett.*, 38, L05503, doi:10.1029/2011GL046583, 2011.
- 2487 232. Rignot, E., J. Mouginot, and B. Scheuchl, Ice flow of the Antarctic Ice
 2488 Sheet, *Science*, 333(6048), 1427–1430, doi:10.1126/science.1208336, 2011.
- 2489 233. Riva R.E., Gunter B.C., Urban T.J., Vermeersen B.L., Lindenbergh R.C., Helsen
 2490 M.M., and others, Glacial isostatic adjustment over Antarctica from combined ICESat
 2491 and GRACE satellite data, *Earth and Planetary Science Letters* 288(3), 516-523, 2009.

- 2492 234. Riva, R. E. M., J. L. Bamber, D. A. Lavallée, and B. Wouters, Sea-level
 2493 fingerprint of continental water and ice mass change from GRACE, *Geophys. Res. Lett.*,
 2494 37, L19605, doi:10.1029/2010GL044770, 2010.
- 2495 235. Rodell, M., I. Velicogna, and J. S. Famiglietti, Satellite-based estimates of
 2496 groundwater depletion in India, *Nature*, 460, 999-1002, doi:10.1038/nature08238,
 2497 2009.
- 2498 236. Roemmich, D., Owens, W.B., The ARGO project: global ocean observations for
 2499 understanding for understanding and prediction of climate variability. *Oceanography*
 2500 13 (2), 45–50, 2000.
- 2501 237. Roemmich, D., W. J. Gould, and J. Gilson, 135 years of global ocean warming
 2502 between the Challenger expedition and the Argo Programme, *Nature Climate Change*,
 2503 2(6), 425-428, doi:10.1038/nclimate1461, 2012.
- 2504 238. Roemmich, D, Gilson J, Sutton P, Zilberman N. 2016. [Multidecadal change of](#)
 2505 [the South Pacific gyre circulation](#). *Journal of Physical Oceanography*. 46:1871-
 2506 1883. [10.1175/jpo-d-15-0237.1](#), 2016.
- 2507 239. Roemmich, D. and J. Gilson. The 2004–2008 mean and annual cycle of
 2508 temperature, salinity, and steric height in the global ocean from the Argo Program,
 2509 *Progress in Oceanography*, Volume 82, Issue 2, August 2009, Pages 81-100, 2009.
- 2510 240. Rohrig E, Biomass and productivity. In: Rohrig E (edt.) *Ecosystems of the*
 2511 *world*. Elsevier, New York, pp 165-174, 1991.
- 2512 241. Sabine C.L. et al., The oceanic sink for anthropogenic CO₂ *Science* 305:367-
 2513 371 doi:10.1126/science.1097403, 2004.
- 2514 242. Sahagian D., Global physical effects of anthropogenic hydrological alterations:
 2515 sea level and water redistribution *Global and Planetary Change* 25:39-48
 2516 doi:10.1016/S0921-8181(00)00020-5, 2000.
- 2517 243. Sahagian, D. L., F. W. Schwartz, and D. K. Jacobs, Direct anthropogenic
 2518 contributions to sea level rise in the twentieth century, *Nature*, 367, 54-57,
 2519 doi:10.1038/367054a0, 1994.
- 2520 244. Sasgen I., Konrad H., Ivins E.R., Van den Broeke M.R., Bamber J.L., Martinec
 2521 Z., Klemann V., Antarctic ice-mass balance 2003 to 2012: regional reanalysis of
 2522 GRACE satellite gravimetry measurements with improved estimate of glacial-isostatic
 2523 adjustment based on GPS uplift rates, *The Cryosphere*, 7, 1499-1512, 2013.
- 2524 245. Sasgen I., Martín-Español A., Horvath A., Klemann V., Petrie E.J., Wouters B.,
 2525 and others Joint inversion estimate of regional glacial isostatic adjustment in Antarctica
 2526 considering a lateral varying Earth structure (ESA STSE Project REGINA),
 2527 *Geophysical Journal International* 211, 3, , 1534-1553, 2017.
- 2528 246. Sasgen, I., Van Den Broeke, M., Bamber, J. L., Rignot, E., Sørensen, L. S.,
 2529 Wouters, B., Martinec, Z., Velicogna, I. & Simonsen, S. B., Timing and origin of recent
 2530 regional ice-mass loss in Greenland. *Earth and Planetary Science Letters*, 333, 293-
 2531 303, 2012.
- 2532 247. Sasgen, I., Konrad, H., Ivins, E. R., Van den Broeke, M. R., Bamber, J. L.,
 2533 Martinec, Z., & Klemann, V., Antarctic ice-mass balance 2003 to 2012: regional
 2534 reanalysis of GRACE satellite gravimetry measurements with improved estimate of
 2535 glacial-isostatic adjustment based on GPS uplift rates. *The Cryosphere*, 7, 1499- 1512,
 2536 2013.
- 2537 248. Sasgen, I., Martín-Español, A., Horvath, A., Klemann, V., Petrie, E. J., Wouters,
 2538 B., & Konrad, Joint inversion estimate of regional glacial isostatic adjustment in
 2539 Antarctica considering a lateral varying Earth structure (ESA STSE Project REGINA).
 2540 *Geophysical Journal International*, 211, 3, 1534-1553, 2017.

- 2541 249. Scanlon, B. R., I. Jolly, M. Sophocleous, and L. Zhang, Global impacts of
 2542 conversions from natural to agricultural ecosystems on water resources: Quantity versus
 2543 quality, *Water Resources Res.*, 43, 3, W03437, 2007.
- 2544 250. Scanlon, B. R., C. C. Faunt, L. Longuevergne, R. C. Reedy, W. M. Alley, V. L.
 2545 McGuire, and P. B. McMahon, Groundwater depletion and sustainability of irrigation
 2546 in the U.S. High Plains and Central Valley, *PNAS*, 109, 9320-9325,
 2547 doi:10.1073/pnas.1200311109, 2012a.
- 2548 251. Scanlon, B. R., L. Longuevergne, and D. Long, Ground referencing GRACE
 2549 satellite estimates of groundwater storage changes in the California Central Valley,
 2550 USA, *Water Resour. Res.*, 48, W04520, doi:10.1029/2011WR011312, 2012b.
- 2551 252. Scanlon, B. R., Zhang, Z., Save, H., Sun, A. Y., Schmied, H. M., van Beek, L.
 2552 P., & Longuevergne, L., Global models underestimate large decadal declining and rising
 2553 water storage trends relative to GRACE satellite data. *PNAS*, 201704665, 2018.
- 2554 253. Schrama, E. J., Wouters, B. & Rietbroek, R., A mascon approach to assess ice
 2555 sheet and glacier mass balances and their uncertainties from GRACE data. *Journal of*
 2556 *Geophysical Research: Solid Earth*, 119, 6048-6066, 2014.
- 2557 254. Schellekens, J., Dutra, E., Martínez-de la Torre, A., Balsamo, G., van Dijk, A.,
 2558 Weiland, F. S., & Fink, G., A global water resources ensemble of hydrological models:
 2559 the earth2Observe Tier-1 dataset. *Earth System Science Data*, 9(2), 389, 2017.
- 2560 255. Schwatke C, Dettmering D, Bosch W, Seitz F, DAHITI – an innovative approach
 2561 for estimating water level time series over inland waters using multi-mission satellite
 2562 altimetry, *Hydrol. Earth Syst. Sci.*, 19, 4345-4364, 2015.
- 2563 256. Shamsudduha, M., R. G. Taylor, and L. Longuevergne, Monitoring groundwater
 2564 storage changes in the highly seasonal humid tropics: Validation of GRACE
 2565 measurements in the Bengal Basin, *Water Resour. Res.*, 48, W02508,
 2566 doi:10.1029/2011WR010993, 2012.
- 2567 257. Sheng Y, Song C, Wang J, Lyons EA, Knox BR, Cox JS, Gao F., Representative
 2568 lake water extent mapping at continental scales using multi-temporal Landsat-8 imagery
 2569 *Remote Sensing of Environment* in press:doi:10.1016/j.rse.2015.1012.1041, 2016.
- 2570 258. Shepherd, A., Ivins E.R., Geruo A., Barletta V.R., Bentley M.J., Bettadpur S.,
 2571 and others, A reconciled estimate of ice-sheet mass balance. *Science*, 338(6111), 1183-
 2572 1189, doi:10.1126/science.1228102, 2012.
- 2573 259. Shukla J, Nobre C, Sellers P., Amazon Deforestation and Climate Change
 2574 *Science* 247:1322-1325 doi:10.1126/science.247.4948.1322, 1990.
- 2575 260. Singh A, Seitz F, Schwatke C., Inter-annual water storage changes in the Aral
 2576 Sea from multi-mission satellite altimetry, optical remote sensing, and GRACE satellite
 2577 gravimetry *Remote Sens Environ* 123:187-195, 2012.
- 2578 261. Slangen, A.B.A., Meyssignac, B., Agosta, C., Champollion, N., Church, J.A.,
 2579 Fettweis, X., Ligtenberg, S.R.M., Marzeion, B., Melet, A., Palmer, M.D., Richter, K.,
 2580 Roberts, C.D., Spada, G., Evaluating model simulations of 20th century sea-level rise.
 2581 Part 1: global mean sea-level change. *J. Clim.* 30(21): 8539–
 2582 8563. <https://dx.doi.org/10.1175/jcli-d-17-0110.1>, 2017.
- 2583 262. Sloan S, Sayer JA., Forest Resources Assessment of 2015 shows positive global
 2584 trends but forest loss and degradation persist in poor tropical countries, *Forest Ecol*
 2585 *Manag*, 352:134-145 doi:10.1016/j.foreco.2015.06.013, 2015.
- 2586 263. Smith LC, Sheng Y, MacDonald GM, Hinzman LD, Disappearing Arctic lakes
 2587 *Science* 308:1429-1429 doi:10.1126/science.1108142, 2005.
- 2588 264. Solomon, S. et al. (eds.), Climate Change 2007: The Physical Science Basis.
 2589 Contribution of Working Group I to the Fourth Assessment Report of the

- 2590 Intergovernmental Panel on Climate Change, Cambridge Univ. Press, Cambridge, UK.,
2591 2007.
- 2592 265. Song C, Huang B, Ke L., Modeling and analysis of lake water storage changes
2593 on the Tibetan Plateau using multi-mission satellite data *Remote Sens Environ* 135:25-
2594 35 doi:10.1016/j.rse.2013.03.013, 2013.
- 2595 266. Spada G., Stocchi P., SELEN: A Fortran 90 program for solving the “sea-level
2596 equation”, *Computers & Geosciences* 33.4, 538-562, 2007.
- 2597 267. Spada G., Galassi G., New estimates of secular sea level rise from tide gauge
2598 data and GIA modelling, *Geophysical Journal International* 191(3): 1067-1094, 2012.
- 2599 268. Spada G., Galassi G., Spectral analysis of sea level during the altimetry era, and
2600 evidence for GIA and glacial melting fingerprints, *Global and Planetary Change*
2601 143:34-49, 2016.
- 2602 269. Spada G., Glacial isostatic adjustment and contemporary sea level rise: An
2603 overview. *Surveys in Geophysics* 38(1), 153-185, 2017.
- 2604 270. Spracklen DV, Arnold SR, Taylor CM., Observations of increased tropical
2605 rainfall preceded by air passage over forests *Nature* 489:282-U127
2606 doi:10.1038/nature11390, 2012.
- 2607 271. Sutterley T.C., Velicogna I., Csatho B., van den Broeke M., Rezvan-Behbahani
2608 S., Babonis G., Evaluating Greenland glacial isostatic adjustment corrections using
2609 GRACE, altimetry and surface mass balance data *Environmental Research Letters* 9(1),
2610 014004, 2014.
- 2611 272. Strassberg, G., B. R. Scanlon, and M. Rodell, Comparison of seasonal terrestrial
2612 water storage variations from GRACE with groundwater-level measurements from the
2613 High Plains Aquifer (USA), *Geophys. Res. Lett.*, 34, L14402,
2614 doi:10.1029/2007GL030139, 2007.
- 2615 273. Swenson S, Wahr J., Monitoring the water balance of Lake Victoria, East Africa,
2616 from space *J Hydro* 370:163-176, 2009.
- 2617 274. Syed, T. H., J. S. Famiglietti, D. P. Chambers, J. K. Willis, and K. Hilburn,
2618 Satellite-based global ocean mass balance reveals water cycle acceleration and
2619 increasing continental freshwater discharge, 1994–2006, *Proc. Natl. Acad. Sci. U. S. A.*,
2620 107, 17,916–17,921, doi:10.1073/pnas.1003292107, 2010.
- 2621 275. Stammer, D., and Cazenave A., *Satellite Altimetry Over Oceans and Land*
2622 *Surfaces*, 617 pp., CRC Press, Taylor and Francis Group, Boca Raton, New York,
2623 London, ISBN: 13: 978-1-4987-4345-7, 2018.
- 2624 276. Tamisiea, M. E., Leuliette, E. W., Davis, J. L., and Mitrovica, J. X., Constraining
2625 hydrological and cryospheric mass flux in southeastern Alaska using space-based
2626 gravity measurements. *Geophysical Research Letters*, 32:L20501,
2627 doi:10.1029/2005GL023961, 2005.
- 2628 277. Tamisiea M.E., Ongoing glacial isostatic contributions to observations of sea
2629 level change, *Geophysical Journal International* 186(3):1036, 2011.
- 2630 278. Tapley, B. D., S. Bettadpur, J. C. Ries, P. F. Thompson, and M. M. Watkins,
2631 GRACE measurements of mass variability in the Earth system. *Science* 305, 503–505,
2632 doi: 10.1126/science.1099192, 2004.
- 2633 279. Tapley, B. D., Bettadpur, S., Ries, J. C., Thompson, P. F., and Watkins, M. M.,
2634 The Gravity Recovery and Climate Experiment; Mission Overview and Early Results,
2635 *Geophys. Res. Lett.*, Vol. 31, No. 9, L09607, 10.1029/2004GL019920, 2004.
- 2636 280. Taylor, R. G., B. Scanlon, P. Döll, M. Rodell, R. van Beek, Y. Wada, L.
2637 Longuevergne, M. LeBlanc, J. S. Famiglietti, M. Edmunds, L. Konikow, T. R. Green,
2638 J. Chen, M. Taniguchi, M. F. P. Bierkens, A. MacDonald, Y. Fan, R. M. Maxwell, Y.
2639 Yechieli, J. J. Gurdak, D. M. Allen, M. Shamsudduha, K. Hiscock, P. J.-F. Yeh, I.

- 2640 Holman and H. Treidel, Groundwater and climate change, *Nature Clim. Change*, 3, 322-
 2641 329, doi:10.1038/nclimate1744, 2013.
- 2642 281. Thompson, P.R., and M.A. Merrifield, A unique asymmetry in the pattern of
 2643 recent sea level change, *Geophys. Res. Lett.*, 41, 7675-7683, 2014.
- 2644 282. Tiwari, V. M., J. Wahr, and S. Swenson, Dwindling groundwater resources in
 2645 northern India, from satellite gravity observations, *Geophys. Res. Lett.*, 36, L18401,
 2646 doi:10.1029/2009GL039401, 2009.
- 2647 283. Tourian M, Elmi O, Chen Q, Devaraju B, Roohi S, Sneeuw N, A spaceborne
 2648 multisensor approach to monitor the desiccation of Lake Urmia in Iran *Remote Sens
 2649 Environ* 156:349-360, 2015.
- 2650 284. Turcotte DL, Schubert G, Geodynamics. Cambridge University Press,
 2651 Cambridge, 2014.
- 2652 285. Valladeau, G., J. F. Legeais, M. Ablain, S. Guinehut, and N. Picot, “Comparing
 2653 Altimetry with Tide Gauges and Argo Profiling Floats for Data Quality Assessment and
 2654 Mean Sea Level Studies.” *Marine Geodesy* 35 (sup1):42–60.
 2655 <https://doi.org/10.1080/01490419.2012.718226>, 2012.
- 2656 286. Van Den Broeke, M. R., Enderlin, E. M., Howat, I. M., Kuipers Munneke, P.,
 2657 Noël, B. P. Y., Van De Berg, W. J., Van Meijgaard, E. & Wouters, B., On the recent
 2658 contribution of the Greenland ice sheet to sea level change. *The Cryosphere*, 10, 1933-
 2659 1946, 2016.
- 2660 287. Velicogna, I., Increasing rates of ice mass loss from the Greenland and Antarctic
 2661 ice sheets revealed by GRACE. *Geophysical Research Letters*, 36, 2009.
- 2662 288. van der Werf GR et al., Global fire emissions and the contribution of
 2663 deforestation, savanna, forest, agricultural, and peat fires (1997-2009) *Atmos Chem
 2664 Phys* 10:11707-11735 doi:10.5194/acp-10-11707-2010, 2010.
- 2665 289. Van Dijk, A. I. J. M., L. J. Renzullo, Y. Wada, and P. Tregoning, A global water
 2666 cycle reanalysis (2003–2012) merging satellite gravimetry and altimetry observations
 2667 with a hydrological multi-model ensemble, *Hydrol. Earth Syst. Sci.*, 18, 2955-2973,
 2668 doi:10.5194/hess-18-2955-2014, 2014.
- 2669 290. Velicogna, I., Sutterley, T. C., & Van Den Broeke, M. R., Regional acceleration
 2670 in ice mass loss from Greenland and Antarctica using GRACE time-variable gravity
 2671 data. *Geophysical Research Letters*, 41(22), 8130-8137, 2014.
- 2672 291. Velicogna, I., Wahr, J., Measurements of Time-VARIABLE Gravity Show Mass
 2673 Loss in Antarctica, *Science*, DOI: 10.1126/science.1123785, 2006.
- 2674 292. von Schuckmann, K., J.-B. Sallée, D. Chambers, P.-Y. Le Traon, C. Cabanes,
 2675 F. Gaillard, S. Speich, and M. Hamon, Monitoring ocean heat content from the current
 2676 generation of global ocean observing systems, *Ocean Science*, 10, 547-557,
 2677 DOI:10.5194/os-10-547-2012, 2014.
- 2678 293. von Schuckmann K., Palmer M.D., Trenberth K.E., Cazenave A., D. Chambers,
 2679 Champollion N. et al., Earth’s energy imbalance: an imperative for monitoring, *Nature
 2680 Climate Change*, 26, 138-144, 2016.
- 2681 294. Vörösmarty CJ, Sahagian D, Anthropogenic disturbance of the terrestrial water
 2682 cycle *Bioscience* 50:753-765 doi:10.1641/0006-
 2683 3568(2000)050[0753:Adottw]2.0.Co;2, 2000.
- 2684 295. Voss, K. A., J. S. Famiglietti, M. Lo, C. de Linage, M. Rodell, and S. C.
 2685 Swenson, Groundwater depletion in the Middle East from GRACE with implications
 2686 for transboundary water management in the Tigris-Euphrates-Western Iran region,
 2687 *Water Resour. Res.*, 49, doi:10.1002/wrcr.20078, 2013.
- 2688 296. Watson, Christopher S., Neil J. White, John A. Church, Matt A. King, Reed J.
 2689 Burgette, and Benoit Legresy, “Unabated Global Mean Sea-Level Rise over the Satellite

- 2690 Altimeter Era.” *Nature Climate Change* 5 (6):565–68.
 2691 <https://doi.org/10.1038/nclimate2635>, 2015.
- 2692 297. Wada, Y., L. P. H. van Beek, C. M. van Kempen, J. W. T. M. Reckman, S.
 2693 Vasak, and M. F. P. Bierkens, Global depletion of groundwater resources, *Geophys.*
 2694 *Res. Lett.*, 37, L20402, doi:10.1029/2010GL044571, 2010.
- 2695 298. Wada, Y., Modelling groundwater depletion at regional and global scales:
 2696 Present state and future prospects, *Surv. Geophys.*, 37, 419-451, doi:10.1007/s10712-
 2697 015-9347-x, Special Issue: ISSI Workshop on Remote Sensing and Water Resources,
 2698 2017.
- 2699 299. Wada, Y., L. P. H. van Beek, and M. F. P. Bierkens, Nonsustainable groundwater
 2700 sustaining irrigation: A global assessment, *Water Resour. Res.*, 48, W00L06,
 2701 doi:10.1029/2011WR010562, Special Issue: Toward Sustainable Groundwater in
 2702 Agriculture, 2012a.
- 2703 300. Wada, Y., L. P. H. van Beek, F. C. Sperna Weiland, B. F. Chao, Y.-H. Wu, and
 2704 M. F. P. Bierkens, Past and future contribution of global groundwater depletion to sea-
 2705 level rise, *Geophys. Res. Lett.*, 39, L09402, doi:10.1029/2012GL051230, 2012b.
- 2706 301. Wada, Y., M.-H. Lo, P. J.-F. Yeh, J. T. Reager, J. S. Famiglietti, R.-J. Wu, and
 2707 Y.-H. Tseng, Fate of water pumped from underground causing sea level rise, *Nature*
 2708 *Clim. Change*, doi:10.1038/nclimate3001, early online, 2016.
- 2709 302. Wada, Y., Reager, J. T., Chao, B. F., Wang, J., Lo, M. H., Song, C. and Gardner,
 2710 A. S., Satellite Altimetry-Based Sea Level at Global and Regional Scales. In *Integrative*
 2711 *Study of the Mean Sea Level and Its Components* (pp. 133-154). Springer International
 2712 Publishing, 2017.
- 2713 303. Wang J, Sheng Y, Hinkel KM, Lyons EA, Drained thaw lake basin recovery on
 2714 the western Arctic Coastal Plain of Alaska using high-resolution digital elevation
 2715 models and remote sensing imagery *Remote Sensing of Environment* 119:325-336
 2716 doi:10.1016/j.rse.2011.10.027, 2012.
- 2717 304. Wang J, Sheng Y, Tong TSD, Monitoring decadal lake dynamics across the
 2718 Yangtze Basin downstream of Three Gorges Dam *Remote Sensing of Environment*
 2719 152:251-269 doi:10.1016/j.rse.2014.06.004, 2014.
- 2720 305. Wahr J., Nerem R.S. and Bettadpur S.V., The pole tide and its effect on GRACE
 2721 time-variable gravity measurements: Implications for estimates of surface mass
 2722 variations. *Journal of Geophysical Research: Solid Earth* 120(6), 4597-4615, 2015.
- 2723 306. Watkins, M. M., Wiese, D. N., Yuan, D.-N., Boening, C., and Landerer, F. W.,
 2724 Improved methods for observing Earth's time variable mass distribution with GRACE
 2725 using spherical cap mascons. *Journal of Geophysical Research (Solid Earth)*,
 2726 120:2648–2671, doi:10.1002/2014JB011547, 2015.
- 2727 307. Wenzel M and J Schroter, Reconstruction of regional mean sea level anomalies
 2728 from tide gauges using neural networks, *J. Geophys. Res.* 115.
 2729 doi:10.1029/2009JC005630, 2010.
- 2730 308. Wessem J. M. et al., Modeling the climate and surface mass balance of polar ice
 2731 sheets using RACMO2, part 2: Antarctica, *the Cryosphere*, 2017.
- 2732 309. Whitehouse, P. L., et al., A new glacial isostatic adjustment model for
 2733 Antarctica: calibrating the deglacial model using observations of relative sea-level and
 2734 present-day uplift rates, *Geophys Journal Int.*, 190, 1464-1482, 2012.
- 2735 310. Wiese, D. N., Landerer, F. W., and Watkins, M. M., Quantifying and reducing
 2736 leakage errors in the JPL RL05M GRACE mascon solution. *Water Resources Research*,
 2737 52:7490–7502, doi:10.1002/2016WR019344, 2016.

- 2738 311. Willis, J.K., Chambers, D.T., Nerem, R.S., Assessing the globally averaged sea
2739 level budget on seasonal to interannual time scales, *J. Geophys. Res.* 113, C06015.
2740 doi:10.1029/2007JC004517, 2008.
- 2741 312. Wisser, D., S. Frolking, S. Hagen, and M. F. P. Bierkens, Beyond peak reservoir
2742 storage? A global estimate of declining water storage capacity in large reservoirs, *Water*
2743 *Resour. Res.*, 49, 5732–5739, doi:10.1002/wrcr.20452, 2013.
- 2744 313. Whitehouse, P.L., Bentley M.J., Milne G.A., King M.A., Thomas I.D., A new
2745 glacial isostatic adjustment model for Antarctica: calibrating the deglacial model using
2746 observations of relative sea-level and present-day uplift rates, *Geophysical Journal*
2747 *International* 190, 1464-1482, 2012.
- 2748 314. Wiese, D., Yuan, D., Boening, C., Landerer, F. & Watkins, M., JPL GRACE
2749 Mascon Ocean, Ice, and Hydrology Equivalent Water Height RL05M. 1 CRI Filtered,
2750 Ver. 2, PO. DAAC, CA, USA. Dataset provided by Wiese in Nov/Dec 2017, 2016.
- 2751 315. Wijffels, S. E., D. Roemmich, D. Monselesan, J. Church, J. Gilson, Ocean
2752 temperatures chronicle the ongoing warming of Earth. *Nature Climate Change*, (6),116-
2753 118, bdoi:10.1038/nclimate2924, 2016.
- 2754 316. Wöppelmann, G., and M. Marcos, Vertical land motion as a key to
2755 understanding sea level change and variability, *Rev. Geophys.*, 54, 64–92,
2756 doi:10.1002/2015RG000502, 2016.
- 2757 317. Wouters, B., Bamber, J. Á., Van den Broeke, M. R., Lenaerts, J. T. M., & Sasgen,
2758 I., Limits in detecting acceleration of ice sheet mass loss due to climate
2759 variability. *Nature Geoscience*, 6(8), 613, 2013.
- 2760 318. Wouters, B., R. E. M. Riva, D. A. Lavallée, and J. L. Bamber, Seasonal
2761 variations in sea level induced by continental water mass: First results from GRACE,
2762 *Geophys. Res. Lett.*, 38(3), doi:10.1029/2010GL046128, 2011.
- 2763 319. Wouters, B., Chambers, D. & Schrama, E., GRACE observes small-scale mass
2764 loss in Greenland. *Geophysical Research Letters*, 35, 2008.
- 2765 320. Wu X., Heflin M.B., Schotman H., Vermeersen B.L., Dong D., Gross R. S., and
2766 .others, Simultaneous estimation of global present-day water transport and glacial
2767 isostatic adjustment. *Nature Geoscience* 3.9: 642-646, 2010.
- 2768 321. Yi, S., Sun, W., Heki, K., and Qian, A., An increase in the rate of global mean
2769 sea level rise since 2010. *Geophysical Research Letters*, 42:3998–4006,
2770 doi:10.1002/2015GL063902, 2015.
- 2771 322. Zawadzki L., M. Ablain, Estimating a drift in TOPEX-A Global Mean Sea Level
2772 using Poseidon-1 measurements, paper presented at the OSTST meeting, La Rochelle,
2773 2016.
- 2774 323. Zhang G, Yao T, Xie H, Kang S, Lei Y, Increased mass over the Tibetan Plateau:
2775 From lakes or glaciers? *Geophys Res Lett*:1-6, 2013.
- 2776 324. Zemp, M., Frey, H., Gärtner-Roer, I., Nussbaumer, S., Hoelzle, M., Paul, F.,
2777 Haeberli, W., Denzinger, F., Ahlstrøm, A., Anderson, B., Bajracharya, S., Baroni, C.,
2778 Braun, L., Cáceres, B., Casassa, G., Cobos, G., Dávila, L., Delgado Granados, H.,
2779 Demuth, M., Espizua, L., Fischer, A., Fujita, K., Gadek, B., Ghazanfar, A., Hagen, J.,
2780 Holmlund, P., Karimi, N., Li, Z., Pelto, M., Pitte, P., Popovnin, V., Portocarrero, C.,
2781 Prinz, R., Sangewar, C., Severskiy, I., Sigurdsson, O., Soruco, A., Usubaliev, R. and
2782 Vincent, C., Historically unprecedented global glacier decline in the early 21st century,
2783 *Journal of Glaciology*, 61, 745–762, 2015.
- 2784 325. Zwally, J.H., J. Li, J.W. Robbins, J.L. Saba, D.H. Yi, A.C. Brenner, 2016,
2785 Mass gains of the Antarctic ice sheet exceed losses, *Journal of Glaciology*, 61, 1013-
2786 1036, doi :10.3189/2015JoG15J071.
- 2787

2788